Noname manuscript No.
(will be inserted by the editor)

A discontinuous Galerkin method for non-linear electro-thermo-mechanical problems

Application to shape memory composite materials

Lina Homsi · Ludovic Noels

Received: date / Accepted: date

Abstract A coupled Electro-Thermo-Mechanical Discontinuous Galerkin (DG) method is developed considering the non-linear interactions of electrical, thermal, and mechanical fields. In order to develop a stable discontinuous Galerkin formulation the governing equations are expressed in terms of energetically conjugated fields gradients and fluxes. Moreover, the DG method is formulated in finite deformations and finite fields variations. The multi-physics DG formulation is shown to satisfy the consistency condition, and the uniqueness and optimal convergence rate properties are derived under the assumption of small deformation. First the numerical properties are verified on a simple numerical example, and then the framework is applied to simulate the response of smart composite materials in which the shape memory effect of the matrix is triggered by the Joule effect.

Keywords Discontinuous Galerkin Method · Electro-thermo-mechanics · non-linear elliptic problems · smart composites

1 Introduction

The emergence of complex multi-physics materials, such as multi-functional and shape-memory materials, see the reviews [37,36,18,51] as a non-exhaustive list, has motivated the development of reliable, accurate, and efficient multi-physics numerical models. As an example, Shape Memory Polymer (SMP) [9,44] can fix a temporary deformed configuration and recover their initial shape upon application of a stimulus such as temperature [34], light [35], electric field [17], magnetic field [56], water [29], or solvent [41]. Temperature triggered SMP take advantage of a property change at the glass transition temperature T_g: Below T_g, the movement of the polymer segments is frozen and the polymers are considered to be in a glassy

L. Homsi, L. Noels
University of Liège, Department of Aerospace and Mechanical Engineering, Computational & Multiscale Mechanics of Materials (CM3),
Quartier Polytech 1, Allée de la Découverte 9, B-4000 Liège, Belgium
Tel.: +32 4 366 48 26
Fax: +32 4 366 95 05
E-mail: {Lina.Homsi,L.Noels}@ulg.ac.be

state. Once they are heated above T_g the chains become weak and the polymers are considered to be in a rubbery state, such that the materials can be deformed with minimal force. However, SMP have the drawback of low strength and stiffness when they are used for structural applications. This drawback can be overcome by dispersing continuous or discontinuous reinforcements throughout a polymer matrix, leading to Shape Memory Polymer Composites (SMPC) [45, 14]. Besides improving the mechanical properties, the fillers can improve the shape memory recovery stress and, in addition, act as triggering mechanisms. For example, carbon fibers exhibit conductivity which can be exploited as a shape memory triggering mechanism since the increase of temperature required to trigger the Shape Memory effect of the matrix is obtained through Joule effect by applying an electric current. Henceforth SMPC are seeing a growing interest in the area of deployable structures, sensors, actuators etc

However, several difficulties arise when modeling the response of this kind of materials. On the one hand, multi-physics numerical models involving strong coupling are required. On the other hand, as SMP are capable of large deformations (high recovery strain) and as the field variations are important, the numerical methods ought to be formulated in a finite deformation and fields variation setting. As a result the governing equations involve strong non-linear coupling. Muliana *et al.* [47] have studied the time dependent response of active piezoelectric fiber and polymer composite materials in a multi-scale approach. Rothe *et al.* [55] have considered Electro-Thermo-Elasticity in a small strain setting, where they have focused on the numerical treatment of the monolithic approach, with the development of a one dimensional analytical solution in the purpose of code verification. In particular Zhupanska *et al.* [74] have discussed the governing equations describing electromagnetic, thermal, and mechanical field interactions. Nevertheless these contributions are still limited to small deformation settings.

In this work, a multi-field coupling resolution strategy is used for the resolution of electrical, energy, and momentum conservation equations by means of the Discontinuous Galerkin (DG) Finite Element Method (FEM) to solve Electro-Thermo-Mechanical (ETM) coupling. The main idea of the DG formalism is to approximate the solution by piece-wise continuous polynomial functions, and to constrain weakly the compatibility between elements. The inter-elements weak enforcement of the continuity allows using discontinuous polynomial spaces of high degree and facilitates handling elements of different types and dynamic mesh modifications. Indeed, the possibility of using irregular and non conforming meshes in an algorithm makes it suitable for time dependent transient problems. It also allows having hanging nodes and different polynomial degrees at the interface, with a view to hp-adaptivity. These DG opportunities and their merits have been illustrated and discussed by Kaufmann et al. [32]. In addition, since the DG method allows discontinuities of the physical unknowns within the interior of the problem domain, it is a natural approach to capture the jumps across the material interface in coupled problems. Above all, DG methods are also characterized by their flexibility in terms of mesh design while keeping their high order accuracy [28] and their high scalability in parallel simulations [50, 8] while optimal convergence rates are still achieved.

However, if not correctly formulated, discontinuous methods can exhibit instabilities, and the numerical results fail to approximate the exact solution. It is, therefore, important to develop a DG FEM which leads to reliable results for a wide

variety of problems. By using an adequate inter element flux definition combined to stabilization techniques, the shortcomings of non-stabilized DG methods can be overcome [49,52,54]. Since the seminal work of Reed *et al.* [53], DG methods have been developed to solve hyperbolic, parabolic, and elliptic problems [13]. Most of DG methods for elliptic and parabolic problems rely on the Interior Penalty (IP) method. The main principle of IP, as introduced in [15,69], is to constrain weakly the compatibility through the use of compatibility and/or stabilization terms, instead of building it into the finite element, which enables the use of discontinuous polynomial spaces of high degree. The interest in the symmetric interior penalty (SIPG) methods, in which the compatibility terms symmetrizes the formulation and which will be considered in this work, has been renewed by Wheeler [69] due to demands for optimality in the convergence rates with the mesh size h_s, *i.e.* the rates of the convergence is k in the H^1-norm and $k+1$ in the L^2-norm, where k is the polynomial approximation degree. However there exist different possible choices of traces and numerical fluxes as discussed by Arnold *et al.* [5], who have provided an analysis of a large class of discontinuous methods for second order elliptic problems with different numerical fluxes, and demonstrated that correctly formulated IP, NIPG (Non-Symmetric Interior Penalty), LDG (Local discontinuous Galerkin), and other DG methods are consistent and stables methods. In particular Arnold *et al.* [5] have proposed a framework for dealing with linear elliptic problems by means of DG methods and demonstrated that DG methods which are completely consistent and stable achieve optimal error estimates, and that the inconsistent DG methods like the pure penalty methods can still achieve optimal error estimates provided they are super-penalized. Besides, Georgoulis [19] has derived anisotropic *hp*-error bounds for linear second order elliptic diffusion convection reaction using Discontinuous Galerkin finite element methods (SIPG and NIPG), on shape-regular and anisotropic elements, and for isotropic and anisotropic polynomial degrees for the element bases. He has also observed optimal order of convergence in the L^2-norm for the SIPG formulation when a uniform mesh size refinement for different values of k is employed. Moreover, he has shown that the solution of the adjoint problem suffers from sub-optimal rates of convergence when a NIPG formulation is used. Yadav *et al.* [71] have extended the DG methods from a linear self-adjoint elliptic problem to a second order non-linear elliptic problem. The non-linear system resulting from DG methods is then analyzed based on a fixed point argument. They have also shown that the error estimate in the L^2-norm for piece-wise polynomials of degree $k \geq 1$ is $k+1$. They have also provided numerical results to illustrate the theoretical results. Gudi *et al.* [23] have proposed an analysis for the most popular DG schemes such as SIPG, NIPG, and LDG methods for one dimension linear and non-linear elliptic problems, and the error estimate has been studied for each of these methods by reformulating the problems in a fixed point form. In addition, according to Gudi *et al.* [22], optimal errors in the H^1-norm and in L^2-norm are proved for SIPG for polynomial degrees larger or equal to 2, and a loss in the optimality in the L^2-norm is observed for NIPG and LDG. In that work a deterioration in the order of convergence in the mesh size h_s is noted when linear polynomials are used.

DG FEM have been widely developed to solve mechanical problems such as non-linear solid mechanics [49,62,61], (nearly) incompressible elasticity [25,39], strain-gradient elasticity [16], strain gradient plasticity [43] strain gradient damage models [67], plate equations [24,16,6,66], shell equations [48], as a non-exhaustive

list. Truster *et al.* [63,64] have derived a Variational Multiscale Discontinuous Galerkin (VMDG) method to account for geometric and material non-linearities in which computable expressions emerge during the course of the derivation for the stability tensor and numerical flux weighting tensors. Recently, DG has been used to solve coupled problems. For instance Wheeler and Sun [60] have proposed a primal DG method with interior penalty (IP) terms to solve coupled reactive transport in porous media. Liu *et al.* [40] have developed an incomplete IP method for convection-dominated thermo-poro-mechanics. Furthermore, Zheng et al. [73] have proposed a DG method to solve thermo-elastic coupling due to temperature and pressure dependent thermal contact resistance. In that work the DG method is used to simulate the temperature jump, and the mechanical sub-problem is solved by the DG finite element method with a penalty function. In [27], a coupled non-linear Electro-Thermal DG method, has been derived by the authors in terms of energetically conjugated fields gradients and fluxes. This conjugated pair has been obtained by a particular choice of the test functions ($\delta f_T = \delta(\frac{1}{T})$, $\delta f_V = \delta(\frac{V}{T})$) and of the trial functions ($f_T = \frac{1}{T}$, $f_V = \frac{-V}{T}$), where T is the temperature and V is the electrical potential [42,72,38], which has allowed developing a stable non-linear DG formulation with optimal convergence rate.

The main aim of this work is to derive a consistent and stable DG FEM for ETM coupling analyzes, which, to the authors knowledge, has not been introduced yet. To this end, the constitutive equations governing the ETM coupling are formulated in Section 2 as a function of the displacement $\boldsymbol{u}$, the electric potential V and the temperature T, under the form $f(\boldsymbol{u}, \frac{-V}{T}, \frac{1}{T})$. In Section 3, the DG method is first formulated in finite deformations and finite fields variations, resulting into a set of non-linear coupled equations, and then implemented within a three-dimensional finite element code. In particular, the parallel feature of the finite element method relies on the ghost elements method developed for DG formulation [8,70]. Afterwards, the uniqueness and optimal numerical properties are derived for Electro-Thermo-Elasticity stated in a small deformation setting in Section 4. In particular, the convergence rates of the error in both the energy and L^2-norms are shown to be optimal with respect to the mesh size h_s in terms of the polynomial degree approximation k (respectively in order k and $k+1$). This section concludes with a numerical test supporting the developed theory, including the scalability property of the implementation. Finally the methodology is applied to study the Electro-Thermo-Mechanical behavior of SMPC in Section 5, in which a simple transversely isotropic hyperelastic formulation is used to model carbon fibers and an elasto-viscoplastic large deformation formulation is considered to model the SMP. In particular, the shape memory effect of SMPC unit cells electrically activated is studied in the large deformation regime.

2 Strong formulation of the Electro-Thermo-Mechanical problem

In this section an overview of the basic equations that govern Electro-Thermo-Mechanical coupled phenomena is presented. The body in its reference configuration $\Omega_0 \in \mathrm{R}^d$, where d is the spatial dimension, whose Dirichlet boundary $\partial_\mathrm{D}\Omega_0$ and Neumann boundary $\partial_\mathrm{N}\Omega_0$ are the outer boundaries $\partial\Omega_0$ of the domain, is

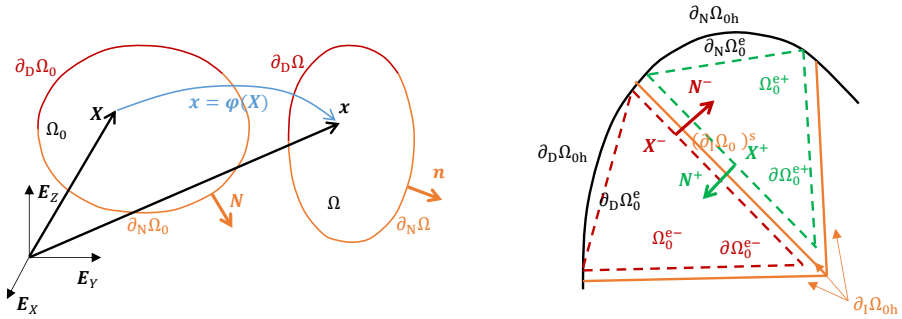

(a) Reference and current configurations (b) Body discretization

Fig. 1 Definition of (a) the reference and current configurations of the body, (b) the body discretization.

subjected to a deformation mapping $\boldsymbol{x} = \boldsymbol{\varphi}(\boldsymbol{X})$ defining the current configuration $\Omega \in \mathrm{R}^d$, see Fig. 1(a). The deformation gradient tensor is defined as

$$\boldsymbol{F} = \frac{\partial \boldsymbol{x}}{\partial \boldsymbol{X}} = \boldsymbol{x} \otimes \nabla_0 \text{ with } J = \det(\boldsymbol{F}), \tag{1}$$

its Jacobian, and where $\nabla_0 = \frac{\partial}{\partial \boldsymbol{X}}$ is the gradient with respect to the reference configuration. The displacement field reads $\boldsymbol{u} = \boldsymbol{x} - \boldsymbol{X}$. Finally, the material properties may in general depend on the position $\boldsymbol{X}$.

2.1 Balance equations

The first balance equation is the equation of motion which is the balance of linear momentum in the absence of (inertial and external) body forces with respect to the reference frame

$$\nabla_0 \cdot \boldsymbol{P}^{\mathrm{T}} = 0 \; \forall \boldsymbol{X} \in \Omega_0, \tag{2}$$

where $\boldsymbol{P}$ is the first Piola-Kirchhoff tensor, which is expressed in terms of the Cauchy stress as

$$\boldsymbol{P} = \boldsymbol{\sigma} \cdot \boldsymbol{F}^{-\mathrm{T}} J. \tag{3}$$

The second balance equation is the electrical contribution which is the conservation of the electric current density flow. Defining the flow of electric current density with respect to the reference surface

$$\boldsymbol{J}_{\mathrm{e}} = \boldsymbol{j}_{\mathrm{e}} \cdot \boldsymbol{F}^{-\mathrm{T}} J, \tag{4}$$

where $\boldsymbol{j}_{\mathrm{e}}$ is the flow of electric current density with respect to the current surface, the second balance equation reads

$$\nabla_0 \cdot \boldsymbol{J}_{\mathrm{e}} = 0 \; \forall \boldsymbol{X} \in \Omega_0. \tag{5}$$

The third balance equation is the conservation of the energy flux. The energy flux with respect to the reference surface reads

$$\boldsymbol{J}_{\mathrm{y}} = \boldsymbol{Q} + V \boldsymbol{J}_{\mathrm{e}} = \boldsymbol{j}_{\mathrm{y}} \cdot \boldsymbol{F}^{-\mathrm{T}} J = (\boldsymbol{q} + V \boldsymbol{j}_{\mathrm{e}}) \cdot \boldsymbol{F}^{-\mathrm{T}} J, \tag{6}$$

where $\boldsymbol{Q}$ and $\boldsymbol{q}$ are respectively the heat flux per unit surface in the reference and current configurations, V is the electrical potential, and where $\boldsymbol{j}_{\mathrm{y}}$ is the energy flux with respect to the current surface. Then the conservation of energy flux is stated as

$$\nabla_0 \cdot \boldsymbol{J}_{\mathrm{y}} = -\rho_0 \dot{y} + \bar{F} \; \forall \boldsymbol{X} \in \Omega_0 \,, \tag{7}$$

where y is the internal energy per unit mass and $\bar{F}$ represents all the body energy sources per unit reference volume.

2.2 Constitutive models

The first Piola-Kirchhoff stress tensor is evaluated under the generic form

$$\boldsymbol{P} = \mathbb{P}(\boldsymbol{F},\, \dot{\boldsymbol{F}},\, V,\, T;\, \boldsymbol{\xi}(\tau < \mathrm{t})) \,, \tag{8}$$

where T is the temperature, and $\boldsymbol{\xi}(\tau < t)$ is the set of internal variables evaluated at time τ lower than the current time t. In the applications, we will consider thermo-mechanical transverse isotropic and SMP thermo-mechanical constitutive behaviors, see A.

In this work, we consider the thermo-electric coupling written in the current configuration under the matrix form

$$\mathbf{j} = \begin{pmatrix} \boldsymbol{j}_{\mathrm{e}} \\ \boldsymbol{j}_{\mathrm{y}} \end{pmatrix} = \begin{pmatrix} \boldsymbol{l} & \alpha \boldsymbol{l} \\ V\boldsymbol{l} + \alpha T \boldsymbol{l} & \boldsymbol{k} + \alpha V \boldsymbol{l} + \alpha^2 T \boldsymbol{l} \end{pmatrix} \begin{pmatrix} -\nabla V \\ -\nabla T \end{pmatrix} , \tag{9}$$

where $\boldsymbol{k}$ denotes the symmetric tensor of thermal conductivity coefficients, $\boldsymbol{l}$ denotes the symmetric tensor of electric conductivity coefficients, and α is the Seebeck coefficient. The coefficients can be temperature and electric potential dependent. Moreover $\nabla = \frac{\partial}{\partial \boldsymbol{x}}$ is the gradient with respect to the current configuration. Using Eqs. (4) and (6), this last set of equations is rewritten

$$\mathbf{J} = \begin{pmatrix} \boldsymbol{J}_{\mathrm{e}} \\ \boldsymbol{J}_{\mathrm{y}} \end{pmatrix} = \begin{pmatrix} \boldsymbol{L} & \alpha \boldsymbol{L} \\ V\boldsymbol{L} + \alpha T \boldsymbol{L} & \boldsymbol{K} + \alpha V \boldsymbol{L} + \alpha^2 T \boldsymbol{L} \end{pmatrix} \begin{pmatrix} -\nabla_0 V \\ -\nabla_0 T \end{pmatrix} , \tag{10}$$

where

$$\begin{aligned} \boldsymbol{K}(\boldsymbol{F},\, T,\, V) &= \boldsymbol{F}^{-1} \cdot \boldsymbol{k}(T,\, V) \cdot \boldsymbol{F}^{-\mathrm{T}} J \;\; \text{and} \\ \boldsymbol{L}(\boldsymbol{F},\, T,\, V) &= \boldsymbol{F}^{-1} \cdot \boldsymbol{l}(T,\, V) \cdot \boldsymbol{F}^{-\mathrm{T}} J \,, \end{aligned} \tag{11}$$

are the coefficient tensors expressed in the reference configuration.

However, in the relation (9), the vectors $\mathbf{J}$ and $(\nabla_0 V^{\mathrm{T}}\ \nabla_0 T^{\mathrm{T}})^{\mathrm{T}}$ are not energetically conjugated, see the discussions in [42,72,38,27]. Therefore we define the fields $\mathbf{M} = (f_{\mathrm{V}}\ f_{\mathrm{T}})^{\mathrm{T}}$ with $f_{\mathrm{V}} = -\frac{V}{T}$ and $f_{\mathrm{T}} = \frac{1}{T}$, and the gradients of the fields vector in the reference frame are defined by $\nabla_0 \mathbf{M}$, a $2d \times 1$ vector in terms of

$$\nabla_0 \mathbf{M} = \begin{pmatrix} \nabla_0 f_{\mathrm{V}} \\ \nabla_0 f_{\mathrm{T}} \end{pmatrix} = \begin{pmatrix} -\frac{1}{T}\boldsymbol{I} & \frac{V}{T^2}\boldsymbol{I} \\ 0 & -\frac{1}{T^2}\boldsymbol{I} \end{pmatrix} \begin{pmatrix} \nabla_0 V \\ \nabla_0 T \end{pmatrix} . \tag{12}$$

As a result the set of Eqs. (10) is rewritten as

$$\mathbf{J} = \mathbf{Z}_0(\boldsymbol{F},\, f_{\mathrm{V}},\, f_{\mathrm{T}})\, \nabla_0 \mathbf{M} \,, \tag{13}$$

with the coefficient matrix expressed in the reference configuration

$$\mathbf{Z}_0(\boldsymbol{F},\, f_{\mathrm{V}},\, f_{\mathrm{T}}) = \begin{pmatrix} \boldsymbol{L}_1(\boldsymbol{F},\, f_{\mathrm{T}}) & \boldsymbol{L}_2(\boldsymbol{F},\, f_{\mathrm{T}},\, f_{\mathrm{T}}) \\ \boldsymbol{L}_2(\boldsymbol{F},\, f_{\mathrm{T}},\, f_{\mathrm{T}}) & \boldsymbol{J}_{\mathrm{y}1}(\boldsymbol{F},\, f_{\mathrm{V}},\, f_{\mathrm{T}}) \end{pmatrix}, \tag{14}$$

where

$$\begin{aligned} \boldsymbol{L}_1(\boldsymbol{F},\, f_{\mathrm{T}}) &= \frac{1}{f_{\mathrm{T}}}\boldsymbol{L}\,;\;\; \boldsymbol{L}_2(\boldsymbol{F},\, f_{\mathrm{T}},\, f_{\mathrm{T}}) = -\frac{f_{\mathrm{V}}}{f_{\mathrm{T}}^2}\boldsymbol{L} + \alpha\frac{1}{f_{\mathrm{T}}^2}\boldsymbol{L}\,;\ \text{and} \\ \boldsymbol{J}_{\mathrm{y}1}(\boldsymbol{F},\, f_{\mathrm{V}},\, f_{\mathrm{T}}) &= \frac{1}{f_{\mathrm{T}}^2}\boldsymbol{K} - 2\alpha\frac{f_{\mathrm{V}}}{f_{\mathrm{T}}^3}\boldsymbol{L} + \alpha^2\frac{1}{f_{\mathrm{T}}^3}\boldsymbol{L} + \frac{f_{\mathrm{V}}^2}{f_{\mathrm{T}}^3}\boldsymbol{L}\,. \end{aligned} \tag{15}$$

From Eq. (13), it can be seen that the symmetric coefficients matrix $\mathbf{Z}_0$ is positive definite since $\boldsymbol{L}_1$ and $\boldsymbol{J}_{\mathrm{y}1} - \boldsymbol{L}_2^{\mathrm{T}} \cdot \boldsymbol{L}_1^{-1} \cdot \boldsymbol{L}_2 = \frac{1}{f_{\mathrm{T}}^2}\boldsymbol{K}$ are positive definite for $T > 0$.

2.3 Boundary conditions

The body boundary $\partial\Omega_0$, see Fig. 1(a), is divided into a Neumann part $\partial_{\mathrm{N}}\Omega_0$ on which the surface traction $\boldsymbol{P}\cdot\boldsymbol{N}$, the electric current density $\boldsymbol{J}_{\mathrm{e}}\cdot\boldsymbol{N}$, and the energy density $\boldsymbol{J}_{\mathrm{y}}\cdot\boldsymbol{N}$ per unit reference surface, are respectively constrained to $\bar{\boldsymbol{T}}$, $\bar{J}_{\mathrm{e}}$, and $\bar{J}_{\mathrm{y}}$, and into a Dirichlet part $\partial_{\mathrm{N}}\Omega_0$, on which the displacement field $\boldsymbol{u}$, the f_{V}-field, and the f_{T}-field are respectively constrained to $\bar{\boldsymbol{u}}$, $\bar{f}_{\mathrm{V}}$, and $\bar{f}_{\mathrm{T}}$. In these relations, $\boldsymbol{N}$ is the outward unit normal in the reference configuration.

Note that to simplify the notations of the equations we have assumed that the Neumann and Dirichlet parts coincide for the three fields, but in all generalities the developed methodology remains applicable if they are different.

2.4 Strong form summary

The set of governing equations (2, 5, and 7) is thus stated as finding $\boldsymbol{u}, \mathbf{M} \in \left[\mathrm{H}^2(\Omega_0)\right]^d \times \mathrm{H}^2(\Omega_0) \times \mathrm{H}^{2^+}(\Omega_0)$ such that

$$\begin{cases} \nabla_0 \cdot \boldsymbol{P}^{\mathrm{T}} = 0 & \forall \boldsymbol{X} \in \Omega_0\,, \\ \nabla_0^{\mathrm{T}}\,(\mathbf{J}) = \mathbf{I}_{\mathrm{i}} & \forall \boldsymbol{X} \in \Omega_0\,, \end{cases} \tag{16}$$

where ∇_0 is also used to represent a vector operator in the reference configuration, $\mathbf{I}_{\mathrm{i}} = \begin{pmatrix} 0 & -\rho_0\dot{y} + \bar{F} \end{pmatrix}^{\mathrm{T}}$ represents the contributions of the internal energy rate and the body energy sources, and where the notation $\mathrm{H}^{2^+}(\Omega_0)$ is used to consider only positive values in the Hilbert space H^2.

This set of governing equations is completed by the Neumann boundary conditions

$$\begin{cases} \boldsymbol{P}\cdot\boldsymbol{N} = \bar{\boldsymbol{T}} & \forall \boldsymbol{X} \in \partial_{\mathrm{N}}\Omega_0\,, \\ \mathbf{J}_{\boldsymbol{N}} = \begin{pmatrix} \boldsymbol{N} & \mathbf{0} \\ \mathbf{0} & \boldsymbol{N} \end{pmatrix}^{\mathrm{T}} \mathbf{J} = \bar{\mathbf{J}} & \forall \boldsymbol{X} \in \partial_{\mathrm{N}}\Omega_0\,, \end{cases} \tag{17}$$

where $\bar{\mathbf{J}} = (\bar{J}_\mathrm{e}\ \bar{J}_\mathrm{y})^\mathrm{T}$ and $\mathbf{J}_{\boldsymbol{N}}$ is the flux per unit reference surface, and by the Dirichlet boundary conditions

$$\begin{cases} \boldsymbol{u} = \bar{\boldsymbol{u}} & \forall \boldsymbol{X} \in \partial_\mathrm{D}\Omega_0\,, \\ \mathbf{M} = \bar{\mathbf{M}} & \forall \boldsymbol{X} \in \partial_\mathrm{D}\Omega_0\,, \end{cases} \tag{18}$$

where $\bar{\mathbf{M}} = (\bar{f}_\mathrm{V}\ \bar{f}_\mathrm{T})^\mathrm{T}$.

Finally, the constitutive Eqs. (13, 8) read

$$\begin{cases} \boldsymbol{P} = \mathbb{P}(\boldsymbol{F},\, \dot{\boldsymbol{F}},\, \mathbf{M};\, \boldsymbol{\xi}(\tau < \mathrm{t}))\,, \\ \mathbf{J} = \mathbf{Z}_0(\boldsymbol{F}\,, \mathbf{M})\, \nabla_0 \mathbf{M}\,. \end{cases} \tag{19}$$

3 Weak Discontinuous Galerkin formulation

In this section we first derive the weak DG formulation of the problem stated under the strong form (16-19). Then we introduce a finite-element discretization of the test and trial functions, before briefly summarizing the resolution process.

3.1 Weak DG form derivation

Let $\Omega_{0\mathrm{h}}$ be a shape regular family of discretization of Ω_0, such that $\Omega_{0\mathrm{h}} = \cup_\mathrm{e}\Omega_0^\mathrm{e}$, see Fig. 1(b), with $h_\mathrm{s} = \max_{\Omega_0^\mathrm{e}\in\Omega_{0\mathrm{h}}} \mathrm{diam}(\Omega_0^\mathrm{e})$ for $\Omega_0^\mathrm{e} \in \Omega_{0\mathrm{h}}$ with $\partial\Omega_0^\mathrm{e} = \partial_\mathrm{N}\Omega_0^\mathrm{e} \cup \partial_\mathrm{D}\Omega_0^\mathrm{e} \cup \partial_\mathrm{I}\Omega_0^\mathrm{e}$, and where $\partial_\mathrm{I}\Omega_{0\mathrm{h}} = \cup_\mathrm{e}\partial_\mathrm{I}\Omega_0^\mathrm{e} \setminus \partial\Omega_{0\mathrm{h}}$, is the intersecting boundary of the finite elements. Finally $(\partial_{\mathrm{DI}}\Omega_0)^\mathrm{s}$ is a face either on $\partial_\mathrm{I}\Omega_{0\mathrm{h}}$ or on $\partial_\mathrm{D}\Omega_{0\mathrm{h}}$, with $\sum_\mathrm{s}(\partial_{\mathrm{DI}}\Omega_0)^\mathrm{s} = \partial_\mathrm{I}\Omega_{0\mathrm{h}} \cup \partial_\mathrm{D}\Omega_{0\mathrm{h}}$.

Since, at the interface between two elements, Fig. 1(b), each interior edge $(\partial_\mathrm{I}\Omega_0)^\mathrm{s}$ is shared by two elements $^-$ and $^+$, where $(\partial_\mathrm{I}\Omega_0)^\mathrm{s} \subset \partial_\mathrm{I}\Omega_0^{\mathrm{e}^-}$ and $(\partial_\mathrm{I}\Omega_0)^\mathrm{s} \subset \partial_\mathrm{I}\Omega_0^{\mathrm{e}^+}$, we can define two useful operators, the jump operator $[\![\cdot]\!] = \left[\cdot^+ - \cdot^-\right]$ that computes the discontinuity between the elements and the average operator $\langle\cdot\rangle = \frac{1}{2}\left(\cdot^+ + \cdot^-\right)$ which is the mean between two element values. Those two operators can be extended on the Dirichlet boundary $\partial_\mathrm{D}\Omega_{0\mathrm{h}}$ as $\langle\cdot\rangle = \cdot$, $[\![\cdot]\!] = (-\cdot)$.

The discontinuous Galerkin method results from the integration by parts on the elements of the governing equations multiplied by discontinuous test functions. Let us multiply the governing equations (16) by discontinuous test functions $\delta\boldsymbol{u}$ and $\delta\mathbf{M}$, and integrate on $\Omega_{0\mathrm{h}}$, yielding

$$0 = \sum_\mathrm{e} \int_{\Omega_0^\mathrm{e}} (\boldsymbol{P}(\boldsymbol{F},\, \mathbf{M}) \cdot \nabla_0) \cdot \delta\boldsymbol{u}\mathrm{d}\Omega_0 \qquad \forall \delta\boldsymbol{u} \in \mathit{\Pi}_\mathrm{e}\left[\mathrm{H}^1(\Omega_0^\mathrm{e})\right]^d\,; \tag{20}$$

$$\sum_\mathrm{e} \int_{\Omega_0^\mathrm{e}} \mathbf{I}_\mathrm{i}^\mathrm{T} \delta\mathbf{M}\mathrm{d}\Omega_0 = \sum_\mathrm{e} \int_{\Omega_0^\mathrm{e}} \left(\nabla_0^\mathrm{T}\mathbf{J}(\boldsymbol{F}\,, \mathbf{M}\,, \nabla_0\mathbf{M})\right)^\mathrm{T} \delta\mathbf{M}\mathrm{d}\Omega_0$$
$$\forall \delta\mathbf{M} \in \mathit{\Pi}_\mathrm{e}\mathrm{H}^1(\Omega_0^\mathrm{e}) \times \mathit{\Pi}_\mathrm{e}\mathrm{H}^1(\Omega_0^\mathrm{e})\,. \tag{21}$$

By performing an integration by parts on each element, and by using the divergence theorem, these equations become

$$\int_{\partial_{\mathrm{N}}\Omega_{0\mathrm{h}}} \delta\boldsymbol{u}\cdot\bar{\boldsymbol{T}}\mathrm{d}\mathrm{S}_0 = \int_{\Omega_{0\mathrm{h}}} \boldsymbol{P}(\boldsymbol{F},\mathbf{M}) : \nabla_0\delta\boldsymbol{u}\mathrm{d}\Omega_0 + \int_{\partial_{\mathrm{I}}\Omega_{0\mathrm{h}}} [\![\delta\boldsymbol{u}\cdot\boldsymbol{P}(\boldsymbol{F},\mathbf{M})]\!]\cdot\mathbf{N}^-\mathrm{d}\mathrm{S}_0 - \int_{\partial_{\mathrm{D}}\Omega_{0\mathrm{h}}} \delta\boldsymbol{u}\cdot\boldsymbol{P}(\boldsymbol{F},\mathbf{M})\cdot\boldsymbol{N}\mathrm{d}\mathrm{S}_0 \quad \forall\delta\boldsymbol{u}\in\left[\mathrm{H}^1(\Omega_0^{\mathrm{e}})\right]^d \text{;(22)}$$

$$-\int_{\Omega_{0\mathrm{h}}} \mathbf{I}_{\mathrm{i}}^{\mathrm{T}}\delta\mathbf{M}\mathrm{d}\Omega_0 + \int_{\partial_{\mathrm{N}}\Omega_{0\mathrm{h}}} \delta\mathbf{M}^{\mathrm{T}}\bar{\mathbf{J}}\mathrm{d}\mathrm{S}_0 = \int_{\Omega_{0\mathrm{h}}} (\nabla_0\delta\mathbf{M})^{\mathrm{T}}\,\mathbf{J}(\boldsymbol{F}\,,\mathbf{M}\,,\nabla_0\mathbf{M})\mathrm{d}\Omega_0 + \int_{\partial_{\mathrm{I}}\Omega_{0\mathrm{h}}} \left[\!\!\left[\delta\mathbf{M}_{\mathbf{N}}^{\mathrm{T}}\mathbf{J}(\boldsymbol{F}\,,\mathbf{M}\,,\nabla_0\mathbf{M})\right]\!\!\right]\mathrm{d}\mathrm{S}_0 - \int_{\partial_{\mathrm{D}}\Omega_{0\mathrm{h}}} \delta\mathbf{M}_{\mathbf{N}}^{\mathrm{T}}\mathbf{J}(\boldsymbol{F}\,,\mathbf{M}\,,\nabla_0\mathbf{M})\mathrm{d}\mathrm{S}_0 \quad \forall\delta\mathbf{M}\in\mathit{\Pi}_{\mathrm{e}}\mathrm{H}^1(\Omega_0^{\mathrm{e}})\times\mathit{\Pi}_{\mathrm{e}}\mathrm{H}^1(\Omega_0^{\mathrm{e}}) \text{;(23)}$$

where the vector $\mathbf{M}_{\mathbf{N}} = \begin{pmatrix} \boldsymbol{N}^{\text{-}} & \mathbf{0} \\ \mathbf{0} & \boldsymbol{N}^{\text{-}} \end{pmatrix}\mathbf{M}$ has been introduced for simplicity, where $\boldsymbol{N}^-$ is defined as the reference outward unit normal of the minus element $\Omega_0^{\mathrm{e}^-}$, whereas $\boldsymbol{N}^+$ is the reference outward unit normal of its neighboring element, with $\boldsymbol{N}^+ = -\boldsymbol{N}^-$, and where we have used the Neumann boundary conditions (17). However, when considering the jump operators, consistency is satisfied as long as the jump on the test function is accounted for, while the stress terms can be substituted by a numerical flux such as the average value. The set of Eqs. (22-23) thus becomes

$$\int_{\partial_{\mathrm{N}}\Omega_{0\mathrm{h}}} \delta\boldsymbol{u}\cdot\bar{\boldsymbol{T}}\mathrm{d}\mathrm{S}_0 = \int_{\Omega_{0\mathrm{h}}} \boldsymbol{P}(\boldsymbol{F},\mathbf{M}) : \nabla_0\delta\boldsymbol{u}\mathrm{d}\Omega_0 + \int_{\partial_{\mathrm{I}}\Omega_{0\mathrm{h}}\cup\partial_{\mathrm{D}}\Omega_{0\mathrm{h}}} [\![\delta\boldsymbol{u}]\!]\cdot\langle\boldsymbol{P}(\boldsymbol{F},\mathbf{M})\rangle\cdot\boldsymbol{N}^-\mathrm{d}\mathrm{S}_0 \quad \forall\delta\boldsymbol{u}\in\mathit{\Pi}_{\mathrm{e}}\left[\mathrm{H}^1(\Omega_0^{\mathrm{e}})\right]^d \text{;(24)}$$

$$-\int_{\Omega_{0\mathrm{h}}} \mathbf{I}_{\mathrm{i}}^{\mathrm{T}}\delta\mathbf{M}\mathrm{d}\Omega_0 + \int_{\partial_{\mathrm{N}}\Omega_{0\mathrm{h}}} \delta\mathbf{M}^{\mathrm{T}}\bar{\mathbf{J}}\mathrm{d}\mathrm{S}_0 = \int_{\Omega_{0\mathrm{h}}} (\nabla_0\delta\mathbf{M})^{\mathrm{T}}\,\mathbf{J}(\boldsymbol{F}\,,\mathbf{M}\,,\nabla_0\mathbf{M})\mathrm{d}\Omega_0 + \int_{\partial_{\mathrm{I}}\Omega_{0\mathrm{h}}\cup\partial_{\mathrm{D}}\Omega_{0\mathrm{h}}} \left[\!\!\left[\delta\mathbf{M}_{\mathbf{N}}^{\mathrm{T}}\right]\!\!\right]\langle\mathbf{J}(\boldsymbol{F}\,,\mathbf{M}\,,\nabla_0\mathbf{M})\rangle\,\mathrm{d}\mathrm{S}_0 \;\forall\delta\mathbf{M}\in\mathit{\Pi}_{\mathrm{e}}\mathrm{H}^1(\Omega_0^{\mathrm{e}})\times\mathit{\Pi}_{\mathrm{e}}\mathrm{H}^1(\Omega_0^{\mathrm{e}}) \text{;(25)}$$

where we have considered the definitions of the operators on the Dirichlet boundary.

In order to define the compatibility and stability terms, we define, on the one hand, the four-order tensor $\boldsymbol{\mathcal{H}} = \frac{\partial\boldsymbol{P}}{\partial\boldsymbol{F}}\,(\boldsymbol{F}=\boldsymbol{I},\,\mathbf{M}=\mathbf{M}_0)$ and, on the other hand, the second order tensor $\boldsymbol{\alpha}_{\mathrm{th}}$ such that $\boldsymbol{\alpha}_{\mathrm{th}} : \boldsymbol{\mathcal{H}} = -\frac{\partial\boldsymbol{P}}{\partial T}\,(\boldsymbol{F}=\boldsymbol{I},\,\mathbf{M}=\mathbf{M}_0)$, with $\mathbf{M}_0\in\mathit{\Pi}_{\mathrm{e}}\mathrm{H}^1(\Omega_0^{\mathrm{e}})\times\mathit{\Pi}_{\mathrm{e}}\mathrm{H}^{1^+}(\Omega_0^{\mathrm{e}})$ the initial values of $\mathbf{M}$. As a result both $\boldsymbol{\mathcal{H}}$ and $\boldsymbol{\alpha}_{\mathrm{th}} : \boldsymbol{\mathcal{H}}$ are constant during the simulation as it has been shown that this leads to accurate results in elasto-plasticity [50]. However, evolving terms could also be considered as discussed in [63,64]. Moreover, we define the $d\times d\times 2$ matrix $\boldsymbol{\mathcal{Y}}(\mathbf{M}) = \frac{\partial\boldsymbol{P}}{\partial\mathbf{M}}$. Assuming the stress tensor depends only on f_{T} and not on f_{V}, we have $\boldsymbol{\mathcal{Y}}(\mathbf{M})\delta\mathbf{M} = \boldsymbol{\alpha}_{\mathrm{th}} : \boldsymbol{\mathcal{H}}\dfrac{1}{f_{\mathrm{T}}^2}\delta f_{\mathrm{T}}$, with $\boldsymbol{\mathcal{Y}}_0 = \boldsymbol{\mathcal{Y}}(\mathbf{M}_0)$.

The compatibility of the displacement fields on the element interfaces and on the Dirichlet boundary is thus added to the weak form (24-25), leading to

$$\begin{aligned}
&\int_{\partial_{\mathrm{N}}\Omega_{0\mathrm{h}}} \delta\boldsymbol{u}\cdot\bar{\boldsymbol{T}}\mathrm{d}\mathrm{S}_0 - \int_{\partial_{\mathrm{D}}\Omega_{0\mathrm{h}}} \bar{\boldsymbol{u}}\cdot(\boldsymbol{\mathcal{H}}:\nabla_0\delta\boldsymbol{u})\cdot\boldsymbol{N}\mathrm{d}\mathrm{S}_0 - \\
&\int_{\partial_{\mathrm{D}}\Omega_{0\mathrm{h}}} \delta\boldsymbol{u}\cdot\left(\boldsymbol{\mathcal{Y}}(\bar{\mathbf{M}})\bar{\mathbf{M}} - \boldsymbol{\mathcal{Y}}(\bar{\mathbf{M}}_0)\bar{\mathbf{M}}_0\right)\cdot\boldsymbol{N}\mathrm{d}\mathrm{S}_0 = \\
&\int_{\Omega_{0\mathrm{h}}} \boldsymbol{P}(\boldsymbol{F},\mathbf{M}):\nabla_0\delta\boldsymbol{u}\mathrm{d}\Omega_0 + \int_{\partial_{\mathrm{I}}\Omega_{0\mathrm{h}}\cup\partial_{\mathrm{D}}\Omega_{0\mathrm{h}}} [\![\delta\boldsymbol{u}]\!]\cdot\langle\boldsymbol{P}(\boldsymbol{F},\mathbf{M})\rangle\cdot\boldsymbol{N}^-\mathrm{d}\mathrm{S}_0 + \\
&\int_{\partial_{\mathrm{I}}\Omega_{0\mathrm{h}}\cup\partial_{\mathrm{D}}\Omega_{0\mathrm{h}}} [\![\boldsymbol{u}]\!]\cdot\langle\boldsymbol{\mathcal{H}}:\nabla_0\delta\boldsymbol{u}\rangle\cdot\boldsymbol{N}^-\mathrm{d}\mathrm{S}_0 + \\
&\int_{\partial_{\mathrm{D}}\Omega_{0\mathrm{h}}} [\![\delta\boldsymbol{u}]\!]\cdot\langle\boldsymbol{\mathcal{Y}}(\mathbf{M})\mathbf{M} - \boldsymbol{\mathcal{Y}}(\mathbf{M}_0)\mathbf{M}_0\rangle\cdot\boldsymbol{N}^-\mathrm{d}\mathrm{S}_0 \quad \forall\delta\boldsymbol{u}\in\mathit{\Pi}_{\mathrm{e}}\left[\mathrm{H}^1(\Omega_0^{\mathrm{e}})\right]^d \quad (26)\\
&-\int_{\Omega_{0\mathrm{h}}} \mathbf{I}_{\mathrm{i}}^{\mathrm{T}}\delta\mathbf{M}\mathrm{d}\Omega_0 + \int_{\partial_{\mathrm{N}}\Omega_{0\mathrm{h}}} \delta\mathbf{M}^{\mathrm{T}}\bar{\mathbf{J}}\mathrm{d}\mathrm{S}_0 - \int_{\partial_{\mathrm{D}}\Omega_{0\mathrm{h}}} \bar{\mathbf{M}}_{\mathbf{N}}^{\mathrm{T}}\left(\mathbf{Z}_0(\boldsymbol{F},\bar{\mathbf{M}})\nabla_0\delta\mathbf{M}\right)\mathrm{d}\mathrm{S}_0 = \\
&\int_{\Omega_{0\mathrm{h}}} (\nabla_0\delta\mathbf{M})^{\mathrm{T}}\,\mathbf{J}(\boldsymbol{F},\mathbf{M},\nabla_0\mathbf{M})\mathrm{d}\Omega_0 + \int_{\partial_{\mathrm{I}}\Omega_{0\mathrm{h}}\cup\partial_{\mathrm{D}}\Omega_{0\mathrm{h}}} \left[\!\left[\delta\mathbf{M}_{\mathbf{N}}^{\mathrm{T}}\right]\!\right]\langle\mathbf{J}(\boldsymbol{F},\mathbf{M},\nabla_0\mathbf{M})\rangle\,\mathrm{d}\mathrm{S}_0 \\
&+\int_{\partial_{\mathrm{I}}\Omega_{0\mathrm{h}}} \left[\!\left[\mathbf{M}_{\mathbf{N}}^{\mathrm{T}}\right]\!\right]\langle\mathbf{Z}_0(\mathbf{F},\mathbf{M})\nabla_0\delta\mathbf{M}\rangle\,\mathrm{d}\mathrm{S}_0 + \int_{\partial_{\mathrm{D}}\Omega_{0\mathrm{h}}} \left[\!\left[\mathbf{M}_{\mathbf{N}}^{\mathrm{T}}\right]\!\right]\langle\mathbf{Z}_0(\mathbf{F},\bar{\mathbf{M}})\nabla_0\delta\mathbf{M}\rangle\,\mathrm{d}\mathrm{S}_0 \\
&\forall\delta\mathbf{M}\in\mathit{\Pi}_{\mathrm{e}}\mathrm{H}^1(\Omega_0^{\mathrm{e}})\times\mathit{\Pi}_{\mathrm{e}}\mathrm{H}^1(\Omega_0^{\mathrm{e}}) \quad (27)
\end{aligned}$$

Some remarks arise from this formulation

- In the compatibility terms, the operator $\boldsymbol{\mathcal{H}}$ has been considered as constant but not the operator $\mathbf{Z}_0$. As a result, the optimality of the convergence rate will only be demonstrated when linearizing the mechanical equations, and when stating the equations in a small deformation setting. This is due to the complexity of the mechanical behavior (19a) which is history-dependent, preventing to write a non-linear equation under a form similar to the considered electro-thermal coupling (19b).
- The last term of Eq. (26) appears from the fact that the term in $[\![\delta\boldsymbol{u}]\!]\cdot\langle\boldsymbol{P}(\boldsymbol{F},\mathbf{M})\rangle\cdot\boldsymbol{N}^-\mathrm{d}\mathrm{S}_0$ acting on the Dirichlet boundary condition prevents a symmetric operator to be obtained and as such would prevent the optimal convergence rate in the L^2-norm to be achieved, as it will be shown in Section 4.

What remains to be done is to stabilize the method through quadratic terms weighted by a stabilization parameter $\mathcal{B}$ and the mesh size h_{s}, leading to state the

problem as finding $\boldsymbol{u}$, $\mathbf{M} \in \left[\mathit{\Pi}_{\mathrm{e}}\mathrm{H}^1(\Omega_0^{\mathrm{e}})\right]^d \times \mathit{\Pi}_{\mathrm{e}}\mathrm{H}^1(\Omega_0^{\mathrm{e}}) \times \mathit{\Pi}_{\mathrm{e}}\mathrm{H}^{1^+}(\Omega_0^{\mathrm{e}})$ such that

$$\int_{\partial_{\mathrm{N}}\Omega_{0\mathrm{h}}} \delta\boldsymbol{u}\cdot\bar{\boldsymbol{T}}\mathrm{d}\mathrm{S}_0 - \int_{\partial_{\mathrm{D}}\Omega_{0\mathrm{h}}} \bar{\boldsymbol{u}}\cdot(\boldsymbol{\mathcal{H}}:\nabla_0\delta\boldsymbol{u})\cdot\boldsymbol{N}\mathrm{d}\mathrm{S}_0 +$$
$$\int_{\partial_{\mathrm{D}}\Omega_{0\mathrm{h}}} \bar{\boldsymbol{u}}\otimes\boldsymbol{N} : \left(\frac{\boldsymbol{\mathcal{H}}\mathcal{B}}{h_{\mathrm{s}}}\right) : \delta\boldsymbol{u}\otimes\boldsymbol{N}\mathrm{d}\mathrm{S}_0 -$$
$$\int_{\partial_{\mathrm{D}}\Omega_{0\mathrm{h}}} \delta\boldsymbol{u}\cdot\left(\boldsymbol{\mathcal{Y}}(\bar{\mathbf{M}})\bar{\mathbf{M}} - \boldsymbol{\mathcal{Y}}(\bar{\mathbf{M}}_0)\bar{\mathbf{M}}_0\right)\cdot\boldsymbol{N}\mathrm{d}\mathrm{S}_0 = \int_{\Omega_{0\mathrm{h}}} \boldsymbol{P}(\boldsymbol{F},\mathbf{M}) : \nabla_0\delta\boldsymbol{u}\mathrm{d}\Omega_0 +$$
$$\int_{\partial_{\mathrm{I}}\Omega_{0\mathrm{h}}\cup\partial_{\mathrm{D}}\Omega_{0\mathrm{h}}} [\![\delta\boldsymbol{u}]\!]\cdot\langle\boldsymbol{P}(\boldsymbol{F},\mathbf{M})\rangle\cdot\boldsymbol{N}^-\mathrm{d}\mathrm{S}_0 +$$
$$\int_{\partial_{\mathrm{I}}\Omega_{0\mathrm{h}}\cup\partial_{\mathrm{D}}\Omega_{0\mathrm{h}}} [\![\boldsymbol{u}]\!]\otimes\boldsymbol{N} : \left\langle\frac{\boldsymbol{\mathcal{H}}\mathcal{B}}{h_{\mathrm{s}}}\right\rangle : [\![\delta\boldsymbol{u}]\!]\otimes\boldsymbol{N}\mathrm{d}\mathrm{S}_0 +$$
$$\int_{\partial_{\mathrm{I}}\Omega_{0\mathrm{h}}\cup\partial_{\mathrm{D}}\Omega_{0\mathrm{h}}} [\![\boldsymbol{u}]\!]\cdot\langle\boldsymbol{\mathcal{H}}:\nabla_0\delta\boldsymbol{u}\rangle\cdot\boldsymbol{N}^-\mathrm{d}\mathrm{S}_0 +$$
$$\int_{\partial_{\mathrm{D}}\Omega_{0\mathrm{h}}} [\![\delta\boldsymbol{u}]\!]\cdot\langle\boldsymbol{\mathcal{Y}}(\mathbf{M})\mathbf{M} - \boldsymbol{\mathcal{Y}}(\mathbf{M}_0)\mathbf{M}_0\rangle\cdot\boldsymbol{N}^-\mathrm{d}\mathrm{S}_0 \quad \forall\delta\boldsymbol{u}\in\mathit{\Pi}_{\mathrm{e}}\left[\mathrm{H}^1(\Omega_0^{\mathrm{e}})\right]^d ; \quad (28)$$
$$-\int_{\Omega_{0\mathrm{h}}} \mathbf{I}_{\mathrm{i}}^{\mathrm{T}}\delta\mathbf{M}\mathrm{d}\Omega_0 + \int_{\partial_{\mathrm{N}}\Omega_{0\mathrm{h}}} \delta\mathbf{M}^{\mathrm{T}}\bar{\mathbf{J}}\mathrm{d}\mathrm{S}_0 - \int_{\partial_{\mathrm{D}}\Omega_{0\mathrm{h}}} \bar{\mathbf{M}}_{\mathbf{N}}^{\mathrm{T}}\left(\mathbf{Z}_0(\boldsymbol{F},\bar{\mathbf{M}})\nabla_0\delta\mathbf{M}\right)\mathrm{d}\mathrm{S}_0 +$$
$$\int_{\partial_{\mathrm{D}}\Omega_{0\mathrm{h}}} \delta\mathbf{M}_{\mathbf{N}}^{\mathrm{T}}\left(\frac{\mathcal{B}}{h_{\mathrm{s}}}\mathbf{Z}_0(\boldsymbol{F},\bar{\mathbf{M}})\right)\bar{\mathbf{M}}_{\mathbf{N}}\mathrm{d}\mathrm{S}_0 = \int_{\Omega_{0\mathrm{h}}} (\nabla_0\delta\mathbf{M})^{\mathrm{T}}\,\mathbf{J}(\boldsymbol{F},\mathbf{M},\nabla_0\mathbf{M})\mathrm{d}\Omega_0 +$$
$$\int_{\partial_{\mathrm{I}}\Omega_{0\mathrm{h}}} \left[\!\left[\delta\mathbf{M}_{\mathbf{N}}^{\mathrm{T}}\right]\!\right]\left\langle\frac{\mathcal{B}}{h_{\mathrm{s}}}\mathbf{Z}_0(\mathbf{F},\mathbf{M})\right\rangle[\![\mathbf{M}_{\mathbf{N}}]\!]\,\mathrm{d}\mathrm{S}_0 +$$
$$\int_{\partial_{\mathrm{D}}\Omega_{0\mathrm{h}}} \left[\!\left[\delta\mathbf{M}_{\mathbf{N}}^{\mathrm{T}}\right]\!\right]\left\langle\frac{\mathcal{B}}{h_{\mathrm{s}}}\mathbf{Z}_0(\mathbf{F},\bar{\mathbf{M}})\right\rangle[\![\mathbf{M}_{\mathbf{N}}]\!]\,\mathrm{d}\mathrm{S}_0 +$$
$$\int_{\partial_{\mathrm{I}}\Omega_{0\mathrm{h}}\cup\partial_{\mathrm{D}}\Omega_{0\mathrm{h}}} \left[\!\left[\delta\mathbf{M}_{\mathbf{N}}^{\mathrm{T}}\right]\!\right]\langle\mathbf{J}(\boldsymbol{F},\mathbf{M},\nabla_0\mathbf{M})\rangle\,\mathrm{d}\mathrm{S}_0 +$$
$$\int_{\partial_{\mathrm{I}}\Omega_{0\mathrm{h}}} \left[\!\left[\mathbf{M}_{\mathbf{N}}^{\mathrm{T}}\right]\!\right]\langle\mathbf{Z}_0(\mathbf{F},\mathbf{M})\nabla_0\delta\mathbf{M}\rangle\,\mathrm{d}\mathrm{S}_0 + \int_{\partial_{\mathrm{D}}\Omega_{0\mathrm{h}}} \left[\!\left[\mathbf{M}_{\mathbf{N}}^{\mathrm{T}}\right]\!\right]\left\langle\mathbf{Z}_0(\mathbf{F},\bar{\mathbf{M}})\nabla_0\delta\mathbf{M}\right\rangle\mathrm{d}\mathrm{S}_0$$
$$\forall\delta\mathbf{M}\in\mathit{\Pi}_{\mathrm{e}}\mathrm{H}^1(\Omega_0^{\mathrm{e}})\times\mathit{\Pi}_{\mathrm{e}}\mathrm{H}^1(\Omega_0^{\mathrm{e}}), \quad (29)$$

where the notation $\bar{\mathbf{M}}_{\mathbf{N}} = \begin{pmatrix}\boldsymbol{N} & \mathbf{0}\\ \mathbf{0} & \boldsymbol{N}\end{pmatrix}\bar{\mathbf{M}} = \bar{\mathbf{N}}_{\mathbf{M}}\bar{\mathbf{M}}$ has been introduced.

The manifold of the trial functions $\mathbf{G}^{\mathrm{T}} = (\boldsymbol{u}^{\mathrm{T}} \;\; \mathbf{M}^{\mathrm{T}})$ is defined as

$$\mathrm{X}_s^{(+)} = \left\{\begin{array}{l}\mathbf{G}\in\left[\mathrm{L}^2(\Omega_{0\mathrm{h}})\right]^d\times\mathrm{L}^2(\Omega_{0\mathrm{h}})\times\mathrm{L}^{2^{(+)}}(\Omega_{0\mathrm{h}}) \;\text{ such that}\\ \quad \mathbf{G}_{|\Omega_0^{\mathrm{e}}}\in[\mathrm{H}^s(\Omega_0^{\mathrm{e}})]^d\times\mathrm{H}^s(\Omega_0^{\mathrm{e}})\times\mathrm{H}^{s^{(+)}}(\Omega_0^{\mathrm{e}}) \;\; \forall\Omega_0^{\mathrm{e}}\in\Omega_{0\mathrm{h}}\end{array}\right\}. \quad (30)$$

For the future use, we define $\mathrm{X}^{(+)}$ as $\mathrm{X}_2^{(+)}$ and X^+ the manifold such that $\mathrm{f}_{\mathrm{T}} > 0$, while X is the manifold for which $\mathrm{f}_{\mathrm{T}} \lesseqgtr 0$, with $\mathrm{X}^+ \subset \mathrm{X}$. It should be noted that the trial functions in the previous equations of the weak formulation belong to $\left[\mathrm{H}^1(\Omega_0^{\mathrm{e}})\right]^d \times \mathrm{H}^1(\Omega_0^{\mathrm{e}}) \times \mathrm{H}^{1^+}(\Omega_0^{\mathrm{e}})$; however for the numerical analysis, we will need to be in $\left[\mathrm{H}^2(\Omega_0^{\mathrm{e}})\right]^d \times \mathrm{H}^2(\Omega_0^{\mathrm{e}}) \times \mathrm{H}^{2^+}(\Omega_0^{\mathrm{e}})$, as it will be discussed in Section 4.

Therefore the weak form (28-29) is reformulated as finding $\mathbf{G} \in \mathrm{X}^+$ such that

$$\begin{cases} \mathrm{A}(\boldsymbol{F},\, \mathbf{M};\, \delta\boldsymbol{u}) & = \mathrm{B}(\delta\boldsymbol{u}) \\ \mathrm{C}(\boldsymbol{F},\, \mathbf{M};\, \delta\mathbf{M}) & = \mathrm{D}(\boldsymbol{F};\, \delta\mathbf{M}) - \int_{\Omega_{0\mathrm{h}}} \delta\mathbf{M}^{\mathrm{T}}\mathbf{I}_{\mathrm{i}}\mathrm{d}\Omega_0 \end{cases} \quad \forall \delta\mathbf{G} \in \mathrm{X}\,, \tag{31}$$

where $\mathrm{A}(\boldsymbol{F},\, \mathbf{M};\, \delta\boldsymbol{u})$ ($\mathrm{B}(\delta\boldsymbol{u})$) is directly deduced from the right-hand (left-hand) side of Eq. (28), and where $\mathrm{C}(\boldsymbol{F},\, \mathbf{M};\, \delta\mathbf{M})$ ($\mathrm{D}(\boldsymbol{F};\, \delta\mathbf{M})$) is directly deduced from the right-hand (left-hand) side of Eq. (29).

3.2 The finite element discretization of the coupled problem

In the computational model we consider the approximation $\mathbf{G}_{\mathrm{h}}^{\mathrm{T}} = \left(\boldsymbol{u}_{\mathrm{h}}^{\mathrm{T}}\ f_{\mathrm{V_h}}\ f_{\mathrm{T_h}}\right)$ of the trial function defined in a finite dimensional space of real valued piece-wise polynomial functions. The following manifold is thus introduced

$$\mathrm{X}^{k^{(+)}} = \left\{ \begin{array}{l} \mathbf{G}_{\mathrm{h}} \in \left[\mathrm{L}^2(\Omega_{0\mathrm{h}})\right]^d \times \mathrm{L}^2(\Omega_{0\mathrm{h}}) \times \mathrm{L}^{2^{(+)}}(\Omega_{0\mathrm{h}}) \ \text{ such that} \\ \quad \mathbf{G}_{\mathrm{h}}\,|_{\Omega_0^{\mathrm{e}}} \in [\mathbb{P}^k(\Omega_0^{\mathrm{e}})]^d \times \mathbb{P}^k(\Omega_0^{\mathrm{e}}) \times \mathbb{P}^{k^{(+)}}(\Omega_0^{\mathrm{e}})\ \forall \Omega_0^{\mathrm{e}} \in \Omega_{0\mathrm{h}} \end{array} \right\}, \tag{32}$$

where $\mathbb{P}^k(\Omega_0^{\mathrm{e}})$ is the space of polynomial functions of order up to k and $\mathbb{P}^{k^+}$ means that the polynomial approximation remains positive.

The discretization of the system is carried out using the discontinuous Galerkin Finite element method by introducing the same shape functions for the trial functions $\boldsymbol{u}$ and $\mathbf{M}$, and for the test functions $\delta\boldsymbol{u}$ and $\delta\mathbf{M}$, which are thus interpolated as

$$\boldsymbol{u}_{\mathrm{h}} = N_{\boldsymbol{u}}^a\, \mathbf{u}^a\,, \quad \mathbf{M}_{\mathrm{h}} = \mathbf{N}_{\mathbf{M}}^a\, \mathbf{M}^a\,, \tag{33}$$

$$\delta\boldsymbol{u}_{\mathrm{h}} = N_{\boldsymbol{u}}^a\, \delta\mathbf{u}^a\,, \quad \delta\mathbf{M}_{\mathrm{h}} = \mathbf{N}_{\mathbf{M}}^a\, \delta\mathbf{M}^a\,, \tag{34}$$

where $(\delta)\mathbf{u}^a$ and $(\delta)\mathbf{M}^a$ denote the nodal values of respectively $(\delta)\boldsymbol{u}_{\mathrm{h}}$ and $(\delta)\mathbf{M}_{\mathrm{h}}$ at node a, and where $\mathbf{N}_{\mathbf{M}}^a = \begin{pmatrix} N_{\mathrm{f_V}}^a & 0 \\ 0 & N_{\mathrm{f_T}}^a \end{pmatrix}$ is a matrix of the shape functions.

The finite element approximation of the weak form (31) is thus stated as finding $\mathbf{G}_{\mathrm{h}} \in \mathrm{X}^{k^+}$ such that

$$\begin{cases} \mathrm{A}(\boldsymbol{F}_{\mathrm{h}},\, \mathbf{M}_{\mathrm{h}};\, \delta\boldsymbol{u}_{\mathrm{h}}) & = \mathrm{B}(\delta\boldsymbol{u}_{\mathrm{h}}) \\ \mathrm{C}(\boldsymbol{F}_{\mathrm{h}},\, \mathbf{M}_{\mathrm{h}};\, \delta\mathbf{M}_{\mathrm{h}}) & = \mathrm{D}(\boldsymbol{F}_{\mathrm{h}};\, \delta\mathbf{M}_{\mathrm{h}}) - \int_{\Omega_{0\mathrm{h}}} \delta\mathbf{M}_{\mathrm{h}}^{\mathrm{T}}\mathbf{I}_{\mathrm{i_h}}\mathrm{d}\Omega_0 \end{cases} \quad \forall \delta\mathbf{G}_{\mathrm{h}} \in \mathrm{X}^k\,. \tag{35}$$

3.3 The system resolution in parallel

The set of Eqs. (35) can be rewritten under the form

$$\mathbf{F}_{\mathrm{ext}}^a\left(\mathbf{G}^b\right) = \mathbf{F}_{\mathrm{int}}^a\left(\mathbf{G}^b\right) + \mathbf{F}_{\mathrm{I}}^a\left(\mathbf{G}^b\right)\,, \tag{36}$$

where $\mathbf{G}^b$ is a $(d+2)\times 1$ vector gathering the unknowns at node b with $\mathbf{G}^b = (\mathbf{u}^{b^{\mathrm{T}}}\ \mathbf{M}^{b^{\mathrm{T}}})^{\mathrm{T}}$, $\mathbf{F}_{\mathrm{ext}}^a$ corresponds to the contributions of $\mathrm{B}(\delta\boldsymbol{u}_{\mathrm{h}})$ and $\mathrm{D}(\boldsymbol{F}_{\mathrm{h}};\, \delta\mathbf{M}_{\mathrm{h}})$ at node a, $\mathbf{F}_{\mathrm{int}}^a$ corresponds to the volume contributions of $\mathrm{A}(\boldsymbol{F}_{\mathrm{h}},\, \mathbf{M}_{\mathrm{h}};\, \delta\boldsymbol{u}_{\mathrm{h}})$, $\mathrm{C}(\boldsymbol{F}_{\mathrm{h}},\, \mathbf{M}_{\mathrm{h}};\, \delta\mathbf{M}_{\mathrm{h}})$, and $\mathbf{I}_{\mathrm{i_h}}$, and where $\mathbf{F}_{\mathrm{I}}^a$ corresponds to the interface contributions of

A($\boldsymbol{F}_{\mathrm{h}}$, $\mathbf{M}_{\mathrm{h}}$; $\delta\boldsymbol{u}_{\mathrm{h}}$) and C($\boldsymbol{F}_{\mathrm{h}}$, $\mathbf{M}_{\mathrm{h}}$; $\delta\mathbf{M}_{\mathrm{h}}$). The expressions of these forces are detailed in B.1.

The non-linear Eqs. (36) are linearized by means of an implicit formulation and solved using the Newton-Raphson scheme using as initial guess the last solution. To this end, the forces are written in a residual form. The predictor at iteration 0, reads $\mathbf{G}^c = \mathbf{G}^{c0}$, and the residual at iteration i reads

$$\mathbf{F}^a_{\mathrm{ext}}\left(\mathbf{G}^{c^i}\right) - \mathbf{F}^a_{\mathrm{int}}\left(\mathbf{G}^{c^i}\right) - \mathbf{F}^a_{\mathrm{I}}\left(\mathbf{G}^{c^i}\right) = \mathbf{R}^a\left(\mathbf{G}^{c^i}\right) . \tag{37}$$

At iteration i, the first-order Taylor development yields the system to be solved, *i.e.*

$$\left(\frac{\partial \mathbf{F}^a_{\mathrm{ext}}}{\partial \mathbf{G}^b} - \frac{\partial \mathbf{F}^a_{\mathrm{int}}}{\partial \mathbf{G}^b} - \frac{\partial \mathbf{F}^a_{\mathrm{I}}}{\partial \mathbf{G}^b}\right)|_{\mathbf{G}=\mathbf{G}^{c^i}} \Delta\mathbf{G}^b = -\mathbf{R}^a\left(\mathbf{G}^{c^i}\right) . \tag{38}$$

The explicit expression of the tangent matrix of the coupled Electro-Thermo-Mechanical system $\mathbb{K}^{ab}_{\mathbf{G}} = \frac{\partial \mathbf{F}^a_{\mathrm{ext}}}{\partial \mathbf{G}^b} - \frac{\partial \mathbf{F}^a_{\mathrm{int}}}{\partial \mathbf{G}^b} - \frac{\partial \mathbf{F}^a_{\mathrm{I}}}{\partial \mathbf{G}^b}$ is given in B.2. Finally, the resolution of the system (38) yields the correction $\Delta\mathbf{G}^b = \left(\mathbf{G}^b - \mathbf{G}^{bi}\right)$.

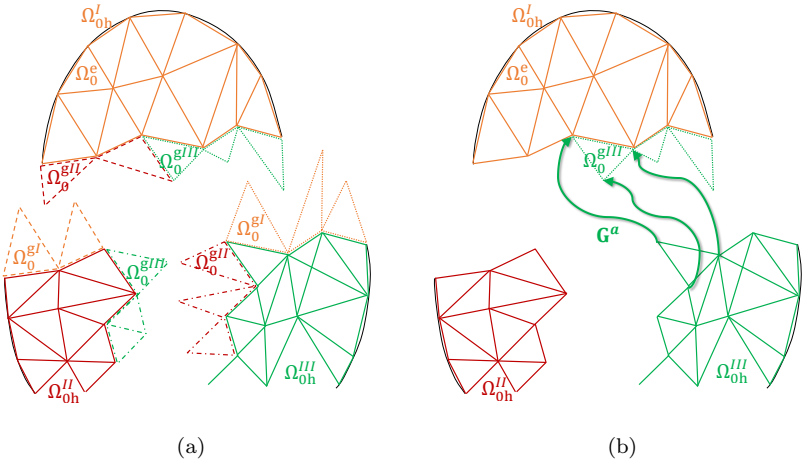

Fig. 2 Parallel implementation using ghost elements with (a) the different partitions $\Omega^i_{0\mathrm{h}}$ with their ghost elements $\Omega^{\mathrm{g}j}_0$ corresponding to the elements of the partition $\Omega^j_{0\mathrm{h}}$ having a common interface, and (b) the exchange of the nodal field $\mathbf{G}^b$ from the element in partition $\Omega^j_{0\mathrm{h}}$ to the ghost element $\Omega^{\mathrm{g}j}_0$ in partition $\Omega^i_{0\mathrm{h}}$.

The DG method has been implemented in Gmsh [20] in parallel using the ghost elements method suggested in [8,70]. In this approach, the discretization $\Omega_{0\mathrm{h}}$ is divided in partitions $\Omega^i_{0\mathrm{h}}$ using the METIS library [31], see Fig. 2(a). On top of its own bulk elements Ω^{e}_0, the partition $\Omega^i_{0\mathrm{h}}$ also owns the ghost elements $\Omega^{\mathrm{g}j}_0$ which correspond to the bulk elements of the partition $\Omega^j_{0\mathrm{h}}$ sharing a common partitions interface, see Fig. 2(a). The resolution steps are thus

- Step #1: Each partition $\Omega^i_{0\mathrm{h}}$ evaluates the bulk nodal forces $\mathbf{F}^a_{\mathrm{int}}$ (36) and stiffness matrix $\frac{\partial \mathbf{F}^a_{\mathrm{int}}}{\partial \mathbf{G}^b}$ (38) by performing a quadrature rule on its own elements Ω^{e}_0. There is no need to evaluate the bulk force and stiffness matrix contributions of the ghost elements $\Omega^{\mathrm{g}j}_0$.
- Step #2: Each partition $\Omega^i_{0\mathrm{h}}$ evaluates the interface nodal forces $\mathbf{F}^a_{\mathrm{I}}$ (36) and stiffness matrix $\frac{\partial \mathbf{F}^a_{\mathrm{I}}}{\partial \mathbf{G}^b}$ (38) by performing a quadrature rule on an interface shared either by two elements Ω^{e}_0 belonging to this partition $\Omega^i_{0\mathrm{h}}$ or by an element Ω^{e}_0 belonging to this partition and a ghost element $\Omega^{\mathrm{g}j}_0$.
- Step #3: The system (38) is then solved using the MUMPS [3] library.
- Step #4: To evaluate correctly the interface forces at partitions boundaries at Step #2 of the next iteration, the ghost elements $\Omega^{\mathrm{g}j}_0$ need to be in the updated deformation state, which requires their nodal values $\mathbf{G}^a$ to be communicated from the original element Ω^{e}_0 lying in partition $\Omega^j_{0\mathrm{h}}$, see Fig. 2(b). This communication is achieved before each new iteration through the network via Message Passing Interface (MPI), whichs is the only communications required by the method.

4 Numerical Properties

The demonstration of the numerical properties for Electro-Thermo-Mechanics coupling is derived following closely the approach developed by Gudi *et al.* [23] for non-linear problems under the assumption $d = 2$, and under the assumptions of temperature independent thermo-mechanical material properties, (however $\boldsymbol{J}_{\mathrm{y}_1}$, $\boldsymbol{L}_1$, $\boldsymbol{L}_2$ remain temperature and electric potential dependent but $\boldsymbol{\mathcal{C}}$ (the matrix form using Voigt notations of the material constant tensor $\boldsymbol{\mathcal{H}}$), and $\boldsymbol{\alpha}_{\mathrm{th}}$ are temperature and electric potential in-dependent), and in the absence of the heat source, such that the term $\bar{F}$ in Eq. (16) is equal to zero. Finally, we also require a framework in small deformation and linear thermo-elasticity in order to demonstrate the stability and convergence rates. Indeed, as explained before the thermo-mechancal response in the non-linear range is history-dependent, preventing to write a non-linear equation under a form similar to the onr of the electro-thermal coupling (19b).

4.1 Strong form in the small deformation setting

Under the discussed assumptions, we can state the weak form (31) under a matrix form with the vector of the unknown fields $\mathbf{G}$. In addition, we can introduce the coefficient matrix $\mathbf{v}$ of size $(5d-3)\times(5d-3)$ such that $\mathbf{v} = \begin{pmatrix} \boldsymbol{\mathcal{C}} & \mathbf{0} & \mathbf{0} \\ \mathbf{0} & \boldsymbol{l}_1 & \boldsymbol{l}_2 \\ \mathbf{0} & \boldsymbol{l}_2 & \boldsymbol{j}_{\mathrm{y}_1} \end{pmatrix}$. In a small deformation setting, we have $\boldsymbol{l}_1 \simeq \boldsymbol{L}_1$, $\boldsymbol{l}_2 \simeq \boldsymbol{L}_2$, and $\boldsymbol{j}_{\mathrm{y}_1} \simeq \boldsymbol{J}_{\mathrm{y}_1}$, and thus $\mathbf{Z} \simeq \mathbf{Z}_0$, the coefficient matrix in the current configuration. Therefore $\mathbf{v}$ can also be written as $\mathbf{v} = \begin{pmatrix} \boldsymbol{\mathcal{C}} & \mathbf{0} \\ \mathbf{0} & \mathbf{Z} \end{pmatrix}$. Moreover, assuming that the stress tensor does not depend

on the electrical potential, we define the matrices $\mathbf{o}(f_{\mathrm{T}}) = \begin{pmatrix} \mathbf{0}\,\mathbf{0} & \dfrac{-\boldsymbol{\mathcal{C}}\boldsymbol{\alpha}_{\mathrm{thc}}}{f_{\mathrm{T}}^2} \\ \mathbf{0}\,\mathbf{0} & \mathbf{0} \\ \mathbf{0}\,\mathbf{0} & \mathbf{0} \end{pmatrix}$ and $\mathbf{o}_0 = \mathbf{o}(f_{\mathrm{T}_0})$ of size $(5d-3)\times(d+2)$. In these matrices, $\boldsymbol{\alpha}_{\mathrm{thc}}$ is a vector of size $(3d-3)\times 1$ with, for $d=3$, $\boldsymbol{\alpha}_{\mathrm{thc}} = \begin{pmatrix} \alpha_{\mathrm{th}} & \alpha_{\mathrm{th}} & \alpha_{\mathrm{th}} & 0 & 0 & 0 \end{pmatrix}^{\mathrm{T}}$, and $\boldsymbol{\mathcal{C}}\boldsymbol{\alpha}_{\mathrm{thc}}$ a vector of size $(3d-3)\times 1$ and given for $d=3$ by $(\boldsymbol{\mathcal{C}}\boldsymbol{\alpha}_{\mathrm{thc}}) = \begin{pmatrix} 3K\alpha_{\mathrm{th}} & 3K\alpha_{\mathrm{th}} & 3K\alpha_{\mathrm{th}} & 0 & 0 & 0 \end{pmatrix}^{\mathrm{T}}$ for isotropic materials, with K the bulk modulus and α_{th} the thermal dilatation. Finally we define $\mathbf{h}$ a matrix of size $(d+2)\times(d+2)$ with, for $d=3$, $\mathbf{h} = \begin{pmatrix} \mathbf{0}\,\mathbf{0} & \mathbf{0} \\ 0\;0 & 0 \\ 0\;0 & \rho \mathrm{c_v} \end{pmatrix}$.

We can now introduce the matrix $\mathbf{w}$ of size $(5d-3)\times 1$ as $\mathbf{w}(\mathbf{G},\nabla\mathbf{G}) = \mathbf{v}(\mathbf{G})\nabla\mathbf{G}$. In this relation $\nabla\mathbf{G}$ is the $(5d-3)\times 1$ vector of the gradient of the unknown fields, which is defined as $\nabla\mathbf{G} = (\nabla)\mathbf{G}$ and is written for $d=3$, using Voigt rules for the mechanical contribution, as

$$(\nabla\mathbf{G}) = \begin{pmatrix} \varepsilon_{\mathrm{xx}} \\ \varepsilon_{\mathrm{yy}} \\ \varepsilon_{\mathrm{zz}} \\ 2\varepsilon_{\mathrm{xy}} \\ 2\varepsilon_{\mathrm{xz}} \\ 2\varepsilon_{\mathrm{yz}} \\ \frac{\partial f_{\mathrm{V}}}{\partial \mathrm{x}} \\ \frac{\partial f_{\mathrm{V}}}{\partial \mathrm{y}} \\ \frac{\partial f_{\mathrm{V}}}{\partial \mathrm{z}} \\ \frac{\partial f_{\mathrm{T}}}{\partial \mathrm{x}} \\ \frac{\partial f_{\mathrm{T}}}{\partial \mathrm{y}} \\ \frac{\partial f_{\mathrm{T}}}{\partial \mathrm{z}} \end{pmatrix} = \begin{pmatrix} \frac{\partial}{\partial \mathrm{x}} & 0 & 0 & 0 & 0 \\ 0 & \frac{\partial}{\partial \mathrm{y}} & 0 & 0 & 0 \\ 0 & 0 & \frac{\partial}{\partial \mathrm{z}} & 0 & 0 \\ \frac{\partial}{\partial \mathrm{y}} & \frac{\partial}{\partial \mathrm{x}} & 0 & 0 & 0 \\ \frac{\partial}{\partial \mathrm{z}} & 0 & \frac{\partial}{\partial \mathrm{x}} & 0 & 0 \\ 0 & \frac{\partial}{\partial \mathrm{z}} & \frac{\partial}{\partial \mathrm{y}} & 0 & 0 \\ 0 & 0 & 0 & \frac{\partial}{\partial \mathrm{x}} & 0 \\ 0 & 0 & 0 & \frac{\partial}{\partial \mathrm{y}} & 0 \\ 0 & 0 & 0 & \frac{\partial}{\partial \mathrm{z}} & 0 \\ 0 & 0 & 0 & 0 & \frac{\partial}{\partial \mathrm{x}} \\ 0 & 0 & 0 & 0 & \frac{\partial}{\partial \mathrm{y}} \\ 0 & 0 & 0 & 0 & \frac{\partial}{\partial \mathrm{z}} \end{pmatrix} \begin{pmatrix} u_{\mathrm{x}} \\ u_{\mathrm{y}} \\ u_{\mathrm{z}} \\ f_{\mathrm{V}} \\ f_{\mathrm{T}} \end{pmatrix}. \tag{39}$$

Similarly, $\boldsymbol{\Sigma}^{\mathrm{T}} = \begin{pmatrix} \sigma_{\mathrm{xx}} & \sigma_{\mathrm{yy}} & \sigma_{\mathrm{zz}} & \tau_{\mathrm{xy}} & \tau_{\mathrm{xz}} & \tau_{\mathrm{yz}} & j_{\mathrm{e_x}} & j_{\mathrm{e_y}} & j_{\mathrm{e_z}} & j_{\mathrm{y_x}} & j_{\mathrm{y_y}} & j_{\mathrm{y_z}} \end{pmatrix}$ represents the energy conjugated stress.

Using these definitions, the constitutive relations (19) are rewritten as

$$\boldsymbol{\Sigma} = \mathbf{v}(\mathbf{G})\nabla\mathbf{G} + \mathbf{o}(\mathbf{G})\mathbf{G} - \mathbf{o}_0\mathbf{G}_0\,, \tag{40}$$

where $\mathbf{G}_0$ is the vector of the initial values $\mathbf{G}_0^{\mathrm{T}} = (u_{\mathrm{x}_0}\; u_{\mathrm{y}_0}\; u_{\mathrm{z}_0}\; f_{\mathrm{V}_0}\; f_{\mathrm{T}_0})$. The set of governing Eqs. (16) is now stated as finding $\mathbf{G} \in \left[\mathrm{H}^2(\Omega_0)\right]^d \times \mathrm{H}^2(\Omega_0) \times \mathrm{H}^{2^+}(\Omega_0)$ such that

$$-\nabla^{\mathrm{T}}\left[\mathbf{w}(\mathbf{G},\nabla\mathbf{G}) + \mathbf{o}(\mathbf{G})\mathbf{G} - \mathbf{o}_0\mathbf{G}_0\right] = \mathbf{h}\,\dot{\mathbf{G}} \qquad \forall \boldsymbol{x} \in \Omega\,. \tag{41}$$

This set of equations is completed with the Dirichlet BC (18) rewritten as

$$\mathbf{G} = \bar{\mathbf{G}} \qquad \forall\, \boldsymbol{x} \in \partial_{\mathrm{D}}\Omega\,, \tag{42}$$

and with the Neumann BC (17) rewritten as

$$\bar{\mathbf{n}}^{\mathrm{T}}(\mathbf{w} + \mathbf{o}\mathbf{G} - \mathbf{o}_0\mathbf{G}_0) = \bar{\mathbf{w}} \qquad \forall\, \mathbf{x} \in \partial_{\mathrm{N}}\Omega, \tag{43}$$

where, for $d = 3$,

$$\bar{\mathbf{n}} = \begin{pmatrix} n_\mathrm{x} & 0 & 0 & 0 & 0 \\ 0 & n_\mathrm{y} & 0 & 0 & 0 \\ 0 & 0 & n_\mathrm{z} & 0 & 0 \\ n_\mathrm{y} & n_\mathrm{x} & 0 & 0 & 0 \\ n_\mathrm{z} & 0 & n_\mathrm{x} & 0 & 0 \\ 0 & n_\mathrm{z} & n_\mathrm{y} & 0 & 0 \\ 0 & 0 & 0 & n_\mathrm{x} & 0 \\ 0 & 0 & 0 & n_\mathrm{y} & 0 \\ 0 & 0 & 0 & n_\mathrm{z} & 0 \\ 0 & 0 & 0 & 0 & n_\mathrm{x} \\ 0 & 0 & 0 & 0 & n_\mathrm{y} \\ 0 & 0 & 0 & 0 & n_\mathrm{z} \end{pmatrix}, \tag{44}$$

represents the unit outward normal in the current configuration, $\bar{\mathbf{G}}^\mathrm{T} = \left(\bar{\boldsymbol{u}}^\mathrm{T}\ \bar{f}_\mathrm{V}\ \bar{f}_\mathrm{T}\right)$ gathers the constrained fields, and where $\bar{\mathbf{w}}^\mathrm{T} = \left(\bar{\boldsymbol{t}}^\mathrm{T}\ \bar{j}_\mathrm{y}\ \bar{j}_\mathrm{e}\right)$ gathers the constrained fluxes.

It can be noticed that the gradient of $(\mathbf{o}(\mathbf{G})\mathbf{G})$ consists of zero components and of the gradient of $(-\frac{(\boldsymbol{\mathcal{C}}\boldsymbol{\alpha}_\mathrm{thc})}{f_\mathrm{T}^2} f_\mathrm{T})$. As the variation $\delta(-\frac{(\boldsymbol{\mathcal{C}}\boldsymbol{\alpha}_\mathrm{thc})}{f_\mathrm{T}^2} f_\mathrm{T}) = \frac{(\boldsymbol{\mathcal{C}}\boldsymbol{\alpha}_\mathrm{thc})}{f_\mathrm{T}^2}\delta f_\mathrm{T}$, the matrix $\mathbf{o}(\mathbf{G})$ can be rearranged in a new form $\tilde{\mathbf{o}}(\mathbf{G})$ of size $(d+2)\times(5d-3)$, such that

$$\nabla^\mathrm{T}\left(\mathbf{o}(\mathbf{G})\mathbf{G}\right) = -\tilde{\mathbf{o}}(\mathbf{G})\nabla\mathbf{G}\,, \tag{45}$$

with, for $d = 3$,

$$\tilde{\mathbf{o}}(\mathbf{G}) = \begin{pmatrix} 0\,0\,0\,0\,0\,0\,0\,0\,0\,0\,0 & -\frac{3K\alpha_\mathrm{th}}{f_\mathrm{T}^2} & 0 & 0 \\ 0\,0\,0\,0\,0\,0\,0\,0\,0\,0\,0 & 0 & -\frac{3K\alpha_\mathrm{th}}{f_\mathrm{T}^2} & 0 \\ 0\,0\,0\,0\,0\,0\,0\,0\,0\,0\,0 & 0 & 0 & -\frac{3K\alpha_\mathrm{th}}{f_\mathrm{T}^2} \\ 0\,0\,0\,0\,0\,0\,0\,0\,0\,0\,0 & 0 & 0 & 0 \\ 0\,0\,0\,0\,0\,0\,0\,0\,0\,0\,0 & 0 & 0 & 0 \end{pmatrix}. \tag{46}$$

The operator $\tilde{\cdot}$ can be seen as the transpose operator that accounts for the definition of the ∇ operator in the matrix form. Therefore Eq. (41) becomes

$$-\nabla^\mathrm{T}(\mathbf{w}(\mathbf{G},\nabla\mathbf{G})) + \tilde{\mathbf{o}}(\mathbf{G})\nabla\mathbf{G} = \mathbf{h}\dot{\mathbf{G}} \qquad \forall \boldsymbol{x} \in \Omega\,. \tag{47}$$

4.2 Weak DG form in the small deformation setting

Assuming a quasi-static process from now on, the associated DG form for the Electro-Thermo-Elasticity problem (47) is defined as finding $\mathbf{G} \in \mathrm{X}^+$ such that

$$\mathrm{a}(\mathbf{G},\delta\mathbf{G}) = \mathrm{b}(\delta\mathbf{G}), \quad \forall\delta\mathbf{G} \in \mathrm{X}\,, \tag{48}$$

with

$$
\begin{aligned}
\mathrm{a}(\mathbf{G},\delta\mathbf{G}) = & \int_{\Omega_\mathrm{h}} (\nabla\delta\mathbf{G})^\mathrm{T}\mathbf{w}(\mathbf{G},\nabla\mathbf{G})\mathrm{d}\Omega + \int_{\Omega_\mathrm{h}} \delta\mathbf{G}^\mathrm{T}\tilde{\mathbf{o}}(\mathbf{G})\nabla\mathbf{G}\mathrm{d}\Omega + \\
& \int_{\partial_\mathrm{I}\Omega_\mathrm{h}\cup\partial_\mathrm{D}\Omega_\mathrm{h}} \left[\!\left[\delta\mathbf{G}_\mathbf{n}^\mathrm{T}\right]\!\right] \langle \mathbf{w}(\mathbf{G},\nabla\mathbf{G})\rangle \,\mathrm{dS} + \\
& \int_{\partial_\mathrm{I}\Omega_\mathrm{h}} \left[\!\left[\mathbf{G}_\mathbf{n}^\mathrm{T}\right]\!\right] \langle \mathbf{v}(\mathbf{G})\nabla\delta\mathbf{G}\rangle \,\mathrm{dS} + \int_{\partial_\mathrm{D}\Omega_\mathrm{h}} \left[\!\left[\mathbf{G}_\mathbf{n}^\mathrm{T}\right]\!\right] \langle \mathbf{v}(\bar{\mathbf{G}})\nabla\delta\mathbf{G}\rangle \,\mathrm{dS} + \\
& \int_{\partial_\mathrm{I}\Omega_\mathrm{h}} \left[\!\left[\mathbf{G}_\mathbf{n}^\mathrm{T}\right]\!\right] \left\langle \frac{\mathbf{v}(\mathbf{G})\mathcal{B}}{h_\mathrm{s}} \right\rangle [\![\delta\mathbf{G}_\mathbf{n}]\!] \,\mathrm{dS} + \int_{\partial_\mathrm{D}\Omega_\mathrm{h}} \left[\!\left[\mathbf{G}_\mathbf{n}^\mathrm{T}\right]\!\right] \left\langle \frac{\mathbf{v}(\bar{\mathbf{G}})\mathcal{B}}{h_\mathrm{s}} \right\rangle [\![\delta\mathbf{G}_\mathbf{n}]\!] \,\mathrm{dS} - \\
& \int_{\partial_\mathrm{I}\Omega_\mathrm{h}\cup\partial_\mathrm{D}\Omega_\mathrm{h}} \left\langle \delta\mathbf{G}_\mathbf{n}^\mathrm{T} \right\rangle [\![\mathbf{o}(\mathbf{G})\mathbf{G} - \mathbf{o}_0\mathbf{G}_0]\!] \,\mathrm{dS} + \\
& \int_{\partial_\mathrm{N}\Omega_\mathrm{h}} \delta\mathbf{G}^\mathrm{T}\bar{\mathbf{n}}^\mathrm{T}(\mathbf{o}(\mathbf{G})\mathbf{G} - \mathbf{o}_0\mathbf{G}_0)\mathrm{dS}\,, \qquad (49)
\end{aligned}
$$

and

$$
\begin{aligned}
\mathrm{b}(\delta\mathbf{G}) = & \int_{\partial_\mathrm{N}\Omega_\mathrm{h}} \delta\mathbf{G}^\mathrm{T}\bar{\mathbf{w}}\mathrm{dS} - \int_{\partial_\mathrm{D}\Omega_\mathrm{h}} \bar{\mathbf{G}}_\mathbf{n}^\mathrm{T}\mathbf{v}(\bar{\mathbf{G}})\nabla\delta\mathbf{G}\,\mathrm{dS} + \\
& \int_{\partial_\mathrm{D}\Omega_\mathrm{h}} \delta\mathbf{G}_\mathbf{n}^\mathrm{T}\frac{\mathbf{v}(\bar{\mathbf{G}})\mathcal{B}}{h_\mathrm{s}}\bar{\mathbf{G}}_\mathbf{n}\,\mathrm{dS} + \int_{\partial_\mathrm{D}\Omega_\mathrm{h}} \delta\mathbf{G}_\mathbf{n}^\mathrm{T}(\mathbf{o}(\bar{\mathbf{G}})\bar{\mathbf{G}} - \mathbf{o}_0\mathbf{G}_0)\mathrm{dS}\,, \qquad (50)
\end{aligned}
$$

where $\mathbf{G}_\mathbf{n} = \bar{\mathbf{n}}^-\mathbf{G}$ is a $(5d-3)\times 1$ vector, which is defined by building $\bar{\mathbf{n}}^-$ using the unit outward normal of the "-" element, $\boldsymbol{n}^-$, following Eq. (44).

Using the identity $[\![\mathrm{ab}]\!] = [\![\mathrm{a}]\!]\langle\mathrm{b}\rangle + \langle\mathrm{a}\rangle[\![\mathrm{b}]\!]$ on $\partial_\mathrm{I}\Omega_\mathrm{h}$, the relation (45), and performing an integration by parts lead to

$$
\begin{aligned}
& \int_{\Omega_\mathrm{h}} \delta\mathbf{G}^\mathrm{T}\tilde{\mathbf{o}}(\mathbf{G})\nabla\mathbf{G}\mathrm{d}\Omega = -\int_{\Omega_\mathrm{h}} \delta\mathbf{G}^\mathrm{T}\nabla^\mathrm{T}(\mathbf{o}(\mathbf{G})\mathbf{G} - \mathbf{o}_0\mathbf{G}_0)\mathrm{d}\Omega = \\
& \sum_\mathrm{e}\int_{\Omega^\mathrm{e}} (\nabla\delta\mathbf{G})^\mathrm{T}(\mathbf{o}(\mathbf{G})\mathbf{G} - \mathbf{o}_0\mathbf{G}_0)\mathrm{d}\Omega - \sum_\mathrm{e}\int_{\partial\Omega^\mathrm{e}} \delta\mathbf{G}_\mathbf{n}^\mathrm{T}(\mathbf{o}(\mathbf{G})\mathbf{G} - \mathbf{o}_0\mathbf{G}_0)\mathrm{dS} = \\
& \int_{\Omega_\mathrm{h}} (\nabla\delta\mathbf{G})^\mathrm{T}(\mathbf{o}(\mathbf{G})\mathbf{G} - \mathbf{o}_0\mathbf{G}_0)\mathrm{d}\Omega - \int_{\partial_\mathrm{N}\Omega_\mathrm{h}} \delta\mathbf{G}_\mathbf{n}^\mathrm{T}(\mathbf{o}(\mathbf{G})\mathbf{G} - \mathbf{o}_0\mathbf{G}_0)\mathrm{dS} \qquad (51) \\
& - \int_{\partial_\mathrm{D}\Omega_\mathrm{h}} \delta\mathbf{G}_\mathbf{n}^\mathrm{T}(\mathbf{o}(\mathbf{G})\mathbf{G} - \mathbf{o}_0\mathbf{G}_0)\mathrm{dS} + \int_{\partial_\mathrm{I}\Omega_\mathrm{h}} \left[\!\left[\delta\mathbf{G}_\mathbf{n}^\mathrm{T}\right]\!\right] \langle \mathbf{o}(\mathbf{G})\mathbf{G} - \mathbf{o}_0\mathbf{G}_0\rangle \,\mathrm{dS} + \\
& \int_{\partial_\mathrm{I}\Omega_\mathrm{h}} \left\langle \delta\mathbf{G}_\mathbf{n}^\mathrm{T} \right\rangle [\![\mathbf{o}(\mathbf{G})\mathbf{G} - \mathbf{o}_0\mathbf{G}_0]\!] \,\mathrm{dS}.
\end{aligned}
$$

Therefore, Eq. (48) can be rewritten as

$$
\mathrm{a}'(\mathbf{G},\delta\mathbf{G}) = \mathrm{b}'(\delta\mathbf{G}), \quad \forall\delta\mathbf{G}\in\mathrm{X}, \qquad (52)
$$

with

$$\begin{aligned}
\mathrm{a}'(\mathbf{G},\delta\mathbf{G}) = &\int_{\Omega_\mathrm{h}} (\nabla\delta\mathbf{G})^\mathrm{T}\mathbf{w}(\mathbf{G},\nabla\mathbf{G})\mathrm{d}\Omega + \int_{\Omega_\mathrm{h}} (\nabla\delta\mathbf{G})^\mathrm{T}(\mathbf{o}(\mathbf{G})\mathbf{G}-\mathbf{o}_0\mathbf{G}_0)\mathrm{d}\Omega + \\
&\int_{\partial_\mathrm{I}\Omega_\mathrm{h}\cup\partial_\mathrm{D}\Omega_\mathrm{h}} \left[\!\left[\delta\mathbf{G}_\mathbf{n}^\mathrm{T}\right]\!\right] \langle \mathbf{w}(\mathbf{G},\nabla\mathbf{G})\rangle \,\mathrm{dS} + \int_{\partial_\mathrm{I}\Omega_\mathrm{h}} \left[\!\left[\mathbf{G}_\mathbf{n}^\mathrm{T}\right]\!\right] \langle \mathbf{v}(\mathbf{G})\nabla\delta\mathbf{G}\rangle \,\mathrm{dS} + \\
&\int_{\partial_\mathrm{D}\Omega_\mathrm{h}} \left[\!\left[\mathbf{G}_\mathbf{n}^\mathrm{T}\right]\!\right] \langle \mathbf{v}(\bar{\mathbf{G}})\nabla\delta\mathbf{G}\rangle \,\mathrm{dS} + \int_{\partial_\mathrm{I}\Omega_\mathrm{h}} \left[\!\left[\mathbf{G}_\mathbf{n}^\mathrm{T}\right]\!\right] \left\langle \frac{\mathbf{v}(\mathbf{G})\mathcal{B}}{h_\mathrm{s}} \right\rangle [\![\delta\mathbf{G}_\mathbf{n}]\!] \,\mathrm{dS} + \\
&\int_{\partial_\mathrm{D}\Omega_\mathrm{h}} \left[\!\left[\mathbf{G}_\mathbf{n}^\mathrm{T}\right]\!\right] \left\langle \frac{\mathbf{v}(\bar{\mathbf{G}})\mathcal{B}}{h_\mathrm{s}} \right\rangle [\![\delta\mathbf{G}_\mathbf{n}]\!] \,\mathrm{dS} + \\
&\int_{\partial_\mathrm{I}\Omega_\mathrm{h}\cup\partial_\mathrm{D}\Omega_\mathrm{h}} \left[\!\left[\delta\mathbf{G}_\mathbf{n}^\mathrm{T}\right]\!\right] \langle \mathbf{o}(\mathbf{G})\mathbf{G}-\mathbf{o}_0\mathbf{G}_0\rangle \,\mathrm{dS} \\
&-\int_{\partial_\mathrm{D}\Omega_\mathrm{h}} \left\langle \delta\mathbf{G}_\mathbf{n}^\mathrm{T}\right\rangle [\![\mathbf{o}(\mathbf{G})\mathbf{G}-\mathbf{o}_0\mathbf{G}_0]\!] \,\mathrm{dS}\,,
\end{aligned} \tag{53}$$

and

$$\begin{aligned}
\mathrm{b}'(\delta\mathbf{G}) = &\int_{\partial_\mathrm{N}\Omega_\mathrm{h}} \delta\mathbf{G}^\mathrm{T}\bar{\mathbf{w}}\mathrm{dS} - \int_{\partial_\mathrm{D}\Omega_\mathrm{h}} \bar{\mathbf{G}}_\mathbf{n}^\mathrm{T}\mathbf{v}(\bar{\mathbf{G}})\nabla\delta\mathbf{G}\,\mathrm{dS} \\
&+\int_{\partial_\mathrm{D}\Omega_\mathrm{h}} \delta\mathbf{G}_\mathbf{n}^\mathrm{T}\frac{\mathbf{v}(\bar{\mathbf{G}})\mathcal{B}}{h_\mathrm{s}}\bar{\mathbf{G}}_\mathbf{n}\,\mathrm{dS} + \int_{\partial_\mathrm{D}\Omega_\mathrm{h}} \delta\mathbf{G}_\mathbf{n}^\mathrm{T}(\mathbf{o}(\bar{\mathbf{G}})\bar{\mathbf{G}}-\mathbf{o}_0\mathbf{G}_0)\mathrm{dS}\,.
\end{aligned} \tag{54}$$

Henceforth, using Eq. (40), it is shown that Eq. (52), which is derived from Eq. (48), corresponds to the weak form (31).

Unlike the usual case in DG, where the interface term involves $\mathbf{o}$ in the average operator $\langle\,\rangle$, Eq. (49) shows that $\mathbf{o}$ is rather involved in the jump operator $[\![\,]\!]$. This comes from the integration by parts in Eq. (51), in which $\mathbf{o}$ is $\mathbf{G}$ dependent. However, this allows the volume and consistency terms in Eq. (52) to be directly expressed in terms of the stress $\boldsymbol{\Sigma} = \mathbf{w} + (\mathbf{o}\mathbf{G} - \mathbf{o}_0\mathbf{G}_0)$, which is convenient when dealing with a non-linear formulation as in Eqs. (31).

4.3 Consistency

To prove the consistency of the method, the exact solution $\mathbf{G}^\mathrm{e} \in \left[\mathrm{H}^2(\Omega)\right]^d \times \mathrm{H}^2(\Omega) \times \mathrm{H}^{2^+}(\Omega)$ of the problem stated by Eq. (47) is considered. This implies $[\![\mathbf{G}^\mathrm{e}]\!] = 0$, $\langle\mathbf{w}\rangle = \mathbf{w}$, $[\![\mathbf{o}(\mathbf{G}^\mathrm{e})\mathbf{G}^\mathrm{e} - \mathbf{o}_0\mathbf{G}_0]\!] = 0$ on $\partial_\mathrm{I}\Omega_\mathrm{h}$, and $[\![\mathbf{G}^\mathrm{e}]\!] = -\bar{\mathbf{G}} = -\mathbf{G}^\mathrm{e}$, $[\![\mathbf{o}(\mathbf{G}^\mathrm{e})\mathbf{G}^\mathrm{e} - \mathbf{o}_0\mathbf{G}_0]\!] = -\mathbf{o}(\bar{\mathbf{G}})\bar{\mathbf{G}} + \mathbf{o}_0\mathbf{G}_0$, $\langle\mathbf{w}\rangle = \mathbf{v}(\bar{\mathbf{G}})\nabla\mathbf{G}^\mathrm{e} = \mathbf{v}(\mathbf{G}^\mathrm{e})\nabla\mathbf{G}^\mathrm{e}$, and $\mathbf{v}(\mathbf{G}) = \mathbf{v}(\bar{\mathbf{G}}) = \mathbf{v}(\mathbf{G}^\mathrm{e})$ on $\partial_\mathrm{D}\Omega_\mathrm{h}$. Therefore, Eq. (48) becomes:

$$\begin{gathered}
\textstyle\int_{\partial_\mathrm{N}\Omega_\mathrm{h}} \delta\mathbf{G}^\mathrm{T}\bar{\mathbf{w}}\mathrm{dS} - \int_{\partial_\mathrm{D}\Omega_\mathrm{h}} \bar{\mathbf{G}}_\mathbf{n}^\mathrm{T}\mathbf{v}(\bar{\mathbf{G}})\nabla\delta\mathbf{G}\,\mathrm{dS} + \int_{\partial_\mathrm{D}\Omega_\mathrm{h}} \delta\mathbf{G}_\mathbf{n}^\mathrm{T}\left(\mathbf{o}(\bar{\mathbf{G}})\bar{\mathbf{G}}-\mathbf{o}_0\mathbf{G}_0\right)\mathrm{dS} + \\
\textstyle\int_{\partial_\mathrm{D}\Omega_\mathrm{h}} \delta\mathbf{G}_\mathbf{n}^\mathrm{T}\frac{\mathbf{v}(\bar{\mathbf{G}})\mathcal{B}}{h_\mathrm{s}}\bar{\mathbf{G}}_\mathbf{n}\,\mathrm{dS} = \int_{\Omega_\mathrm{h}} (\nabla\delta\mathbf{G})^\mathrm{T}\mathbf{w}(\mathbf{G}^\mathrm{e},\nabla\mathbf{G}^\mathrm{e})\mathrm{d}\Omega + \\
\textstyle\int_{\Omega_\mathrm{h}} \delta\mathbf{G}^\mathrm{T}\tilde{\mathbf{o}}(\mathbf{G}^\mathrm{e})\nabla\mathbf{G}^\mathrm{e}\mathrm{d}\Omega + \int_{\partial_\mathrm{I}\Omega_\mathrm{h}} \left[\!\left[\delta\mathbf{G}_\mathbf{n}^\mathrm{T}\right]\!\right] \langle\mathbf{w}(\mathbf{G}^\mathrm{e},\nabla\mathbf{G}^\mathrm{e})\rangle \,\mathrm{dS} - \\
\textstyle\int_{\partial_\mathrm{D}\Omega_\mathrm{h}} \delta\mathbf{G}_\mathbf{n}^\mathrm{T}\mathbf{w}(\mathbf{G}^\mathrm{e},\nabla\mathbf{G}^\mathrm{e})\mathrm{dS} - \int_{\partial_\mathrm{D}\Omega_\mathrm{h}} \mathbf{G}_\mathbf{n}^{\mathrm{e}^\mathrm{T}}\mathbf{v}(\bar{\mathbf{G}})\nabla\delta\mathbf{G}\mathrm{dS} + \int_{\partial_\mathrm{D}\Omega_\mathrm{h}} \delta\mathbf{G}_\mathbf{n}^\mathrm{T}\frac{\mathcal{B}}{h_\mathrm{s}}\mathbf{v}(\bar{\mathbf{G}})\mathbf{G}_\mathbf{n}^\mathrm{e}\mathrm{dS} + \\
\textstyle\int_{\partial_\mathrm{D}\Omega_\mathrm{h}} \delta\mathbf{G}_\mathbf{n}^\mathrm{T}\left(\mathbf{o}(\mathbf{G}^\mathrm{e})\mathbf{G}^\mathrm{e}-\mathbf{o}_0\mathbf{G}_0\right)\mathrm{dS} + \int_{\partial_\mathrm{N}\Omega_\mathrm{h}} \delta\mathbf{G}^\mathrm{T}\bar{\mathbf{n}}^\mathrm{T}\left(\mathbf{o}(\mathbf{G}^\mathrm{e})\mathbf{G}^\mathrm{e}-\mathbf{o}_0\mathbf{G}_0\right)\mathrm{dS}\ \forall\delta\mathbf{G}\in\mathrm{X}\,.
\end{gathered} \tag{55}$$

Integrating the first term of the right hand side by parts leads to

$$\sum_{\mathrm{e}} \int_{\Omega^{\mathrm{e}}} (\nabla \delta \mathbf{G})^{\mathrm{T}} \mathbf{w}(\mathbf{G}^{\mathrm{e}}, \nabla \mathbf{G}^{\mathrm{e}}) \mathrm{d}\Omega = -\sum_{\mathrm{e}} \int_{\Omega^{\mathrm{e}}} \delta \mathbf{G}^{\mathrm{T}} \nabla^{\mathrm{T}} \mathbf{w}(\mathbf{G}^{\mathrm{e}}, \nabla \mathbf{G}^{\mathrm{e}}) \mathrm{d}\Omega + \sum_{\mathrm{e}} \int_{\partial \Omega^{\mathrm{e}}} \delta \mathbf{G}_{\mathbf{n}}^{\mathrm{T}} \mathbf{w}(\mathbf{G}^{\mathrm{e}}, \nabla \mathbf{G}^{\mathrm{e}}) \mathrm{dS},$$

and Eq.(55) becomes

$$\begin{aligned} &\int_{\partial_{\mathrm{N}}\Omega_{\mathrm{h}}} \delta \mathbf{G}^{\mathrm{T}} \bar{\mathbf{w}} \mathrm{dS} - \int_{\partial_{\mathrm{D}}\Omega_{\mathrm{h}}} \bar{\mathbf{G}}_{\mathbf{n}}^{\mathrm{T}} \left(\mathbf{v}(\bar{\mathbf{G}}) \nabla \delta \mathbf{G}\right) \mathrm{dS} + \int_{\partial_{\mathrm{D}}\Omega_{\mathrm{h}}} \delta \mathbf{G}_{\mathbf{n}}^{\mathrm{T}} (\mathbf{o}(\bar{\mathbf{G}}) \bar{\mathbf{G}} - \mathbf{o}_0 \mathbf{G}_0) \mathrm{dS} + \\ &\int_{\partial_{\mathrm{D}}\Omega_{\mathrm{h}}} \delta \mathbf{G}_{\mathbf{n}}^{\mathrm{T}} \left(\tfrac{\mathcal{B}}{h_{\mathrm{s}}} \mathbf{v}(\bar{\mathbf{G}})\right) \bar{\mathbf{G}}_{\mathbf{n}} \mathrm{dS} = -\int_{\Omega_{\mathrm{h}}} \delta \mathbf{G}^{\mathrm{T}} \nabla^{\mathrm{T}} \mathbf{w}(\mathbf{G}^{\mathrm{e}}, \nabla \mathbf{G}^{\mathrm{e}}) \mathrm{d}\Omega + \\ &\int_{\partial_{\mathrm{N}}\Omega_{\mathrm{h}}} \delta \mathbf{G}_{\mathbf{n}}^{\mathrm{T}} \mathbf{w}(\mathbf{G}^{\mathrm{e}}, \nabla \mathbf{G}^{\mathrm{e}}) \mathrm{dS} + \int_{\Omega_{\mathrm{h}}} \delta \mathbf{G}^{\mathrm{T}} \tilde{\mathbf{o}}(\mathbf{G}^{\mathrm{e}}) \nabla \mathbf{G}^{\mathrm{e}} \mathrm{d}\Omega - \int_{\partial_{\mathrm{D}}\Omega_{\mathrm{h}}} \mathbf{G}_{\mathbf{n}}^{\mathrm{e}^{\mathrm{T}}} \mathbf{v}(\bar{\mathbf{G}}) \nabla \delta \mathbf{G} \mathrm{dS} + \\ &\int_{\partial_{\mathrm{D}}\Omega_{\mathrm{h}}} \delta \mathbf{G}_{\mathbf{n}}^{\mathrm{T}} \tfrac{\mathcal{B}}{h_{\mathrm{s}}} \mathbf{v}(\bar{\mathbf{G}}) \mathbf{G}_{\mathbf{n}}^{\mathrm{e}} \mathrm{dS} + \int_{\partial_{\mathrm{D}}\Omega_{\mathrm{h}}} \delta \mathbf{G}_{\mathbf{n}}^{\mathrm{T}} (\mathbf{o}(\mathbf{G}^{\mathrm{e}}) \mathbf{G}^{\mathrm{e}} - \mathbf{o}_0 \mathbf{G}_0) \mathrm{dS} + \\ &\int_{\partial_{\mathrm{N}}\Omega_{\mathrm{h}}} \delta \mathbf{G}^{\mathrm{T}} \bar{\mathbf{n}}^{\mathrm{T}} (\mathbf{o}(\mathbf{G}^{\mathrm{e}}) \mathbf{G}^{\mathrm{e}} - \mathbf{o}_0 \mathbf{G}_0) \mathrm{dS} \quad \forall \delta \mathbf{G} \in \mathrm{X}\,. \end{aligned} \tag{56}$$

The arbitrary nature of the test functions and the use of Eq. (45) lead to recover the set of conservation laws, Eqs. (41), and the boundary conditions, Eqs. (42-43).

4.4 Second order non-self-adjoint elliptic problem

In this part, we will assume that $\partial_{\mathrm{D}}\Omega_{\mathrm{h}} = \partial\Omega_{\mathrm{h}}$. This assumption is not restrictive but simplifies the demonstrations.

Starting from the definition of the matrix $\mathbf{v}(\mathbf{G})$, which is a symmetric and positive definite matrix since its components $\boldsymbol{\mathcal{C}}$ and $\mathbf{Z}$ are positive definite matrices, let us define the minimum and maximum eigenvalues of the matrix $\mathbf{v}(\mathbf{G})$ as $\lambda(\mathbf{G})$ and $\Lambda(\mathbf{G})$; then for all $\xi \in \mathbb{R}_0^{(5d-3)}$

$$0 < \lambda(\mathbf{G})|\xi|^2 \leq \xi_{\mathrm{i}} \mathbf{v}^{\mathrm{ij}}(\mathbf{G}) \xi_{\mathrm{j}} \leq \Lambda(\mathbf{G})|\xi|^2\,. \tag{57}$$

Also by assuming that $\| \mathbf{G} \|_{\mathrm{W}^1_\infty} \leq \alpha$, then there is a positive constant C_α such that

$$0 < C_\alpha < \lambda(\mathbf{G})\,. \tag{58}$$

Let us define

$$\mathbf{Y} = \left\{ \nabla \mathbf{G} \in \left((\mathrm{L}^2(\Omega_{0\mathrm{h}}))^{(5d-3)} \right) |_{\nabla \mathbf{G}_{|\Omega^{\mathrm{e}}} \in \left(\mathrm{H}^1(\Omega_0^{\mathrm{e}})\right)^{(5d-3)} \quad \forall \Omega_0^{\mathrm{e}} \in \Omega_{0\mathrm{h}}} \right\}. \tag{59}$$

In the following analysis, we use the integral form of the Taylor's expansions of $\mathbf{w}(\mathbf{G}, \nabla\mathbf{G}) = \mathbf{v}(\mathbf{G})\nabla\mathbf{G}$, for $(\mathbf{V}, \nabla\mathbf{Q}) \in \mathrm{X}^+ \times \mathbf{Y}$ in terms of $(\mathbf{G}, \nabla\mathbf{G}) \in \mathrm{X}^+ \times \mathbf{Y}$:

$$\begin{aligned} \mathbf{w}(\mathbf{V}, \nabla\mathbf{Q}) - \mathbf{w}(\mathbf{G}, \nabla\mathbf{G}) &= -\mathbf{w}_{\mathbf{G}}(\mathbf{G}, \nabla\mathbf{G})(\mathbf{G} - \mathbf{V}) - \mathbf{w}_{\nabla\mathbf{G}}(\mathbf{G})(\nabla\mathbf{G} - \nabla\mathbf{Q}) + \\ &\quad \bar{\mathbf{R}}_{\mathbf{w}}(\mathbf{G} - \mathbf{V}, \nabla\mathbf{G} - \nabla\mathbf{Q}) \\ &= -\bar{\mathbf{w}}_{\mathbf{G}}(\mathbf{G}, \nabla\mathbf{G})(\mathbf{G} - \mathbf{V}) - \bar{\mathbf{w}}_{\nabla\mathbf{G}}(\mathbf{G})(\nabla\mathbf{G} - \nabla\mathbf{Q})\,, \end{aligned} \tag{60}$$

where $\mathbf{w}_{\mathbf{G}}(\mathbf{G}, \nabla\mathbf{G}) = \mathbf{v}_{\mathbf{G}}(\mathbf{G})\nabla\mathbf{G}$ is the partial derivative of $\mathbf{w}$ with respect to $\mathbf{G}$ (with $\mathbf{v}_{\mathbf{G}}(\mathbf{G})$ the partial derivative of $\mathbf{v}$ with respect to $\mathbf{G}$), $\mathbf{w}_{\nabla\mathbf{G}}(\mathbf{G}) = \mathbf{v}(\mathbf{G})$ is the

partial derivative of $\mathbf{w}$ with respect to $\nabla\mathbf{G}$ expressed in the matrix form (and using Voigt notations), and where $\bar{\mathbf{w}}_{\mathbf{G}}$, $\bar{\mathbf{w}}_{\nabla\mathbf{G}}$, and $\bar{\mathbf{R}}_{\mathbf{w}}$ are the remainder terms, with in particular

$$\begin{aligned}\bar{\mathbf{R}}_{\mathbf{w}}(\mathbf{G}-\mathbf{V},\nabla\mathbf{G}-\nabla\mathbf{Q}) =&(\mathbf{G}-\mathbf{V})^{\mathrm{T}}\bar{\mathbf{w}}_{\mathbf{GG}}(\mathbf{V},\nabla\mathbf{Q})(\mathbf{G}-\mathbf{V})+\\ &2(\mathbf{G}-\mathbf{V})^{\mathrm{T}}\bar{\mathbf{w}}_{\mathbf{G}\nabla\mathbf{G}}(\mathbf{V})(\nabla\mathbf{G}-\nabla\mathbf{Q})\,.\end{aligned} \tag{61}$$

The other remainder terms $\bar{\mathbf{w}}_{\mathbf{G}}$, $\bar{\mathbf{w}}_{\nabla\mathbf{G}}$, $\bar{\mathbf{w}}_{\mathbf{GG}}$, and $\bar{\mathbf{w}}_{\mathbf{G}\nabla\mathbf{G}}$ are given in C.1. Using the definition of $\mathbf{w}$, if $\mathrm{f_T}\geq c^2>0$, then $\bar{\mathbf{w}}_{\mathbf{G}}$, $\bar{\mathbf{w}}_{\mathbf{GG}}\in\mathbf{L}^\infty\left(\Omega\times\mathbb{R}^{(d+1)}\times\mathbb{R}_0^+\times\mathbb{R}^{(5d-3)}\right)$ and $\bar{\mathbf{w}}_{\nabla\mathbf{G}}$, $\bar{\mathbf{w}}_{\mathbf{G}\nabla\mathbf{G}}\in\mathbf{L}^\infty\left(\Omega\times\mathbb{R}^{(d+1)}\times\mathbb{R}_0^+\right)$.

For future use, let us introduce $\mathbf{d}(\mathbf{G},\nabla\mathbf{G})=\tilde{\mathbf{o}}(\mathbf{G})\nabla\mathbf{G}$ a $(d+2)\times 1$ vector, and its partial derivatives $\mathbf{d}_{\nabla\mathbf{G}}(\mathbf{G})=\tilde{\mathbf{o}}(\mathbf{G})$ a $(d+2)\times(5d-3)$ matrix, $\mathbf{d}_{\mathbf{G}}(\mathbf{G},\nabla\mathbf{G})=\tilde{\mathbf{o}}_{\mathbf{G}}(\mathbf{G})\nabla\mathbf{G}$ a $(d+2)\times(d+2)$ matrix, $\mathbf{d}_{\mathbf{GG}}(\mathbf{G},\nabla\mathbf{G})=\tilde{\mathbf{o}}_{\mathbf{GG}}(\mathbf{G})\nabla\mathbf{G}$ a $(d+2)\times(d+2)\times(d+2)$ matrix, and $\mathbf{d}_{\nabla\mathbf{GG}}(\mathbf{G})=\tilde{\mathbf{o}}_{\mathbf{G}}(\mathbf{G})$ a $(d+2)\times(5d-3)\times(d+2)$ matrix. Similarly to Eqs. (60-61), one has

$$\begin{aligned}\mathbf{d}(\mathbf{V},\nabla\mathbf{Q})-\mathbf{d}(\mathbf{G},\nabla\mathbf{G}) =&-\mathbf{d}_{\mathbf{G}}(\mathbf{G},\nabla\mathbf{G})(\mathbf{G}-\mathbf{V})-\mathbf{d}_{\nabla\mathbf{G}}(\mathbf{G})(\nabla\mathbf{G}-\nabla\mathbf{Q})+\\ &\bar{\mathbf{R}}_{\mathbf{d}}(\mathbf{G}-\mathbf{V},\nabla\mathbf{G}-\nabla\mathbf{Q})\\ =&-\bar{\mathbf{d}}_{\mathbf{G}}(\mathbf{G},\nabla\mathbf{G})(\mathbf{G}-\mathbf{V})-\bar{\mathbf{d}}_{\nabla\mathbf{G}}(\mathbf{G})(\nabla\mathbf{G}-\nabla\mathbf{Q})\,,\end{aligned} \tag{62}$$

where

$$\begin{aligned}\bar{\mathbf{R}}_{\mathbf{d}}(\mathbf{G}-\mathbf{V},\nabla\mathbf{G}-\nabla\mathbf{Q}) =&(\mathbf{G}-\mathbf{V})^{\mathrm{T}}\bar{\mathbf{d}}_{\mathbf{GG}}(\mathbf{V},\nabla\mathbf{Q})(\mathbf{G}-\mathbf{V})+\\ &2(\mathbf{G}-\mathbf{V})^{\mathrm{T}}\bar{\mathbf{d}}_{\mathbf{G}\nabla\mathbf{G}}(\mathbf{V})(\nabla\mathbf{G}-\nabla\mathbf{Q})\,.\end{aligned} \tag{63}$$

The other remainder terms $\bar{\mathbf{d}}_{\mathbf{G}}$, $\bar{\mathbf{d}}_{\nabla\mathbf{G}}$, $\bar{\mathbf{d}}_{\mathbf{GG}}$, and $\bar{\mathbf{d}}_{\mathbf{G}\nabla\mathbf{G}}$ are given in C.1. Using the definition of $\mathbf{d}$, if $\mathrm{f_T}\geq c^2>0$, then $\bar{\mathbf{d}}_{\mathbf{G}}$, $\bar{\mathbf{d}}_{\mathbf{GG}}\in\mathbf{L}^\infty\left(\Omega\times\mathbb{R}^{(d+1)}\times\mathbb{R}_0^+\times\mathbb{R}^{(5d-3)}\right)$ and $\bar{\mathbf{d}}_{\nabla\mathbf{G}}$, $\bar{\mathbf{d}}_{\mathbf{G}\nabla\mathbf{G}}$, $\in\mathbf{L}^\infty\left(\Omega\times\mathbb{R}^{(d+2)}\times\mathbb{R}_0^+\right)$.

Finally, we also define the $(5d-3)\times 1$ vector $\mathbf{p}(\mathbf{G})=\mathbf{o}(\mathbf{G})\mathbf{G}$ and its first and second derivatives $\mathbf{p}_{\mathbf{G}}(\mathbf{G})$ of size $(5d-3)\times(d+2)$ and $\mathbf{p}_{\mathbf{GG}}(\mathbf{G})$ of size $(5d-3)\times(d+2)\times(d+2)$ respectively. The Taylor's expansion of this last vector reads

$$\mathbf{p}(\mathbf{V})-\mathbf{p}(\mathbf{G})=-\mathbf{p}_{\mathbf{G}}(\mathbf{G})(\mathbf{G}-\mathbf{V})+\bar{\mathbf{R}}_{\mathbf{p}}(\mathbf{G}-\mathbf{V})=-\bar{\mathbf{p}}_{\mathbf{G}}(\mathbf{G})(\mathbf{G}-\mathbf{V})\,, \tag{64}$$

where

$$\bar{\mathbf{R}}_{\mathbf{p}}(\mathbf{G}-\mathbf{V})=(\mathbf{G}-\mathbf{V})^{\mathrm{T}}\bar{\mathbf{p}}_{\mathbf{GG}}(\mathbf{V})(\mathbf{G}-\mathbf{V})\,, \tag{65}$$

with the other remainder terms $\bar{\mathbf{p}}_{\mathbf{G}}$ and $\bar{\mathbf{p}}_{\mathbf{GG}}$ given in C.1. Using the definition of $\mathbf{p}$, if $\mathrm{f_T}\geq c^2>0$, then $\bar{\mathbf{p}}_{\mathbf{G}}$, $\bar{\mathbf{p}}_{\mathbf{GG}}$, $\in\mathbf{L}^\infty\left(\Omega\times\mathbb{R}^{(d+1)}\times\mathbb{R}_0^+\right)$. However, one has $\mathbf{p}_{\mathbf{G}}^{\mathrm{T}}=\frac{\partial(\mathbf{G}^{\mathrm{T}}\mathbf{o}^{\mathrm{T}}(\mathbf{G}))}{\partial\mathbf{G}}=\mathbf{G}^{\mathrm{T}}\frac{\partial\mathbf{o}^{\mathrm{T}}(\mathbf{G})}{\partial\mathbf{G}}+\mathbf{o}^{\mathrm{T}}(\mathbf{G})$, which once computed explicitly as to derive Eq. (45) leads to $\mathbf{p}_{\mathbf{G}}=-\mathbf{o}(\mathbf{G})$, and Eq. (65) becomes

$$\bar{\mathbf{R}}_{\mathbf{p}}(\mathbf{G}-\mathbf{V})=-(\mathbf{G}-\mathbf{V})\bar{\mathbf{o}}_{\mathbf{G}}(\mathbf{V})(\mathbf{G}-\mathbf{V})\,. \tag{66}$$

Since for $\mathrm{f_T}\geq c^2>0$, $\mathbf{w}$, $\mathbf{o}$, and $\mathbf{d}$ are twice continuously differentiable function with all the derivatives through the second order locally bounded in a ball around $\mathbf{G}\in[\mathbb{R}]^d\times\mathbb{R}\times\mathbb{R}_0^+$ as it will be shown in Section 4.5, we denote by C_{y}

$$\begin{aligned}C_{\mathrm{y}}=&\max\Big\{\|\,\mathbf{w},\mathbf{d}\,\|_{\mathrm{W}^2_\infty(\Omega\times\mathbb{R}^{(d+1)}\times\mathbb{R}_0^+\times\mathbb{R}^{(5d-3)})},\\ &\|\,\bar{\mathbf{w}}_{\mathbf{G}},\bar{\mathbf{w}}_{\mathbf{GG}},\bar{\mathbf{d}}_{\mathbf{G}},\bar{\mathbf{d}}_{\mathbf{GG}}\,\|_{\mathrm{L}^\infty(\Omega\times\mathbb{R}^{(d+1)}\times\mathbb{R}_0^+\times\mathbb{R}^{(5d-3)})}\\ &\|\,\bar{\mathbf{w}}_{\nabla\mathbf{G}},\bar{\mathbf{w}}_{\mathbf{G}\nabla\mathbf{G}},\bar{\mathbf{o}}_{\mathbf{G}},\bar{\mathbf{d}}_{\nabla\mathbf{G}},\bar{\mathbf{d}}_{\nabla\mathbf{GG}}\,\|_{\mathrm{L}^\infty(\Omega\times\mathbb{R}^{(d+1)}\times\mathbb{R}_0^+)}\Big\}.\end{aligned} \tag{67}$$

Let us define the solution $\mathbf{G}^{\mathrm{e}} \in \left[\mathrm{H}^2(\Omega)\right]^d \times \mathrm{H}^2(\Omega) \times \mathrm{H}^{2^+}(\Omega)$ of the strong form stated by Eqs. (41-43). Since $[\![\mathbf{G}^{\mathrm{e}}_{\mathbf{n}}]\!] = 0$ on $\partial_{\mathrm{I}}\Omega^{\mathrm{e}}$ and $[\![\mathbf{G}^{\mathrm{e}}_{\mathbf{n}}]\!] = -\mathbf{G}^{\mathrm{e}}_{\mathbf{n}} = -\bar{\mathbf{G}}_{\mathbf{n}}$ on $\partial_{\mathrm{D}}\Omega^{\mathrm{e}}$, and since Eq. (48) satisfies the consistency condition, we have

$$\begin{aligned}
&\mathrm{a}(\mathbf{G}^{\mathrm{e}}, \delta\mathbf{G}) = \int_{\Omega_{\mathrm{h}}} (\nabla\delta\mathbf{G})^{\mathrm{T}} \mathbf{w}(\mathbf{G}^{\mathrm{e}}, \nabla\mathbf{G}^{\mathrm{e}}) \mathrm{d}\Omega + \int_{\Omega_{\mathrm{h}}} \delta\mathbf{G}^{\mathrm{T}} \tilde{\mathbf{o}}(\mathbf{G}^{\mathrm{e}}) \nabla\mathbf{G}^{\mathrm{e}} \mathrm{d}\Omega + \\
&\int_{\partial_{\mathrm{I}}\Omega_{\mathrm{h}}} \left[\!\left[\delta\mathbf{G}^{\mathrm{T}}_{\mathbf{n}}\right]\!\right] \langle \mathbf{w}(\mathbf{G}^{\mathrm{e}}, \nabla\mathbf{G}^{\mathrm{e}}) \rangle \, \mathrm{dS} - \int_{\partial_{\mathrm{D}}\Omega_{\mathrm{h}}} \delta\mathbf{G}^{\mathrm{T}}_{\mathbf{n}} \mathbf{w}(\mathbf{G}^{\mathrm{e}}, \nabla\mathbf{G}^{\mathrm{e}}) \mathrm{dS} - \\
&\int_{\partial_{\mathrm{D}}\Omega_{\mathrm{h}}} \mathbf{G}^{\mathrm{e}^{\mathrm{T}}}_{\mathbf{n}} \mathbf{v}(\mathbf{G}^{\mathrm{e}}) \nabla\delta\mathbf{G} \mathrm{dS} + \int_{\partial_{\mathrm{D}}\Omega_{\mathrm{h}}} \mathbf{G}^{\mathrm{e}^{\mathrm{T}}}_{\mathbf{n}} \frac{\mathbf{v}(\mathbf{G}^{\mathrm{e}})\mathcal{B}}{h_{\mathrm{s}}} \delta\mathbf{G}_{\mathbf{n}} \mathrm{dS} + \\
&\int_{\partial_{\mathrm{D}}\Omega_{\mathrm{h}}} \delta\mathbf{G}^{\mathrm{T}}_{\mathbf{n}} (\mathbf{o}(\mathbf{G}^{\mathrm{e}})\mathbf{G}^{\mathrm{e}} - \mathbf{o}_0\mathbf{G}_0) \mathrm{dS} = \mathrm{b}(\delta\mathbf{G}) \quad \forall \delta\mathbf{G} \in \mathrm{X},
\end{aligned} \tag{68}$$

with

$$\begin{aligned}
\mathrm{b}(\delta\mathbf{G}) = &- \int_{\partial_{\mathrm{D}}\Omega_{\mathrm{h}}} \bar{\mathbf{G}}^{\mathrm{T}}_{\mathbf{n}} \left(\mathbf{v}(\bar{\mathbf{G}}) \nabla\delta\mathbf{G}\right) \mathrm{dS} + \int_{\partial_{\mathrm{D}}\Omega_{\mathrm{h}}} \delta\mathbf{G}^{\mathrm{T}}_{\mathbf{n}} (\mathbf{o}(\bar{\mathbf{G}})\bar{\mathbf{G}} - \mathbf{o}_0\mathbf{G}_0) \mathrm{dS} + \\
&\int_{\partial_{\mathrm{D}}\Omega_{\mathrm{h}}} \delta\mathbf{G}^{\mathrm{T}}_{\mathbf{n}} \left(\frac{\mathcal{B}}{h_{\mathrm{s}}} \mathbf{v}(\bar{\mathbf{G}})\right) \bar{\mathbf{G}}_{\mathbf{n}} \mathrm{dS}.
\end{aligned} \tag{69}$$

Therefore, using $\delta\mathbf{G} = \delta\mathbf{G}_{\mathrm{h}} \in \mathrm{X}^k$ in Eq. (68), subtracting the DG discretization (48) from Eq. (68), then adding and subtracting successively the two terms $\int_{\partial_{\mathrm{I}}\Omega_{\mathrm{h}}} \left[\!\left[\mathbf{G}^{\mathrm{e}^{\mathrm{T}}}_{\mathbf{n}} - \mathbf{G}^{\mathrm{T}}_{\mathrm{h}_{\mathbf{n}}}\right]\!\right] \langle \mathbf{w}_{\nabla\mathbf{G}}(\mathbf{G}^{\mathrm{e}}) \nabla\delta\mathbf{G}_{\mathrm{h}} \rangle \, \mathrm{dS}$, and $\int_{\partial_{\mathrm{I}}\Omega_{\mathrm{h}}} \left[\!\left[\mathbf{G}^{\mathrm{e}^{\mathrm{T}}}_{\mathbf{n}} - \mathbf{G}^{\mathrm{T}}_{\mathrm{h}_{\mathbf{n}}}\right]\!\right] \left\langle \frac{\mathcal{B}}{\mathrm{h_s}} \mathbf{w}_{\nabla\mathbf{G}}(\mathbf{G}^{\mathrm{e}}) \right\rangle [\![\delta\mathbf{G}_{\mathrm{h}_{\mathbf{n}}}]\!] \, \mathrm{dS}$ to this last relation, and using $[\![\mathbf{o}(\mathbf{G}^{\mathrm{e}})\mathbf{G}^{\mathrm{e}} - \mathbf{o}_0\mathbf{G}_0]\!] = 0$, $[\![\mathbf{G}^{\mathrm{e}}_{\mathbf{n}}]\!] = 0$ on $\partial_{\mathrm{I}}\Omega_{\mathrm{h}}$, and $[\![\mathbf{G}^{\mathrm{e}}_{\mathbf{n}}]\!] = -\mathbf{G}^{\mathrm{e}}_{\mathbf{n}} = -\bar{\mathbf{G}}_{\mathbf{n}}$, $[\![\mathbf{o}(\mathbf{G}^{\mathrm{e}})\mathbf{G}^{\mathrm{e}} - \mathbf{o}_0\mathbf{G}_0]\!] = -\mathbf{o}(\bar{\mathbf{G}})\bar{\mathbf{G}} + \mathbf{o}_0\mathbf{G}_0$ on $\partial_{\mathrm{D}}\Omega_{\mathrm{h}}$, one gets

$$\begin{aligned}
0 = &\int_{\Omega_{\mathrm{h}}} \left(\nabla\delta\mathbf{G}_{\mathrm{h}}\right)^{\mathrm{T}} \left(\mathbf{w}(\mathbf{G}^{\mathrm{e}}, \nabla\mathbf{G}^{\mathrm{e}}) - \mathbf{w}(\mathbf{G}_{\mathrm{h}}, \nabla\mathbf{G}_{\mathrm{h}})\right) \mathrm{d}\Omega \\
&+ \int_{\Omega_{\mathrm{h}}} \delta\mathbf{G}^{\mathrm{T}}_{\mathrm{h}} \left(\tilde{\mathbf{o}}(\mathbf{G}^{\mathrm{e}}) \nabla\mathbf{G}^{\mathrm{e}} - \tilde{\mathbf{o}}(\mathbf{G}_{\mathrm{h}}) \nabla\mathbf{G}_{\mathrm{h}}\right) \mathrm{d}\Omega \\
&+ \int_{\partial_{\mathrm{I}}\Omega_{\mathrm{h}} \cup \partial_{\mathrm{D}}\Omega_{\mathrm{h}}} \left[\!\left[\delta\mathbf{G}^{\mathrm{T}}_{\mathrm{h}_{\mathbf{n}}}\right]\!\right] \langle \mathbf{w}(\mathbf{G}^{\mathrm{e}}, \nabla\mathbf{G}^{\mathrm{e}}) - \mathbf{w}(\mathbf{G}_{\mathrm{h}}, \nabla\mathbf{G}_{\mathrm{h}}) \rangle \, \mathrm{dS} \\
&+ \int_{\partial_{\mathrm{I}}\Omega_{\mathrm{h}} \cup \partial_{\mathrm{D}}\Omega_{\mathrm{h}}} \left[\!\left[\mathbf{G}^{\mathrm{e}^{\mathrm{T}}}_{\mathbf{n}} - \mathbf{G}^{\mathrm{T}}_{\mathrm{h}_{\mathbf{n}}}\right]\!\right] \langle \mathbf{w}_{\nabla\mathbf{G}}(\mathbf{G}^{\mathrm{e}}) \nabla\delta\mathbf{G}_{\mathrm{h}} \rangle \, \mathrm{dS} \\
&- \int_{\partial_{\mathrm{I}}\Omega_{\mathrm{h}} \cup \partial_{\mathrm{D}}\Omega_{\mathrm{h}}} \left[\!\left[\mathbf{G}^{\mathrm{e}^{\mathrm{T}}} \mathbf{o}^{\mathrm{T}}(\mathbf{G}^{\mathrm{e}}) - \mathbf{G}^{\mathrm{T}}_{\mathrm{h}} \mathbf{o}^{\mathrm{T}}(\mathbf{G}_{\mathrm{h}})\right]\!\right] \langle \delta\mathbf{G}_{\mathrm{h}_{\mathbf{n}}} \rangle \, \mathrm{dS} \\
&- \int_{\partial_{\mathrm{I}}\Omega_{\mathrm{h}}} \left[\!\left[\mathbf{G}^{\mathrm{e}^{\mathrm{T}}}_{\mathbf{n}} - \mathbf{G}^{\mathrm{T}}_{\mathrm{h}_{\mathbf{n}}}\right]\!\right] \langle (\mathbf{w}_{\nabla\mathbf{G}}(\mathbf{G}^{\mathrm{e}}) - \mathbf{w}_{\nabla\mathbf{G}}(\mathbf{G}_{\mathrm{h}})) \nabla\delta\mathbf{G}_{\mathrm{h}} \rangle \, \mathrm{dS} \\
&+ \int_{\partial_{\mathrm{I}}\Omega_{\mathrm{h}} \cup \partial_{\mathrm{D}}\Omega_{\mathrm{h}}} \left[\!\left[\mathbf{G}^{\mathrm{e}^{\mathrm{T}}}_{\mathbf{n}} - \mathbf{G}^{\mathrm{T}}_{\mathrm{h}_{\mathbf{n}}}\right]\!\right] \left\langle \frac{\mathcal{B}}{\mathrm{h_s}} \mathbf{w}_{\nabla\mathbf{G}}(\mathbf{G}^{\mathrm{e}}) \right\rangle [\![\delta\mathbf{G}_{\mathrm{h}_{\mathbf{n}}}]\!] \, \mathrm{dS} \\
&- \int_{\partial_{\mathrm{I}}\Omega_{\mathrm{h}}} \left[\!\left[\mathbf{G}^{\mathrm{e}^{\mathrm{T}}}_{\mathbf{n}} - \mathbf{G}^{\mathrm{T}}_{\mathrm{h}_{\mathbf{n}}}\right]\!\right] \left\langle \frac{\mathcal{B}}{\mathrm{h_s}} (\mathbf{w}_{\nabla\mathbf{G}}(\mathbf{G}^{\mathrm{e}}) - \mathbf{w}_{\nabla\mathbf{G}}(\mathbf{G}_{\mathrm{h}})) \right\rangle [\![\delta\mathbf{G}_{\mathrm{h}_{\mathbf{n}}}]\!] \, \mathrm{dS} \quad \forall \delta\mathbf{G}_{\mathrm{h}} \in \mathrm{X}^k.
\end{aligned} \tag{70}$$

Therefore, by applying the Taylor's expansion (60-66) to the first, second, third, and fifth terms of Eq. (70), see C.2 for details, the latter expression is rewritten

as finding $\mathbf{G}_\mathrm{h} \in \mathrm{X}^{k^+}$ such that:

$$\mathcal{A}(\mathbf{G}^\mathrm{e}; \mathbf{G}^\mathrm{e} - \mathbf{G}_\mathrm{h}, \delta\mathbf{G}_\mathrm{h}) + \mathcal{B}(\mathbf{G}^\mathrm{e}; \mathbf{G}^\mathrm{e} - \mathbf{G}_\mathrm{h}, \delta\mathbf{G}_\mathrm{h}) = \mathcal{N}(\mathbf{G}^\mathrm{e}, \mathbf{G}_\mathrm{h}; \delta\mathbf{G}_\mathrm{h}) \quad \forall \delta\mathbf{G}_\mathrm{h} \in \mathrm{X}^k \,. \tag{71}$$

In this last expression, we have defined for given $\boldsymbol{\psi} \in \mathrm{X}^+, \boldsymbol{\omega} \in \mathrm{X}$ and $\delta\boldsymbol{\omega} \in \mathrm{X}$ the following forms:

$$\begin{aligned}\mathcal{A}(\boldsymbol{\psi}; \boldsymbol{\omega}, \delta\boldsymbol{\omega}) = &\int_{\Omega_\mathrm{h}} \nabla\delta\boldsymbol{\omega}^\mathrm{T} \mathbf{w}_{\nabla\boldsymbol{\psi}}(\boldsymbol{\psi}) \nabla\boldsymbol{\omega} \mathrm{d}\Omega + \int_{\partial_\mathrm{I}\Omega_\mathrm{h} \cup \partial_\mathrm{D}\Omega_\mathrm{h}} \left[\!\left[\delta\boldsymbol{\omega}_\mathbf{n}^\mathrm{T} \right]\!\right] \langle \mathbf{w}_{\nabla\boldsymbol{\psi}}(\boldsymbol{\psi}) \nabla\boldsymbol{\omega} \rangle \,\mathrm{dS} + \\ &\int_{\partial_\mathrm{I}\Omega_\mathrm{h} \cup \partial_\mathrm{D}\Omega_\mathrm{h}} \left[\!\left[\boldsymbol{\omega}_\mathbf{n}^\mathrm{T} \right]\!\right] \langle \mathbf{w}_{\nabla\boldsymbol{\psi}}(\boldsymbol{\psi}) \nabla\delta\boldsymbol{\omega} \rangle \,\mathrm{dS} + \\ &\int_{\partial_\mathrm{I}\Omega_\mathrm{h} \cup \partial_\mathrm{D}\Omega_\mathrm{h}} \left[\!\left[\boldsymbol{\omega}_\mathbf{n}^\mathrm{T} \right]\!\right] \left\langle \frac{\mathcal{B}}{h_\mathrm{s}} \mathbf{w}_{\nabla\boldsymbol{\psi}}(\boldsymbol{\psi}) \right\rangle [\![\delta\boldsymbol{\omega}_\mathbf{n}]\!] \,\mathrm{dS} \,,\end{aligned} \tag{72}$$

$$\begin{aligned}\mathcal{B}(\boldsymbol{\psi}; \boldsymbol{\omega}, \delta\boldsymbol{\omega}) = &\int_{\Omega_\mathrm{h}} \nabla\delta\boldsymbol{\omega}^\mathrm{T} \left(\mathbf{w}_{\boldsymbol{\psi}}(\boldsymbol{\psi}, \nabla\boldsymbol{\psi}) \boldsymbol{\omega} \right) \mathrm{d}\Omega + \int_{\Omega_\mathrm{h}} \delta\boldsymbol{\omega}^\mathrm{T} \mathbf{d}_{\nabla\boldsymbol{\psi}}(\boldsymbol{\psi}) \nabla\boldsymbol{\omega} \mathrm{d}\Omega + \\ &\int_{\partial_\mathrm{I}\Omega_\mathrm{h} \cup \partial_\mathrm{D}\Omega_\mathrm{h}} \left[\!\left[\delta\boldsymbol{\omega}_\mathbf{n}^\mathrm{T} \right]\!\right] \langle \mathbf{w}_{\boldsymbol{\psi}}(\boldsymbol{\psi}, \nabla\boldsymbol{\psi}) \boldsymbol{\omega} \rangle \,\mathrm{dS} + \int_{\Omega_\mathrm{h}} \delta\boldsymbol{\omega}^\mathrm{T} \mathbf{d}_{\boldsymbol{\psi}}(\boldsymbol{\psi}, \nabla\boldsymbol{\psi}) \boldsymbol{\omega} \mathrm{d}\Omega + \\ &\int_{\partial_\mathrm{I}\Omega_\mathrm{h} \cup \partial_\mathrm{D}\Omega_\mathrm{h}} \left[\!\left[\boldsymbol{\omega}_\mathbf{n}^\mathrm{T} \mathbf{d}_{\nabla\boldsymbol{\psi}}^\mathrm{T}(\boldsymbol{\psi}) \right]\!\right] \langle \delta\boldsymbol{\omega} \rangle \,\mathrm{dS} \,,\end{aligned} \tag{73}$$

which gather the terms such that for fixed $\boldsymbol{\psi}$, the form $\mathcal{A}(\boldsymbol{\psi}; .,.)$ and the form $\mathcal{B}(\boldsymbol{\psi}; .,.)$ are bi-linear. The non-linear terms have been gathered in $\mathcal{N}(\mathbf{G}^\mathrm{e}, \mathbf{G}_\mathrm{h}; \delta\mathbf{G}_\mathrm{h})$ as

$$\begin{aligned}\mathcal{N}(\mathbf{G}^\mathrm{e}, \mathbf{G}_\mathrm{h}; \delta\mathbf{G}_\mathrm{h}) = &\int_{\Omega_\mathrm{h}} (\nabla\delta\mathbf{G}_\mathrm{h})^\mathrm{T} (\bar{\mathbf{R}}_\mathbf{w}(\mathbf{G}^\mathrm{e} - \mathbf{G}_\mathrm{h}, \nabla\mathbf{G}^\mathrm{e} - \nabla\mathbf{G}_\mathrm{h})) \mathrm{d}\Omega \\ &+ \int_{\partial_\mathrm{I}\Omega_\mathrm{h} \cup \partial_\mathrm{D}\Omega_\mathrm{h}} \left[\!\left[\delta\mathbf{G}_{\mathrm{h}_\mathbf{n}}^\mathrm{T} \right]\!\right] \left\langle \bar{\mathbf{R}}_\mathbf{w}(\mathbf{G}^\mathrm{e} - \mathbf{G}_\mathrm{h}, \nabla\mathbf{G}^\mathrm{e} - \nabla\mathbf{G}_\mathrm{h}) \right\rangle \mathrm{dS} \\ &+ \int_{\partial_\mathrm{I}\Omega_\mathrm{h}} \left[\!\left[\mathbf{G}_\mathbf{n}^{\mathrm{e}^\mathrm{T}} - \mathbf{G}_{\mathrm{h}_\mathbf{n}}^\mathrm{T} \right]\!\right] \langle (\mathbf{w}_{\nabla\mathbf{G}}(\mathbf{G}^\mathrm{e}) - \mathbf{w}_{\nabla\mathbf{G}}(\mathbf{G}_\mathrm{h})) \nabla\delta\mathbf{G}_\mathrm{h} \rangle \,\mathrm{dS} \\ &+ \int_{\partial_\mathrm{I}\Omega_\mathrm{h}} \left[\!\left[\mathbf{G}_\mathbf{n}^{\mathrm{e}^\mathrm{T}} - \mathbf{G}_{\mathrm{h}_\mathbf{n}}^\mathrm{T} \right]\!\right] \left\langle \frac{\mathcal{B}}{h_\mathrm{s}} (\mathbf{w}_{\nabla\mathbf{G}}(\mathbf{G}^\mathrm{e}) - \mathbf{w}_{\nabla\mathbf{G}}(\mathbf{G}_\mathrm{h})) \right\rangle [\![\delta\mathbf{G}_{\mathrm{h}_\mathbf{n}}]\!] \,\mathrm{dS} \\ &+ \int_{\partial_\mathrm{I}\Omega_\mathrm{h} \cup \partial_\mathrm{D}\Omega_\mathrm{h}} \left[\!\left[(\mathbf{G}^\mathrm{e} - \mathbf{G}_\mathrm{h})^\mathrm{T} \bar{\mathbf{o}}_\mathbf{G}^\mathrm{T}(\mathbf{G}_\mathrm{h}) (\mathbf{G}^\mathrm{e} - \mathbf{G}_\mathrm{h}) \right]\!\right] \langle \delta\mathbf{G}_{\mathrm{h}_\mathbf{n}} \rangle \,\mathrm{dS} \\ &+ \int_{\Omega_\mathrm{h}} \delta\mathbf{G}_\mathrm{h}^\mathrm{T} \bar{\mathbf{R}}_\mathbf{d}(\mathbf{G}^\mathrm{e} - \mathbf{G}_\mathrm{h}, \nabla\mathbf{G}^\mathrm{e} - \nabla\mathbf{G}_\mathrm{h}) \mathrm{d}\Omega \\ &= \mathcal{I}_1 + \mathcal{I}_2 + \mathcal{I}_3 + \mathcal{I}_4 + \mathcal{I}_5 + \mathcal{I}_6 \,.\end{aligned} \tag{74}$$

Compared with the fixed form from Gudi *et al.* [23] for non-linear elliptic problems, the formulations $\mathcal{A}$ and $\mathcal{B}$ are similar, except the last term of $\mathcal{B}(\boldsymbol{\psi}; .,.)$ in which $\mathbf{d}_{\nabla\boldsymbol{\psi}}(\boldsymbol{\psi})$ appears in the $[\![\cdot]\!]$ operator instead of the $\langle\cdot\rangle$ operator. Nevertheless, this term becomes identical with the one in Gudi *et al.* [23] for fixed $\boldsymbol{\psi}$. However the $\mathcal{N}$ is different in the fifth and sixth terms, *i.e.* $\mathcal{I}_5$ and $\mathcal{I}_6$, so they will require

a different treatment. Therefore in the following, we report the methodology developed by Gudi *et al.* [23] without demonstration, except when these two terms $\mathcal{I}_5$ and $\mathcal{I}_6$ explicitly appear, in which case the related demonstration is reported in Appendix.

4.5 Solution uniqueness

Let us first define the mesh dependent norms, which will be considered in the following analysis, for $\mathbf{G} \in \mathrm{X}$

$$|||\ \mathbf{G}\ |||_*^2 = \sum_{\mathrm{e}} \|\nabla \mathbf{G}\|^2_{\mathrm{L}^2(\Omega^{\mathrm{e}})} + \sum_{\mathrm{e}} h_{\mathrm{s}}^{-1} \|\ [\![\mathbf{G}_{\mathbf{n}}]\!]\ \|^2_{\mathrm{L}^2(\partial\Omega^{\mathrm{e}})}, \tag{75}$$

$$|||\ \mathbf{G}\ |||^2 = \sum_{\mathrm{e}} \|\mathbf{G}\|^2_{\mathrm{H}^1(\Omega^{\mathrm{e}})} + \sum_{\mathrm{e}} h_{\mathrm{s}}^{-1} \|\ [\![\mathbf{G}_{\mathbf{n}}]\!]\ \|^2_{\mathrm{L}^2(\partial\Omega^{\mathrm{e}})}, \tag{76}$$

and

$$|||\ \mathbf{G}\ |||_1^2 = \sum_{\mathrm{e}} \|\mathbf{G}\|^2_{\mathrm{H}^1(\Omega^{\mathrm{e}})} + \sum_{\mathrm{e}} h_{\mathrm{s}}\ \|\ \mathbf{G}\ \|^2_{\mathrm{H}^1(\partial\Omega^{\mathrm{e}})} + \sum_{\mathrm{e}} h_{\mathrm{s}}^{-1} \|\ [\![\mathbf{G}_{\mathbf{n}}]\!]\ \|^2_{\mathrm{L}^2(\partial\Omega^{\mathrm{e}})}\,. \tag{77}$$

Let us first assume $\boldsymbol{\eta} = \mathrm{I_h}\mathbf{G} - \mathbf{G}^{\mathrm{e}} \in \mathrm{X}$, with $\mathrm{I_h}\mathbf{G} \in \mathrm{X}^{k^+}$ the interpolant of $\mathbf{G}^{\mathrm{e}}$ in X^{k^+}. The last relation (71) thus becomes

$$\begin{aligned}\mathcal{A}(\mathbf{G}^{\mathrm{e}}; \mathrm{I_h}\mathbf{G} - \mathbf{G}_{\mathrm{h}}, \delta\mathbf{G}_{\mathrm{h}}) + \mathcal{B}(\mathbf{G}^{\mathrm{e}}; \mathrm{I_h}\mathbf{G} - \mathbf{G}_{\mathrm{h}}, \delta\mathbf{G}_{\mathrm{h}}) &= \mathcal{A}(\mathbf{G}^{\mathrm{e}}; \boldsymbol{\eta}, \delta\mathbf{G}_{\mathrm{h}}) + \mathcal{B}(\mathbf{G}^{\mathrm{e}}; \boldsymbol{\eta}, \delta\mathbf{G}_{\mathrm{h}}) \\ &\quad + \mathcal{N}(\mathbf{G}^{\mathrm{e}}, \mathbf{G}_{\mathrm{h}}; \delta\mathbf{G}_{\mathrm{h}}) \quad \forall \delta\mathbf{G}_{\mathrm{h}} \in \mathrm{X}^k.\end{aligned} \tag{78}$$

Now in order to prove the existence of a solution $\mathbf{G}_{\mathrm{h}}$ of the problem stated by Eq. (70), which corresponds to the DG finite element discretization (48), we state the problem in the fixed point formulation and we define a map $\mathrm{S_h} : \mathrm{X}^{k^+} \to \mathrm{X}^{k^+}$ as follows: for a given $\mathbf{y} \in \mathrm{X}^{k^+}$, find $\mathrm{S_h}(\mathbf{y}) = \mathbf{G}_{\mathbf{y}} \in \mathrm{X}^{k^+}$, such that

$$\begin{aligned}\mathcal{A}(\mathbf{G}^{\mathrm{e}}; \mathrm{I_h}\mathbf{G} - \mathbf{G}_{\mathbf{y}}, \delta\mathbf{G}_{\mathrm{h}}) + \mathcal{B}(\mathbf{G}^{\mathrm{e}}; \mathrm{I_h}\mathbf{G} - \mathbf{G}_{\mathbf{y}}, \delta\mathbf{G}_{\mathrm{h}}) &= \mathcal{A}(\mathbf{G}^{\mathrm{e}}; \boldsymbol{\eta}, \boldsymbol{\delta}\mathbf{G}_{\mathrm{h}}) + \mathcal{B}(\mathbf{G}^{\mathrm{e}}; \boldsymbol{\eta}, \delta\mathbf{G}_{\mathrm{h}}) \\ &\quad + \mathcal{N}(\mathbf{G}^{\mathrm{e}}, \mathbf{y}; \delta\mathbf{G}_{\mathrm{h}}) \quad \forall \delta\mathbf{G}_{\mathrm{h}} \in \mathrm{X}^k.\end{aligned} \tag{79}$$

The existence of a unique solution $\mathbf{G}_{\mathrm{h}}$ of the discrete problem (48) is equivalent to the existence of a fixed point of the map $\mathrm{S_h}$, see [23].

For the subsequent analysis, we denote by C^k, a positive generic constant which is independent of the mesh size, but which does depend on the polynomial approximation degree k. We also use several Lemmata reported in C.3.

Lemma 1 (Lower bound) *For $\mathcal{B}$ larger than a constant, which depends on the polynomial approximation, there exist two constants C_1^k and C_2^k, such that*

$$\begin{aligned}\mathcal{A}(\boldsymbol{G}^e; \delta\boldsymbol{G}_h, \delta\boldsymbol{G}_h) + \mathcal{B}(\boldsymbol{G}^e; \delta\boldsymbol{G}_h, \delta\boldsymbol{G}_h) \geq C_1^k\ |||\ \delta\boldsymbol{G}_h\ |||_*^2 - C_2^k\ \|\ \delta\boldsymbol{G}_h\ \|^2_{L^2(\Omega)} \\ \forall \delta\boldsymbol{G}_h \in X^k,\end{aligned} \tag{80}$$

$$\begin{aligned}\mathcal{A}(\boldsymbol{G}^e; \delta\boldsymbol{G}_h, \delta\boldsymbol{G}_h) + \mathcal{B}(\boldsymbol{G}^e; \delta\boldsymbol{G}_h, \delta\boldsymbol{G}_h) \geq C_1^k\ |||\ \delta\boldsymbol{G}_h\ |||^2 - C_2^k\ \|\ \delta\boldsymbol{G}_h\ \|^2_{L^2(\Omega)} \\ \forall \delta\boldsymbol{G}_h \in X^k.\end{aligned} \tag{81}$$

Using the bounds (58) and (67), the Cauchy-Schwartz' inequality, the trace inequality on the finite element space, see Lemma 7, the trace inequality, see Lemma 6, and the inverse inequality, see Lemma 8, the ξ-inequality $-\xi > 0 : |ab| \leq \frac{\xi}{4}a^2 + \frac{1}{\xi}b^2$, as in Wheeler *et al.* [69] and Prudhomme *et al.* [52] analyzes, yields to prove this Lemma. The two constants C_1^k, C_2^k are independent of the mesh size, but require the stability parameter $\mathcal{B}$ to be larger than a constant, which depends on the polynomial degree, $\mathcal{B} > C^k$, to be positive .

Lemma 2 (Upper bound) *There exist $C > 0$ and $C^k > 0$ such that*

$$| \mathcal{A}(\boldsymbol{G}^e; \boldsymbol{m}, \delta\boldsymbol{G}) + \mathcal{B}(\boldsymbol{G}^e; \boldsymbol{m}, \delta\boldsymbol{G}) | \leq C \,|||\, \boldsymbol{m} \,|||_1 \,|||\, \delta\boldsymbol{G} \,|||_1 \quad \forall \boldsymbol{m},\, \delta\boldsymbol{G} \in X, \tag{82}$$

$$| \mathcal{A}(\boldsymbol{G}^e; \boldsymbol{m}, \delta\boldsymbol{G}_h) + \mathcal{B}(\boldsymbol{G}^e; \boldsymbol{m}, \delta\boldsymbol{G}_h) | \leq C^k \,|||\, \boldsymbol{m} \,|||_1 \,|||\, \delta\boldsymbol{G}_h \,||| \quad \forall \boldsymbol{m} \in X,\, \delta\boldsymbol{G}_h \in X^k, \tag{83}$$

$$| \mathcal{A}(\boldsymbol{G}^e; \boldsymbol{m}_h, \delta\boldsymbol{G}_h) + \mathcal{B}(\boldsymbol{G}^e; \boldsymbol{m}_h, \delta\boldsymbol{G}_h) | \leq C^k \,|||\, \boldsymbol{m}_h \,||| \,|||\, \delta\boldsymbol{G}_h \,||| \quad \forall \boldsymbol{m}_h,\, \delta\boldsymbol{G}_h \in X^k. \tag{84}$$

Applying the Hölder's inequality and the bound (67) on each term of $\mathcal{A}(\mathbf{G}^e; \mathbf{m}, \delta\mathbf{G}) + \mathcal{B}(\mathbf{G}^e; \mathbf{m}, \delta\mathbf{G})$, then making use of the Cauchy-Schwartz' inequality, lead to the relation (82). Finally, Eqs. (83) and (84) are easily obtained from the relation between the energy norms on the finite element space, Lemma 9.

Using Lemma 1 and Lemma 2, the stability of the method is demonstrated through the following Lemmata.

Lemma 3 (Auxiliary problem) *We consider the following auxiliary problem, with $\boldsymbol{\phi} \in \left(L^2(\Omega)\right)^{d+2}$:*

$$\begin{aligned} -\nabla^T(\boldsymbol{w}_{\nabla\boldsymbol{G}}(\boldsymbol{G}^e)\nabla\boldsymbol{\psi} + \boldsymbol{w}_{\boldsymbol{G}}(\boldsymbol{G}^e, \nabla\boldsymbol{G}^e)\boldsymbol{\psi}) + \boldsymbol{d}_{\nabla\boldsymbol{G}}(\boldsymbol{G}^e)\nabla\boldsymbol{\psi} + \boldsymbol{d}_{\boldsymbol{G}}(\boldsymbol{G}^e, \nabla\boldsymbol{G}^e)\boldsymbol{\psi} = \boldsymbol{\phi} \quad &\text{on } \Omega, \\ \boldsymbol{\psi} = 0 \quad &\text{on } \partial\Omega. \end{aligned} \tag{85}$$

Assuming regular ellipticity of the operators and that $\boldsymbol{w}_{\boldsymbol{G}}$ and $\boldsymbol{d}_{\boldsymbol{G}}$ satisfy the weak minimum principle [21, Theorem 8.3], there is a unique solution $\boldsymbol{\psi} \in \left[H^2(\Omega)\right]^d \times H^2(\Omega) \times H^2(\Omega)$ to the problem stated by Eq. (85) satisfying the elliptic property

$$\| \boldsymbol{\psi} \|_{H^2(\Omega_h)} \leq C \| \boldsymbol{\phi} \|_{L^2(\Omega_h)} . \tag{86}$$

Moreover, for a given $\boldsymbol{\varphi} \in \left[L^2(\Omega_h)\right]^d \times L^2(\Omega_h) \times L^2(\Omega_h)$ there exists a unique $\boldsymbol{\phi}_h \in X^k$ such that

$$\mathcal{A}(\boldsymbol{G}^e; \delta\boldsymbol{G}_h, \boldsymbol{\phi}_h) + \mathcal{B}(\boldsymbol{G}^e; \delta\boldsymbol{G}_h, \boldsymbol{\phi}_h) = \sum_e \int_{\Omega^e} \boldsymbol{\varphi}^T \delta\boldsymbol{G}_h d\Omega \;\; \forall \delta\boldsymbol{G}_h \in X^k, \tag{87}$$

and there is a constant C^k such that :

$$|||\, \boldsymbol{\phi}_h \,||| \leq C^k \| \boldsymbol{\varphi} \|_{L^2(\Omega_h)} . \tag{88}$$

The proof of the first part is given in [21], by combining [21, Theorem 8.3] to [21, Lemma 9.17].

The second part was demonstrated by Gudi *et al.* [23]: The use of Lemma 1 and Eq. (87) with $\delta\mathbf{G}_\mathrm{h} = \boldsymbol{\phi}_\mathrm{h}$ allows bounding $|||\ \boldsymbol{\phi}_\mathrm{h}\ |||$ in terms of $\|\ \boldsymbol{\varphi}\ \|_{\mathrm{L}^2(\Omega_\mathrm{h})}$ and $\|\ \boldsymbol{\phi}_\mathrm{h}\ \|_{\mathrm{L}^2(\Omega_\mathrm{h})}$; The term $\|\ \boldsymbol{\phi}_\mathrm{h}\ \|_{\mathrm{L}^2(\Omega_\mathrm{h})}$ is then evaluated by using $\boldsymbol{\phi} = \boldsymbol{\phi}_\mathrm{h} \in \mathrm{X}^k$ in Eq. (85), multiplying the result by $\boldsymbol{\phi}_\mathrm{h}$ and integrating it by parts on Ω_h, resulting into $\|\ \boldsymbol{\phi}_\mathrm{h}\ \|^2_{\mathrm{L}^2(\Omega_\mathrm{h})} = \mathcal{A}(\mathbf{G}^\mathrm{e}; \boldsymbol{\psi}, \boldsymbol{\phi}_\mathrm{h}) + \mathcal{B}(\mathbf{G}^\mathrm{e}; \boldsymbol{\psi}, \boldsymbol{\phi}_\mathrm{h})$; Inserting the interpolant $\mathrm{I}_h\boldsymbol{\psi}$ in these last terms, *i.e.* $\|\ \boldsymbol{\phi}_\mathrm{h}\ \|^2_{\mathrm{L}^2(\Omega_\mathrm{h})} = \mathcal{A}(\mathbf{G}^\mathrm{e}; \boldsymbol{\psi} - \mathrm{I}_h\boldsymbol{\psi}, \boldsymbol{\phi}_\mathrm{h}) + \mathcal{B}(\mathbf{G}^\mathrm{e}; \boldsymbol{\psi} - \mathrm{I}_h\boldsymbol{\psi}, \boldsymbol{\phi}_\mathrm{h}) + \mathcal{A}(\mathbf{G}^\mathrm{e}; \mathrm{I}_h\boldsymbol{\psi}, \boldsymbol{\phi}_\mathrm{h}) + \mathcal{B}(\mathbf{G}^\mathrm{e}; \mathrm{I}_h\boldsymbol{\psi}, \boldsymbol{\phi}_\mathrm{h})$, bounding the last two terms by considering $\delta\mathbf{G}_\mathrm{h} = \mathrm{I}_h\boldsymbol{\psi}$ in Eq. (87), and bounding the first two terms by making successive use of Lemma 2 and of the energy bound of the interpolant error, Lemma 10, and using the regular ellipticity Eq. (86) lead to the bound $\|\ \boldsymbol{\phi}_\mathrm{h}\ \|_{\mathrm{L}^2(\Omega_\mathrm{h})} \leq \mathrm{C}^k\ \|\ \boldsymbol{\varphi}\ \|_{\mathrm{L}^2(\Omega_\mathrm{h})}$, and thus to the proof of the solution uniqueness.

Theorem 1 (Solution uniqueness to the problem (79)) *The solution $\boldsymbol{G_y}$ to the problem stated by Eq. (79) is unique for a given $\boldsymbol{y} \in X^{k^+}$ with $S_h(\boldsymbol{y}) = \boldsymbol{G_y}$.*

In order to prove that the solution $\mathbf{G}_\mathbf{y}$ is unique for a given $\mathbf{y} \in \mathrm{X}^{k^+}$, let us assume that there are two distinct solutions $\mathbf{G}_{\mathbf{y}_1}$, $\mathbf{G}_{\mathbf{y}_2}$, such that

$$\begin{aligned} &\mathcal{A}(\mathbf{G}^\mathrm{e}; \mathrm{I}_\mathrm{h}\mathbf{G} - \mathbf{G}_{\mathbf{y}_1}, \delta\mathbf{G}_\mathrm{h}) + \mathcal{B}(\mathbf{G}^\mathrm{e}; \mathrm{I}_\mathrm{h}\mathbf{G} - \mathbf{G}_{\mathbf{y}_1}, \delta\mathbf{G}_\mathrm{h}) \\ &= \mathcal{A}(\mathbf{G}^\mathrm{e}; \mathrm{I}_\mathrm{h}\mathbf{G} - \mathbf{G}_{\mathbf{y}_2}, \delta\mathbf{G}_\mathrm{h}) + \mathcal{B}(\mathbf{G}^\mathrm{e}; \mathrm{I}_\mathrm{h}\mathbf{G} - \mathbf{G}_{\mathbf{y}_2}, \delta\mathbf{G}_\mathrm{h})\ \ \forall\ \ \delta\mathbf{G}_\mathrm{h} \in \mathrm{X}^k. \end{aligned} \tag{89}$$

For fixed $\mathbf{G}^\mathrm{e}$, since $\mathcal{A}$ and $\mathcal{B}$ are bi-linear, this last relation thus becomes

$$\mathcal{A}(\mathbf{G}^\mathrm{e}; \mathbf{G}_{\mathbf{y}_1} - \mathbf{G}_{\mathbf{y}_2}, \delta\mathbf{G}_\mathrm{h}) + \mathcal{B}(\mathbf{G}^\mathrm{e}; \mathbf{G}_{\mathbf{y}_1} - \mathbf{G}_{\mathbf{y}_2}, \delta\mathbf{G}_\mathrm{h}) = 0\ \ \forall\ \ \delta\mathbf{G}_\mathrm{h} \in \mathrm{X}^k. \tag{90}$$

Considering $\boldsymbol{\varphi} = \delta\mathbf{G}_\mathrm{h} = \mathbf{G}_{\mathbf{y}_1} - \mathbf{G}_{\mathbf{y}_2} \in \mathrm{X}^k$ in Lemma 3 consists in stating that there is a unique $\boldsymbol{\Phi}_\mathrm{h} \in \mathrm{X}^k$ solution of the problem Eq. (87), with

$$\mathcal{A}(\mathbf{G}^\mathrm{e}; \mathbf{G}_{\mathbf{y}_1} - \mathbf{G}_{\mathbf{y}_2}, \boldsymbol{\Phi}_\mathrm{h}) + \mathcal{B}(\mathbf{G}^\mathrm{e}; \mathbf{G}_{\mathbf{y}_1} - \mathbf{G}_{\mathbf{y}_2}, \boldsymbol{\Phi}_\mathrm{h}) = \|\ \mathbf{G}_{\mathbf{y}_1} - \mathbf{G}_{\mathbf{y}_2}\ \|^2_{\mathrm{L}^2(\Omega_\mathrm{h})}, \tag{91}$$

and with $|||\ \boldsymbol{\Phi}_\mathrm{h}\ ||| \leq \mathrm{C}^k\ \|\ \mathbf{G}_{\mathbf{y}_1} - \mathbf{G}_{\mathbf{y}_2}\ \|_{\mathrm{L}^2(\Omega_\mathrm{h})}$. The choice $\delta\mathbf{G}_\mathrm{h} = \boldsymbol{\Phi}_\mathrm{h}$ in Eq. (90) leads to $\|\ \mathbf{G}_{\mathbf{y}_1} - \mathbf{G}_{\mathbf{y}_2}\ \|_{\mathrm{L}^2(\Omega_\mathrm{h})} = 0$, demonstrating that the solution $\mathrm{S}_\mathrm{h}(\mathbf{y}) = \mathbf{G}_\mathbf{y}$ is unique.

We will now show that S_h maps a ball $\mathrm{O}_\sigma(\mathrm{I}_\mathrm{h}\mathbf{G}) \subset \mathrm{X}^{k^+}$ into itself and is continuous in the ball. To this end, we define the ball O_σ with radius σ and centered at the interpolant $\mathrm{I}_\mathrm{h}\mathbf{G}$ of $\mathbf{G}^\mathrm{e}$ as

$$\begin{aligned} \mathrm{O}_\sigma(\mathrm{I}_\mathrm{h}\mathbf{G}) &= \left\{ \mathbf{y} \in \mathrm{X}^{k^+} \text{ such that } |||\ \mathrm{I}_\mathrm{h}\mathbf{G} - \mathbf{y}\ |||_1 \leq \sigma \right\}, \\ &\text{with } \sigma = \frac{|||\ \mathrm{I}_\mathrm{h}\mathbf{G} - \mathbf{G}^\mathrm{e}\ |||_1}{h_\mathrm{s}^\varepsilon}\ , \quad 0 < \varepsilon < \frac{1}{4}. \end{aligned} \tag{92}$$

The idea proposed by Gudi *et al.* [23] is to work on a linearized problem in a ball $\mathrm{O}_\sigma(\mathrm{I}_\mathrm{h}\mathbf{G}) \subset \mathrm{X}^{k^+}$ around the interpolant $\mathrm{I}_\mathrm{h}\mathbf{G} \in \mathrm{X}^{k^+}$ of $\mathbf{G}^\mathrm{e}$. Therefore, the non-linear terms $\mathbf{w}$ and $\mathbf{d}$ and their derivatives are locally bounded in the ball $\mathrm{O}_\sigma(\mathrm{I}_\mathrm{h}\mathbf{G}) \subset \mathrm{X}^{k^+}$ since they are continuous. Applying the energy bound of the interpolant error, Lemma 10, in combination with Eq. (92) yields

$$|||\ \mathrm{I}_\mathrm{h}\mathbf{G} - \mathbf{G}^\mathrm{e}\ |||_1 \leq C^k h_\mathrm{s}^{\mu-1}\ \|\ \mathbf{G}^\mathrm{e}\ \|_{\mathrm{H}^s(\Omega_\mathrm{h})} \text{ and } \sigma \leq C^k h_\mathrm{s}^{\mu-1-\varepsilon}\ \|\ \mathbf{G}^\mathrm{e}\ \|_{\mathrm{H}^s(\Omega_\mathrm{h})}, \tag{93}$$

with $\mu = \min\{s, k+1\}$. By assuming $\mathbf{G}^{\mathrm{e}} \in \left[\mathrm{H}^{\frac{5}{2}}(\Omega)\right]^d \times \mathrm{H}^{\frac{5}{2}}(\Omega) \times \mathrm{H}^{\frac{5}{2}^+}(\Omega)$, and by considering $C_{\mathrm{G}} = \| \mathbf{G}^{\mathrm{e}} \|_{\mathrm{H}^{\frac{5}{2}}(\Omega_{\mathrm{h}})}$ and $\mu = s = \frac{5}{2}$, this last relation becomes

$$||| \mathrm{I_h}\mathbf{G} - \mathbf{G}^{\mathrm{e}} |||_1 \leq C^k h_s^{\frac{3}{2}} \| \mathbf{G}^{\mathrm{e}} \|_{\mathrm{H}^{\frac{5}{2}}(\Omega_{\mathrm{h}})} \text{ and } \sigma \leq C^k C_{\mathrm{G}} h_s^{\frac{3}{2}-\varepsilon} \quad \text{if } k \geq 2. \tag{94}$$

Lemma 4 *Let $\boldsymbol{y} \in O_\sigma(I_h\boldsymbol{G})$ and $\delta\boldsymbol{G}_h \in X^k$, then for $d = 2$ the bound of the non-linear term $\mathcal{N}(\boldsymbol{G}^e, \boldsymbol{y}; \delta\boldsymbol{G}_h)$ defined in Eq. (74) reads*

$$| \mathcal{N}(\boldsymbol{G}^e, \boldsymbol{y}; \delta\boldsymbol{G}_h) | \leq C^k C_y \| \boldsymbol{G}^e \|_{H^s(\Omega_h)} {h_s}^{\mu-2-\varepsilon} \sigma ||| \delta\boldsymbol{G}_h |||_1 , \tag{95}$$

with $\mu = min\{s, k+1\}$.

This bound of the non-linear term $\mathcal{N}(\mathbf{G}^{\mathrm{e}}, \mathbf{y}; \delta\mathbf{G}_{\mathrm{h}})$ defined Eq. (79) is derived by bounding every term separately using successively Taylor's series (60 - 66), the generalized Hölder's inequality, the generalized Cauchy-Schwartz' inequality, the definition of C_{y} in Eq. (67), the definition of the ball, Eqs. (92-94), the trace inequalities, Lemma 6, the inverse inequalities for $d = 2$, Lemma 8, and the interpolation inequalities for $d = 2$, Lemma 5. The proof follows from the argumentation reported in [23] and the bound of the non-linear term $\mathcal{N}(\mathbf{G}^{\mathrm{e}}, \mathbf{y}; \delta\mathbf{G}_{\mathrm{h}})$ is nominated by the term with the largest bound, see C.4 for details. Moreover, using the relation between energy norms on the finite element space, Lemma 9, this relation can be rewritten as

$$| \mathcal{N}(\mathbf{G}^{\mathrm{e}}, \mathbf{y}; \delta\mathbf{G}_{\mathrm{h}}) | \leq C^k C_{\mathrm{y}} \| \mathbf{G}^{\mathrm{e}} \|_{\mathrm{H}^s(\Omega_{\mathrm{h}})} {h_{\mathrm{s}}}^{\mu-2-\varepsilon} \sigma ||| \delta\mathbf{G}_{\mathrm{h}} ||| , \tag{96}$$

with $\mu = \min\{s, k+1\}$.

Using the previous Lemmata, Gudi *et al.* [23] have demonstrated the following two Theorems, which are reported here below without demonstration, since they strictly follow the methodology in [23], see also [27,26] for details.

Theorem 2 ($\mathbf{S_h}$ maps $\mathbf{O}_\sigma(\mathbf{I_h}\mathbf{G})$ into itself) *Let $0 < h_s < 1$ and σ be defined by Eq. (93). Then S_h maps the ball $O_\sigma(I_h\boldsymbol{G})$ into itself, with*

$$||| I_h\boldsymbol{G} - \boldsymbol{G}_{\boldsymbol{y}} |||\leq C^{k'} \sigma h_s^{\varepsilon} \text{ if } k \geq 2. \tag{97}$$

For a mesh size h_s small enough and a given ball size σ, $I_h\boldsymbol{G} - \boldsymbol{G}_{\boldsymbol{y}} \longrightarrow 0$, hence S_h maps $O_\sigma(I_h\boldsymbol{G})$ into itself.

Theorem 3 (The continuity of the map $\mathbf{S_h}$ in the ball $\mathbf{O}_\sigma(\mathbf{I_h}\mathbf{G})$) *For $\boldsymbol{y}_1, \boldsymbol{y}_2 \in O_\sigma(I_h\boldsymbol{G})$, let $\boldsymbol{G}_{\boldsymbol{y}_1} = S_h(\boldsymbol{y}_1)$, $\boldsymbol{G}_{\boldsymbol{y}_2} = S_h(\boldsymbol{y}_2)$ be solutions of Eq. (79). Then for $0 < h_s < 1$*

$$||| \boldsymbol{G}_{\boldsymbol{y}_1} - \boldsymbol{G}_{\boldsymbol{y}_2} ||| \leq C^k C_y \| \boldsymbol{G}^e \|_{H^s(\Omega_h)} h_s^{\mu-2-\varepsilon} ||| \boldsymbol{y}_1 - \boldsymbol{y}_2 ||| . \tag{98}$$

Using the Theorems 2, 3 of the map $\mathrm{S_h}$, we can deduced that for all $0 < h_{\mathrm{s}} < 1$, the map $\mathrm{S_h}$ has a fixed point $\mathbf{G}_{\mathrm{h}}$ of the ball $\mathrm{O}_\sigma(\mathrm{I_h}\mathbf{G})$, which is the solution of the non-linear system of Eqs. (48).

4.6 A priori error estimates

As $\mathrm{S_h}$ has a fixed point $\mathbf{G}_\mathrm{h}$, we can use $\mathbf{G}_\mathrm{h}$ instead of $\mathbf{G}_\mathrm{y}$ in Eq. (97), leading to

$$||| \, \mathrm{I_h}\mathbf{G} - \mathbf{G}_\mathrm{h} \, ||| \leq C^{k'} \sigma h_\mathrm{s}^{\varepsilon} = C^{k'} \, ||| \, \mathrm{I_h}\mathbf{G} - \mathbf{G}^\mathrm{e} \, |||_1 \, . \tag{99}$$

Now, for $k \geq 2$, using the relation between energy norms on the finite element space, Lemma 9, and the energy bound of the interpolant error, Lemma 10, Eq. (99) leads to an optimal error convergence in terms of h_s since

$$\begin{aligned} ||| \, \mathbf{G}^\mathrm{e} - \mathbf{G}_\mathrm{h} \, |||_1 \leq & ||| \, \mathbf{G}^\mathrm{e} - \mathrm{I_h}\mathbf{G} \, |||_1 + ||| \, \mathrm{I_h}\mathbf{G} - \mathbf{G}_\mathrm{h} \, |||_1 \\ \leq & ||| \, \mathbf{G}^\mathrm{e} - \mathrm{I_h}\mathbf{G} \, |||_1 + C^{k'} \, ||| \, \mathrm{I_h}\mathbf{G} - \mathbf{G}^\mathrm{e} \, |||_1 \\ \leq & \, (1 + C^{k'}) \, ||| \, \mathbf{G}^\mathrm{e} - \mathrm{I_h}\mathbf{G} \, |||_1 \leq C^{k''} h_\mathrm{s}^{\mu-1} \, \| \, \mathbf{G}^\mathrm{e} \, \|_{\mathrm{H}^s(\Omega_\mathrm{h})}, \end{aligned} \tag{100}$$

where $\mu = \min\{s, k+1\}$, and $C^{k''} = C^k(1 + C^{k'})$.

4.7 Error estimate in the L^2-norm

The optimal order of convergence in the L^2-norm is obtained by applying the duality argument based on the dual problem

$$\begin{aligned} -\nabla^\mathrm{T}(\mathbf{w}_{\nabla\mathbf{G}}(\mathbf{G}^\mathrm{e})\nabla\boldsymbol{\psi} + \mathbf{d}^\mathrm{T}_{\nabla\mathbf{G}}(\mathbf{G}^\mathrm{e})\boldsymbol{\psi}) + \mathbf{w}^\mathrm{T}_{\mathbf{G}}(\mathbf{G}^\mathrm{e}, \nabla\mathbf{G}^\mathrm{e})\nabla\boldsymbol{\psi} + \mathbf{d}_{\mathbf{G}}(\mathbf{G}^\mathrm{e}, \nabla\mathbf{G}^\mathrm{e})\boldsymbol{\psi} = \mathbf{e} \;\; \text{on } \Omega, \\ \boldsymbol{\psi} = \mathbf{0} \;\; \text{on } \partial\Omega \, , \end{aligned} \tag{101}$$

which satisfies the elliptic regularity condition as $\mathbf{w}_{\nabla\mathbf{G}}$ is positive definite and assuming that $\mathbf{d}^\mathrm{T}_{\nabla\mathbf{G}}$ and $\mathbf{d}_{\mathbf{G}}$ satisfy the weak minimum principle [21, Theorem 8.3]. Therefore $\boldsymbol{\psi} \in \left[\mathrm{H}^{2m}(\Omega_\mathrm{h})\right]^d \times \mathrm{H}^{2m}(\Omega_\mathrm{h}) \times \mathrm{H}^{2m}(\Omega_\mathrm{h})$ for $p \geq 2m$ and

$$\| \, \boldsymbol{\psi} \, \|_{\mathrm{H}^\mathrm{p}(\Omega_\mathrm{h})} \leq C \, \| \, \mathbf{e} \, \|_{\mathrm{H}^{\mathrm{p}-2\mathrm{m}}_{(\Omega_\mathrm{h})}} \, , \tag{102}$$

if $\mathbf{e} \in \left[\mathrm{H}^{\mathrm{p}-2\mathrm{m}}(\Omega_\mathrm{h})\right]^d \times \mathrm{H}^{\mathrm{p}-2\mathrm{m}}(\Omega_\mathrm{h}) \times \mathrm{H}^{\mathrm{p}-2\mathrm{m}}(\Omega_\mathrm{h})$.

Let $\mathbf{e} = \mathbf{G}^\mathrm{e} - \mathbf{G}_\mathrm{h} \subset \left[\mathrm{L}^2(\Omega_\mathrm{h})\right]^d \times \mathrm{L}^2(\Omega_\mathrm{h}) \times \mathrm{L}^2(\Omega_\mathrm{h})$ be the error, multiplying Eq. (101) by $\mathbf{e}$, and integrating over Ω_h, yields

$$\begin{aligned} \| \, \mathbf{e} \, \|^2_{\mathrm{L}^2(\Omega_\mathrm{h})} = & \int_{\Omega_\mathrm{h}} \left[\mathbf{w}_{\nabla\mathbf{G}}(\mathbf{G}^\mathrm{e})\nabla\boldsymbol{\psi}\right]^\mathrm{T} \nabla\mathbf{e}\mathrm{d}\Omega + \int_{\Omega_\mathrm{h}} \left[\mathbf{d}^\mathrm{T}_{\nabla\mathbf{G}}(\mathbf{G}^\mathrm{e})\boldsymbol{\psi}\right]^\mathrm{T} \nabla\mathbf{e}\mathrm{d}\Omega + \\ & \int_{\Omega_\mathrm{h}} \left[\mathbf{w}^\mathrm{T}_{\mathbf{G}}(\mathbf{G}^\mathrm{e}, \nabla\mathbf{G}^\mathrm{e})\nabla\boldsymbol{\psi}\right]^\mathrm{T} \mathbf{e}\mathrm{d}\Omega + \int_{\Omega_\mathrm{h}} \left[\mathbf{d}_{\mathbf{G}}(\mathbf{G}^\mathrm{e}, \nabla\mathbf{G}^\mathrm{e})\boldsymbol{\psi}\right]^\mathrm{T} \mathbf{e}\mathrm{d}\Omega - \\ & \sum_\mathrm{e} \int_{\partial\Omega^\mathrm{e}} \left[\mathbf{w}_{\nabla\mathbf{G}}(\mathbf{G}^\mathrm{e})\nabla\boldsymbol{\psi}\right]^\mathrm{T} \mathbf{e}_\mathbf{n}\mathrm{dS} - \sum_\mathrm{e} \int_{\partial\Omega^\mathrm{e}} \left[\mathbf{e}^\mathrm{T}_\mathbf{n}\mathbf{d}^\mathrm{T}_{\nabla\mathbf{G}}(\mathbf{G}^\mathrm{e})\right] \boldsymbol{\psi}\mathrm{dS} \, , \end{aligned} \tag{103}$$

with

$$\| \, \boldsymbol{\psi} \, \|_{\mathrm{H}^2(\Omega_\mathrm{h})} \leq \mathrm{C} \, \| \, \mathbf{e} \, \|_{\mathrm{L}^2(\Omega_\mathrm{h})} \, . \tag{104}$$

Since $[\![\boldsymbol{\psi}]\!] = [\![\nabla\boldsymbol{\psi}]\!] = 0$ on $\partial_{\mathrm{I}}\Omega_{\mathrm{h}}$ and $\boldsymbol{\psi} = 0$ on $\partial_{\mathrm{D}}\Omega_{\mathrm{h}}$, and since $\mathbf{w}_{\nabla\mathbf{G}}$ is symmetric, we have by comparison with Eqs. (72-73) that

$$\| \mathbf{e} \|^2_{\mathrm{L}^2(\Omega_{\mathrm{h}})} = \mathcal{A}(\mathbf{G}^{\mathrm{e}}; \mathbf{e}, \boldsymbol{\psi}) + \mathcal{B}(\mathbf{G}^{\mathrm{e}}; \mathbf{e}, \boldsymbol{\psi}). \tag{105}$$

From Eq. (71), one has

$$\mathcal{A}(\mathbf{G}^{\mathrm{e}}; \mathbf{G}^{\mathrm{e}} - \mathbf{G}_{\mathrm{h}}, \mathrm{I}_{\mathrm{h}}\boldsymbol{\psi}) + \mathcal{B}(\mathbf{G}^{\mathrm{e}}; \mathbf{G}^{\mathrm{e}} - \mathbf{G}_{\mathrm{h}}, \mathrm{I}_{\mathrm{h}}\boldsymbol{\psi}) = \mathcal{N}(\mathbf{G}^{\mathrm{e}}, \mathbf{G}_{\mathrm{h}}; \mathrm{I}_{\mathrm{h}}\boldsymbol{\psi}), \tag{106}$$

since $\mathbf{G}^{\mathrm{e}}$ is the exact solution and $\mathrm{I}_{\mathrm{h}}\boldsymbol{\psi} \in \mathrm{X}^k$, and Eq. (105) is rewritten

$$\| \mathbf{e} \|^2_{\mathrm{L}^2(\Omega_{\mathrm{h}})} = \mathcal{A}(\mathbf{G}^{\mathrm{e}}; \mathbf{e}, \boldsymbol{\psi} - \mathrm{I}_{\mathrm{h}}\boldsymbol{\psi}) + \mathcal{B}(\mathbf{G}^{\mathrm{e}}; \mathbf{e}, \boldsymbol{\psi} - \mathrm{I}_{\mathrm{h}}\boldsymbol{\psi}) + \mathcal{N}(\mathbf{G}^{\mathrm{e}}, \mathbf{G}_{\mathrm{h}}; \mathrm{I}_{\mathrm{h}}\boldsymbol{\psi}). \tag{107}$$

First, using Lemma 2, Eq. (82), the energy bound of the interpolant error, Lemma 10, and Eq. (100), leads to

$$\begin{aligned} | \mathcal{A}(\mathbf{G}^{\mathrm{e}}; \mathbf{e}, \boldsymbol{\psi} - \mathrm{I}_{\mathrm{h}}\boldsymbol{\psi}) + \mathcal{B}(\mathbf{G}^{\mathrm{e}}; \mathbf{e}, \boldsymbol{\psi} - \mathrm{I}_{\mathrm{h}}\boldsymbol{\psi}) | &\leq \mathrm{C}^k \, |\!|\!| \mathbf{e} |\!|\!|_1 \, |\!|\!| \boldsymbol{\psi} - \mathrm{I}_{\mathrm{h}}\boldsymbol{\psi} |\!|\!|_1 \\ &\leq \mathrm{C}^k \, |\!|\!| \mathbf{e} |\!|\!|_1 \; h_{\mathrm{s}} \, \| \boldsymbol{\psi} \|_{\mathrm{H}^2(\Omega_{\mathrm{h}})} \\ &\leq \mathrm{C}^{k''} h_{\mathrm{s}}^{\mu} \, \| \mathbf{G}^{\mathrm{e}} \|_{\mathrm{H}^s(\Omega_{\mathrm{h}})} \| \boldsymbol{\psi} \|_{\mathrm{H}^2(\Omega_{\mathrm{h}})}, \end{aligned} \tag{108}$$

with $\mu = \min\{\mathrm{s}, k+1\}$.

Second, proceeding as to derive Lemma 4 and using the a priori error estimate (99-100), we have, see details in [26]

$$| \mathcal{N}(\mathbf{G}^{\mathrm{e}}, \mathbf{G}_{\mathrm{h}}; \mathrm{I}_{\mathrm{h}}\boldsymbol{\psi}) | \leq C^{k''} C_{\mathrm{y}} h_{\mathrm{s}}^{2\mu-3} \, \| \mathbf{G}^{\mathrm{e}} \|^2_{\mathrm{H}^s(\Omega_{\mathrm{h}})} |\!|\!| \mathrm{I}_{\mathrm{h}}\boldsymbol{\psi} |\!|\!| \, . \tag{109}$$

Finally, since $[\![\boldsymbol{\psi}]\!] = 0$ in Ω, using the energy bound of the interpolant error, Lemma 10, we have

$$\begin{aligned} |\!|\!| \mathrm{I}_{\mathrm{h}}\boldsymbol{\psi} |\!|\!| &\leq |\!|\!| \mathrm{I}_{\mathrm{h}}\boldsymbol{\psi} - \boldsymbol{\psi} |\!|\!|_1 + |\!|\!| \boldsymbol{\psi} |\!|\!|_1 \\ &\leq C^k h_{\mathrm{s}} \, \| \boldsymbol{\psi} \|_{\mathrm{H}^2(\Omega_{\mathrm{h}})} + \| \boldsymbol{\psi} \|_{\mathrm{H}^1(\Omega_{\mathrm{h}})} \leq C^k (h_{\mathrm{s}} + 1) \, \| \boldsymbol{\psi} \|_{\mathrm{H}^2(\Omega_{\mathrm{h}})} \, . \end{aligned} \tag{110}$$

Eventually, combining Eqs. (108-110), Eq. (107) becomes

$$\| \mathbf{e} \|^2_{\mathrm{L}^2(\Omega_{\mathrm{h}})} \leq C^{k''} h_{\mathrm{s}}^{\mu} \left(1 + h_{\mathrm{s}}^{\mu-3} \, \| \mathbf{G}^{\mathrm{e}} \|_{\mathrm{H}^s(\Omega_{\mathrm{h}})} \right) \| \mathbf{G}^{\mathrm{e}} \|_{\mathrm{H}^s(\Omega_{\mathrm{h}})} \| \boldsymbol{\psi} \|_{\mathrm{H}^2(\Omega_{\mathrm{h}})}, \tag{111}$$

with $\mu = \min\{s, k+1\}$, or using Eq. (104), the final result for $k \geq 2$

$$\| \mathbf{e} \|_{\mathrm{L}^2(\Omega_{\mathrm{h}})} \leq C^{k''} h_{\mathrm{s}}^{\mu} \, \| \mathbf{G}^{\mathrm{e}} \|_{\mathrm{H}^s(\Omega_{\mathrm{h}})} \, . \tag{112}$$

This result demonstrates the optimal convergence rate of the method with the mesh-size for cases in which $k \geq 2$, (so that $\mu \geq 3$).

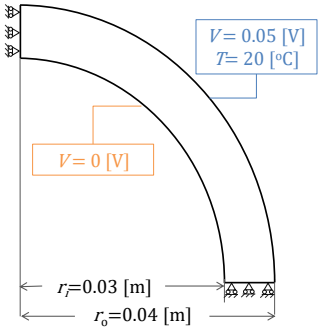

Fig. 3 The schematics and boundary conditions of the quarter of a pipe test

Table 1 Material parameters for the quarter of a pipe test

Parameter	Value
Poisson ratio [−]	0.33
Young's modulus E [Pa]	50×10^9
Thermal expansion $\boldsymbol{\alpha}_{\text{th}}$ [1/K]	diag($2{\times}10^{-6}$)
Thermal conductivity $\boldsymbol{k}$ [W/(K · m)]	diag(1.612)
Seebeck coefficient α [V/K]	1.941×10^{-4}
Electrical conductivity $\boldsymbol{l}$ [S/m]	diag(8.422×10^4)

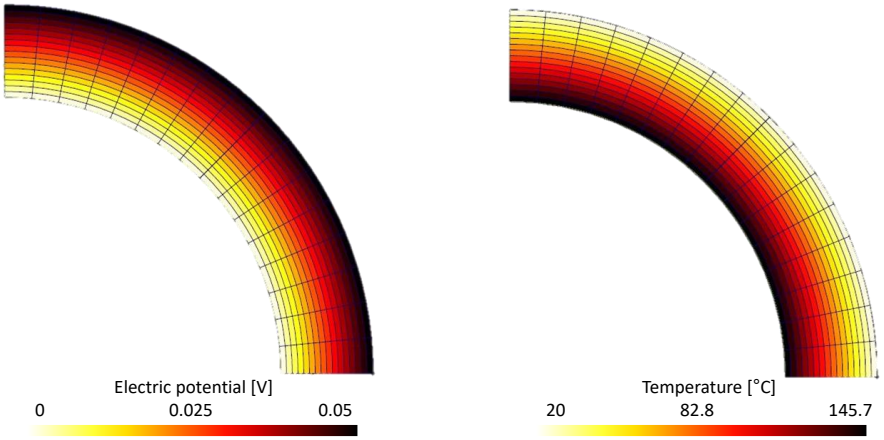

(a) (b)

Fig. 4 The distribution of (a) the electric potential and (b) the temperature for the quarter of a pipe test

4.8 Numerical verification

We consider a quarter of a pipe with the boundary conditions illustrated in Fig. 3. The geometry is extruded to study a 3D-mesh, with plane-strain out-of-plane conditions. The initial value for the temperature is $T_0 = 20$ [°C] and $V_0 = 0$ [V] for the electric potential. The values are also constrained on the inner radius r_i. At the outer radius r_o, the applied electric potential is 0.05 [V], Fig. 3. The

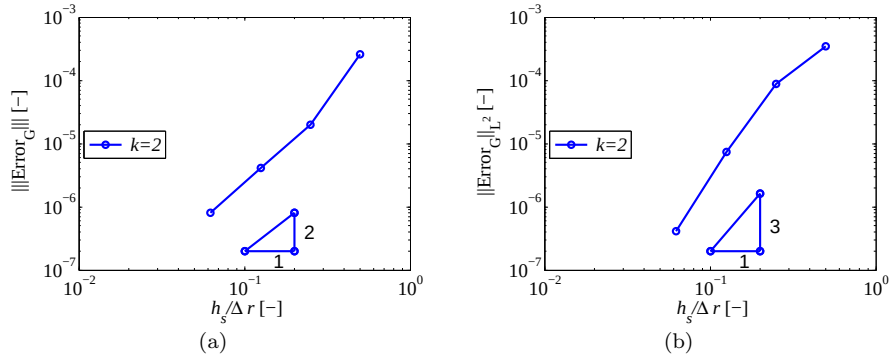

Fig. 5 Error with respect to the mesh size $h_s/\Delta r$, with $\Delta r = r_o - r_i$: (a) in the energy-norm, and (b) in the L^2-norm, for the quarter of a pipe test

material parameters are reported in Table 1. The problem is studied for different mesh refinements of quadratic bricks, and a stabilization parameter $\mathcal{B} = 100$ is considered.

The results for a mesh of $16 \times 16 \times 1$ elements are reported in Fig. 4. The resulting electric potential distribution, Fig. 4(a), induces a temperature gradient from 20 [°C] at the inner face to 145.7 [°C] at the outer face, as shown in Fig. 4(b). Consequently, an expansion of the pipe of 6.35 $\times 10^{-6}$ [m] at the outer radius is observed.

The convergence of the DGFEM is investigated by considering different uniform mesh refinements in Fig. 5. In Fig. 5(a), respectively Fig. 5(b), the errors measured in the energy-norm, respectively in the L^2-norm, are reported in terms of the mesh size h_s; the observed convergence rates are quadratic, respectively cubic, for quadratic polynomial approximations, which agree with the optimal theoretical convergence rates derived in Section 4.6, respectively Section 4.7.

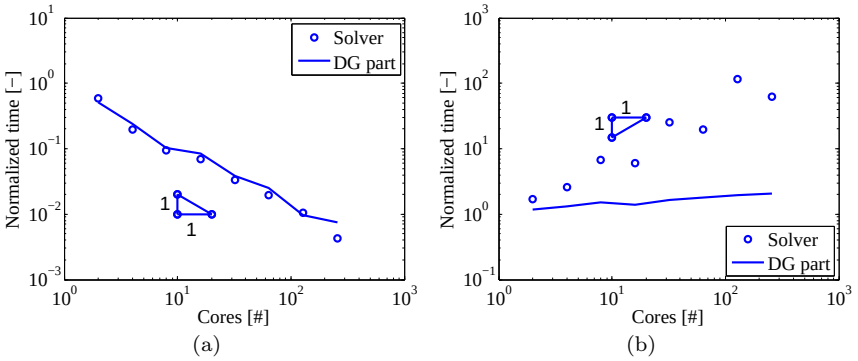

Fig. 6 Scalability test in terms of one processor normalized CPU time for (a) a constant total number of elements divided between the different cores, (b) a constant number of elements per core.

In order to assess the scalability of the parallel implementation presented in Section 3.3, the same numerical application is conducted on a cluster with 43 compute nodes (2752 compute cores). Each compute node contains four 16-core AMD Bulldozer 6272 processors at 2.1 GHz interconnected with a QDR Infiniband network. Two parallel simulation strategies are successively considered:

- Constant total number of elements: A mesh of $32 \times 32 \times 2 = 2048$ quadratic bricks is divided among the different cores of the simulations;
- Constant number of elements per core: The mesh is progressively refined in order to keep 32 quadratic bricks on each core. For the total cores numbers corresponding to $4^i\#$, the global mesh has $2^{i+2} \times 2^{i+2} \times 2$ quadratic bricks, while for the total cores numbers corresponding to $2 \times 4^i\#$, the global mesh has $2^{i+2} \times 2^{i+2} \times 4$ quadratic bricks.

Since the resolution is conducted using a Newton-Raphson process, two computational time evolutions are studied:

- DG part: This gathers the computational time required by one core to evaluate the bulk nodal forces $\mathbf{F}^a_{\text{int}}$ (36) and stiffness matrix $\frac{\partial \mathbf{F}^a_{\text{int}}}{\partial \mathbf{G}^b}$ (38), *i.e.* Step #1 of the algorithm reported in Section 3.3, the interface nodal forces $\mathbf{F}^a_{\text{I}}$ (36) and stiffness matrix $\frac{\partial \mathbf{F}^a_{\text{I}}}{\partial \mathbf{G}^b}$ (38) of the interface elements, *i.e.* Step #2 of the algorithm reported in Section 3.3, and the communication of the nodal values $\mathbf{G}^a$ to the ghost elements, *i.e.* Step #4 of the algorithm reported in Section 3.3.
- Solver: This corresponds to the computational time required by one core during the resolution of the system (38), *i.e.* Step #3 of the algorithm reported in Section 3.3.

Figure 6 reports the computational time –of one core– evolutions normalized with respect to the computational time required for a sequential simulation. When considering a constant total number of elements for the whole structure, see Fig. 6(a), the speed up obtained is close to the theoretical value up to 128 processors for both the DG and solver parts. For 256 processors, the number of elements per core –8– becomes too small to ensure the scalability in the DG part, which includes the nodal values communication. When considering a constant number of elements per core, see Fig. 6(b), the normalized time related to the DG part exhibits a slope almost equal to zero, which shows a good scalability since the force and matrix stiffness evaluations on the cores are not slowed down by the communication burden. Moreover, the solver part increases linearly with the number of cores while the size of the global system increases at a quadratic rate, showing a good scalability. Note that for the latter case two families of points can be seen on Fig. 6(b), which corresponds to the meshes with 2 and 4 layers of elements.

5 Application to Shape Memory Polymer Composites

In this section we model the response of micro-structured Shape Memory Polymers composites (SMPC) subjected to Electro-Thermo-Mechanical histories under a finite deformation setting. To this end we consider the two constitutive behaviors summarized in A: carbon fibers (CF) modeled using a transversely isotropic hyperelastic model with the material properties reported in Table 2, and thermally triggered Shape Memory Polymer (SMP), modeled by an elasto-visco-plastic model,

with the material properties reported in Table 3. The CF mechanical properties are given in [70], while the approximated electrical and thermal parameters are taken from [30,33,11,68]. The thermo-mechanical parameters of the SMP have been calibrated by Srivastava *et al.* [59] to fit the experimental data of tert-butyl acrylate (90% by weight) with crosslinking agent poly (ethylene glycol) dimethacrylate (10% by weight). The parameters related to the conductivity are assumed to correspond to nano-composites and consist of values of the order of magnitude that can be found in [65].

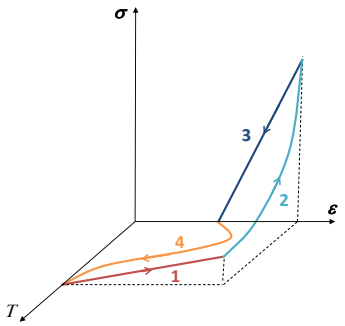

Fig. 7 Thermo-Mechanical cycle of a Shape Memory Polymer

The considered thermally triggered SMP takes advantage of a property change at the glass transition temperature T_g, such that the material can be deformed with minimal force at temperatures above their T_g (hysteretic rubber state), where the polymers are considered as viscous materials. Once cooled below the T_g (glassy state) the SMP becomes rigid again and the polymers are considered as elastic materials. As a result they can maintain the shape that were given to them in their viscous states as long as the temperature remains lower than their glass transition. The typical Thermo-Mechanical cycle for SMP consists of the following steps as shown in Fig. 7:

1. Deforming the polymer at temperature above the glass transition T_g.
2. Fixing the polymer at constant deformation by cooling it to a temperature below T_g
3. Releasing the constraint upon the completion of cooling, to obtain the temporary pre-deformed shape. The polymer holds this temporary shape as long as the temperature remains lower than the glass transition temperature.
4. Heating back the deformed structure above T_g, in order to recover the original shape

The following tests focus in applying the proposed ETM DG formulation to simulate the conductive SMPC behavior at large-deformation regime, when triggered by Joule effect.

Table 2 Carbon fiber properties, see A.1

Parameter	Value
Density ρ [Kg/m^3]	1750
Longitudinal Young's modulus E_{L} [GPa]	230
Transverse Young's modulus E_{T} [GPa]	40
Transverse Poisson ratio ν_{TT} [−]	0.2
Longitudinal-transverse Poisson ratio ν_{LT} [−]	0.256
Transverse shear modulus G_{TT} [GPa]	16.7
Longitudinal shear modulus G_{LT} [GPa]	24
Thermal expansion α_{th} [1/K]	2×10^{-6}
Thermal conductivity $\boldsymbol{k}$ [W/(K · m)]	diag(40)
Seebeck coefficient α [V/K]	3×10^{-6}
Electrical conductivity $\boldsymbol{l}$ [S/m]	diag(10) $\times 10^4$
Heat capacity c_{v} [J/(kg · K)]	712

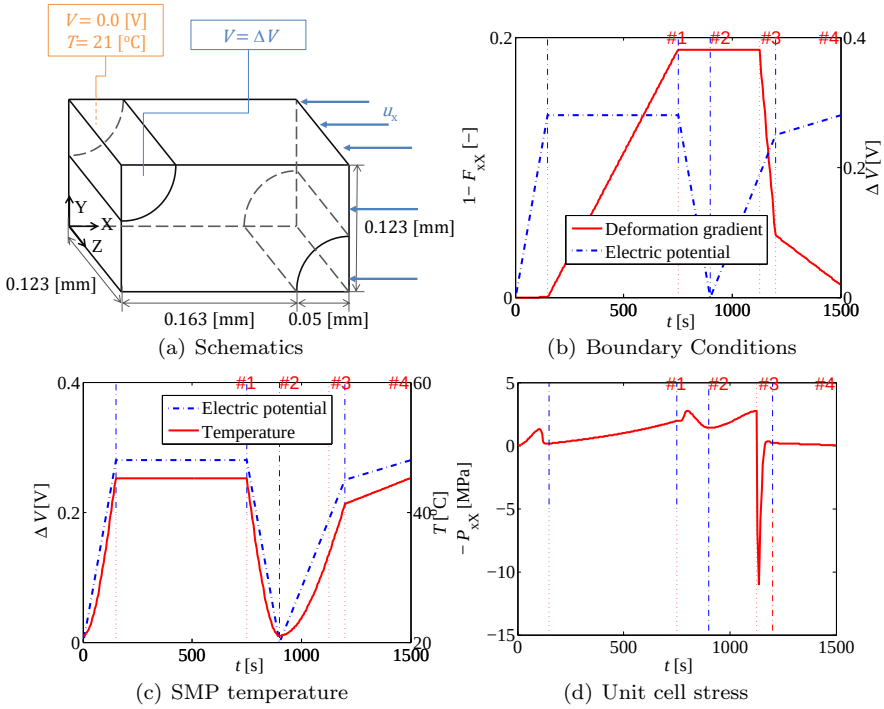

(a) Schematics (b) Boundary Conditions

(c) SMP temperature (d) Unit cell stress

Fig. 8 SMPC unit-cell compression test: (a) Schematics of the unit cell, and (b) boundary conditions in terms of the average deformation gradient and of the applied electric potential difference; (c) Time evolution of the uniform temperature in the SMP, (d) time evolution of the unit cell uniaxial average stress. The vertical '-·-'-lines correspond to the changes of applied electric potential, and the vertical '·'-lines to the changes of applied displacement gradient.

5.1 Electro-Thermo-Mechanical coupling on unit-cell compression test

The geometry of a SMPC unit cell is illustrated in Fig. 8(a) and the applied boundary conditions are the following:

Table 3 Shape memory polymers parameters, see A.2, with β the integration point in the finite increment scheme of the hardening laws, see [26] for details.

Parameter	Value	Parameter	Value
ϵ_r	5.2×10^{-4}	ρ [kg/m^3]	1020
$\dot{\epsilon}_0^{(1)}$ [1/s]	1.73×10^{13}	w	0.6
c_0 [J/(Kg $\cdot$ K)]	1710	c_1[J/Kg]	4.
T_r [K]	310	n [K]	2.1
α_gl [1/K]	13×10^{-5}	α_r [1/K]	25×10^{-5}
G_gl [Pa]	156×10^6	G_r [Pa]	13.4×10^6
L_{G_gl} [Pa/K]	7.4×10^6	L_{G_r} [Pa/K]	0.168×10^6
Q_gl [J]	1.4×10^{-19}	Q_r [J]	0.2×10^{-21}
L_{Q_gl} [J/K]	0.	$\mathrm{L}_{Q_\mathrm{r}}$ [J/K]	0
H_gl [Pa]	1.56×10^6	H_r [Pa]	0.76×10^6
L_{H_gl} [Pa/K]	0.44×10^6	L_{H_r} [Pa/K]	0.006×10^6
ν_gl	0.35	ν_r	0.49
L_{ν_gl} [1/K]	0.	L_{ν_r} [1/K]	0
Δ	2.6	$m^{(1)}$	0.17
h_a	230	g	5.8
b [Pa]	5850×10^6	V' [m^3]	2.16×10^{-27}
z	0.083	r	1.3
s	0.005	a	0.5
d [1/K]	0.015	ζ_gl	0.14
S_{a_0} [Pa]	0	S_{b_0} [Pa]	0
α_p	0.058	φ_0	0
β	0.5	h_a	230
$I_\mathrm{m}^{(2)}$	6.3	N [1/K]	0.045
μ_g [Pa]	1.38×10^6	$m^{(2)}$	0.19
$S_\mathrm{gl}^{(2)}$ [Pa]	58×10^6	$S_\mathrm{r}^{(2)}$ [Pa]	3×10^2
$L_{S_\mathrm{gl}^{(2)}} = L_{S_\mathrm{r}^{(2)}}$ [Pa/K]	0	$\dot{\epsilon}_0^{(2)}$ [1/s]	5.2×10^{-4}
$I_\mathrm{m}^{(3)}$	5	$\mu^{(3)}$ [Pa]	0.75×10^6
h_g	10^{-9}	α [V/K]	3×10^{-7}
$\boldsymbol{k}$ [W/(K $\cdot$ m)]	diag(0.2)	$\boldsymbol{l}$ [S/m]	diag(0.1)

- The displacement is constrained along the three perpendicular faces as follows: the nodes along the XY-plane are fixed in the Z-direction, the nodes along the YZ-plane are fixed in the X-direction, and the nodes along the XZ-plane are fixed in the Y-direction.
- The other three faces are restrained in order to get a uniform deformation, the top face is restrained along the Z-direction, the infront face is restrained along the Y-direction and the right face is restrained along the X-direction.
- The temperature is restrained on the Shape Memory Polymer volume to get a uniform distribution of the temperature.
- The initial value of the electric potential is 0 [V] and the initial value of the temperature is 21 [°C].
- The test is implemented with displacement control in order to simulate a uniaxial compression along the X-direction, following the time evolution reported in Fig. 8(b).
- Simultanously to the displacement control, an electric potential difference is applied between the front and back face following the time evolution reported

in Fig. 8(b), and the initial temperature is constrained at the center of one face of the CF.

A finite element mesh of 2 layers of 40 quadratic bricks is considered and the value of the stabilization parameter is $\mathcal{B}$= 40. Because of the BC, the unit cell is subjected to indirect heating by applying the electric potential with the following Electro-Thermo-Mechanical history:

- Apply an electric field of 0.28 [V] in order to heat the cell above the glass transition temperature of 37 [°C].
- Compress the sample above glass transition.
- Reduce the electric field to 0 [V], in order to cool the cell down to room temperature, while the cell is still under a constrained strain.
- Increase the electric field back to 0.28 [V], which causes an increase in the temperature of the sample to a temperature above the glass transition, and maintain the deformation constant until the cell reaches a value above the glass transition temperature of 37 [°C].
- Once the glass transition temperature is reached in the SMP material, keep increasing the applied potential difference and unload the SMPC unit cell in order to recover the original shape.

The resulting temperature evolution history of the SMP volume versus time is plotted in Fig. 8(c). The particular behavior of SMPC is illustrated through the homogenized stress shown in Fig. 8(d). Deformed shapes of the SMPC unit cell and the corresponding stress distribution along the compression direction are illustrated in Fig. 9. It appears that the force starts to increase (in absolute value) during the heating by Joule effect due to thermal dilation, and a sudden drop can be observed once the temperature reaches the glass transition temperature T_{g}. Then the force increases slightly under the deformation constraint above the glass transition temperature T_{g}. Since the deformation is applied above the glass transition temperature, Fig. 9(a), the stress remains limited in the cell, see Fig. 9(b). Once the temperature starts to decrease, there is an increase of the force as the deformation constraint is still applied. When the temperature is minimal, see Fig. 9(c), the force has almost vanished, which represents a fixation of the deformation, see also the limited stress distribution in Fig. 9(d). Once the temperature starts to increases and reaches back the glass transition temperature T_{g}, see Fig. 9(e), the force starts to sharply decrease and to change sign as the SMPC enters the recovery phase, meaning it tends to recover the original shape, see the important stress distribution in Fig. 9(f). The displacement control is then released and the force tends to vanish as the SMPC cell recovers its original shape above the glass transition temperature T_{g} at around 1200 [s], see Fig. 9(h).

5.2 Electro-Thermo-Mechanical coupling on extruded unit-cell bending test

The aim of the following test is to study the free recovery of a SMPC unit cell subjected to indirect heating by applying an electric potential difference. To this end we study the bending behavior of an extruded unit cell, as illustrated in Fig. 10. the applied boundary conditions are the following:

- The back side of the cell is clamped.

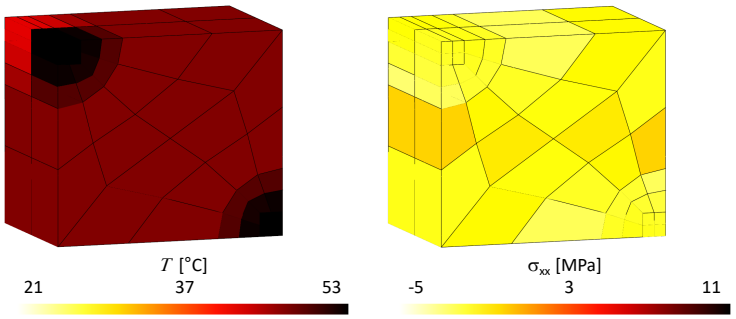

(a) Configuration #1

(b) Configuration #1

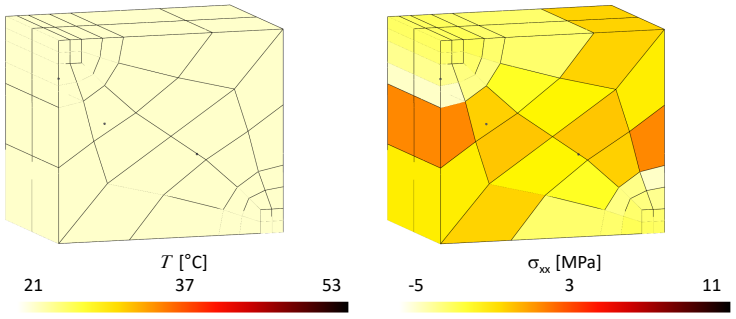

(c) Configuration #2

(d) Configuration #2

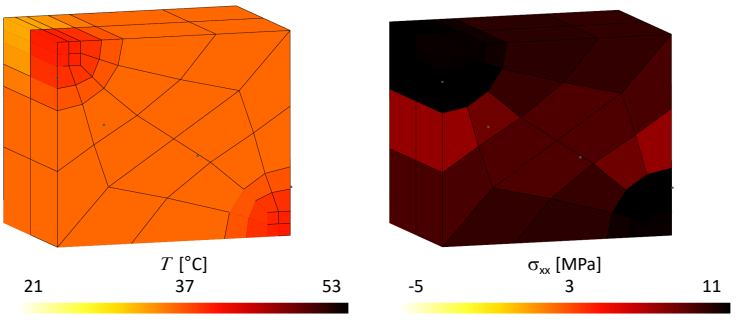

(e) Configuration #3

(f) Configuration #3

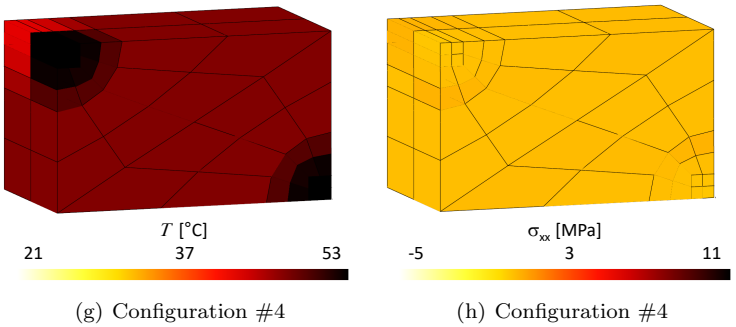

(g) Configuration #4

(h) Configuration #4

Fig. 9 Snapshots of the temperature (left column) and stress (right column) distributions of the of the SMPC unit-cell under compression test during the Electro-Thermo-Mechanical cycle. #1 (t = 750 s): after compression above the glass transition temperature. #2 (t = 900 s): after having released the voltage difference. #3 (t = 1135 s): after having applied again a voltage difference to reheat above the glass transition temperature with partial compression. #4 (t = 1500 s): after having removed the compression above the glass transition temperature.

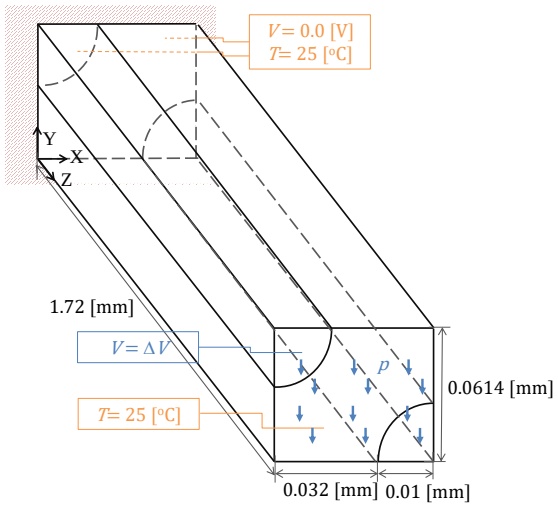

Fig. 10 Schematics of the extruded unit cell under bending

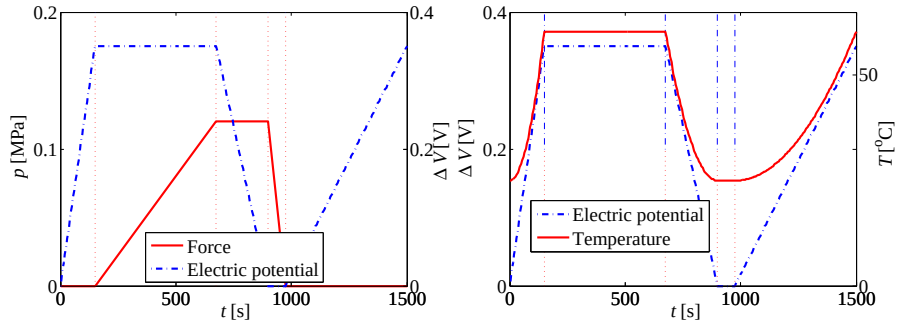

(a) Boundary condition (b) Mid-length temperature

Fig. 11 Time evolution histories of the (a) boundary conditions and (b) temperature at the mid-length of the beam in terms of the applied electric potential difference for the extruded unit cell under bending. The vertical '-·-'-lines correspond to the changes of applied electric potential, and the vertical '··'-lines to the changes of applied force.

- The displacements of the side faces are constrained along the X-direction.
- The temperature is constrained at 25 [°C] on the two extremity faces.
- An electric potential difference is applied between the two extremity faces following the time evolution reported Fig. 11(a).
- A uniform tangential pressure is applied on the front face following the time evolution reported in Fig. 11(a).
- The initial value of the temperature is 25 [°C] and the initial value of the electric potential is 0 [V].

A finite element mesh of 90 quadratic bricks is considered, and the value of the stabilization parameter is $\mathcal{B} = 100$. The applied boundary condition for the force and electric potential versus time are illustrated in Fig. 11(a), with the following Electro-Thermo-Mechanical history:

– Apply an electric field of 0.35 [V] to generate heat and increase the temperature.
– Apply a tangential load per unit surface p on the free in-front face.
– Reduce the electric field to 0 [V], in order to cool the cell down under a constrained strain.
– Remove the force at 25 [°C].
– Increase the electric field back to 0.35 [V] to increase the temperature of the composite cell in order to recover freely the original shape.

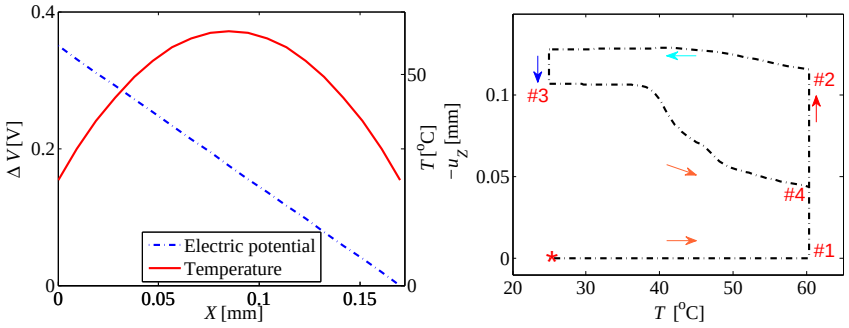

(a) Configuration #1 (b) Activation history

Fig. 12 (a) The distributions of the temperature and electric potential along the extruded unit cell length at configuration #1, and (b) the history of the extruded unit cell under bending triggered by Joule effect

The resulting temperature history is evaluated at the mid-length of the beam and is shown in Fig. 11(b); the electric potential and temperature distributions along the extruded unit-cell length at time t=500 [s] are illustrated in Fig. 12(a). When an electric potential of 0.35 [V] is applied, the temperature increases inside the beam and reaches 60.5 [°C], which is above the glass transition temperature, at the extruded unit-cell mid-length. The distribution of the electric potential is close to linear but the distribution of the temperature is almost quadratic with a maximum value of 60.5 [°C]. Therefore, only a part of the extruded unit-cell has a shape memory effect that can be triggered during the test.

The displacement history of the extruded unit-cell extremity is illustrated in Fig. 12(b), and the successive configurations are reported in Fig. 13. It can be noticed that the cell recovers part of the deformation as the force is removed since, on the one hand, the carbon fibers remain elastic, and, on the other hand, only one part of the beam reaches a value higher than the glass transition. Upon reapplying the electric potential difference, part of the remaining deformation is recovered.

6 Conclusions and perspectives

In this work a DG method has been developed to study non-linear Electro-Thermo-Mechanical coupled problems. Starting from the first principles of solid mechanics, electrical and thermal field theories formulated in terms of energetically conjugated

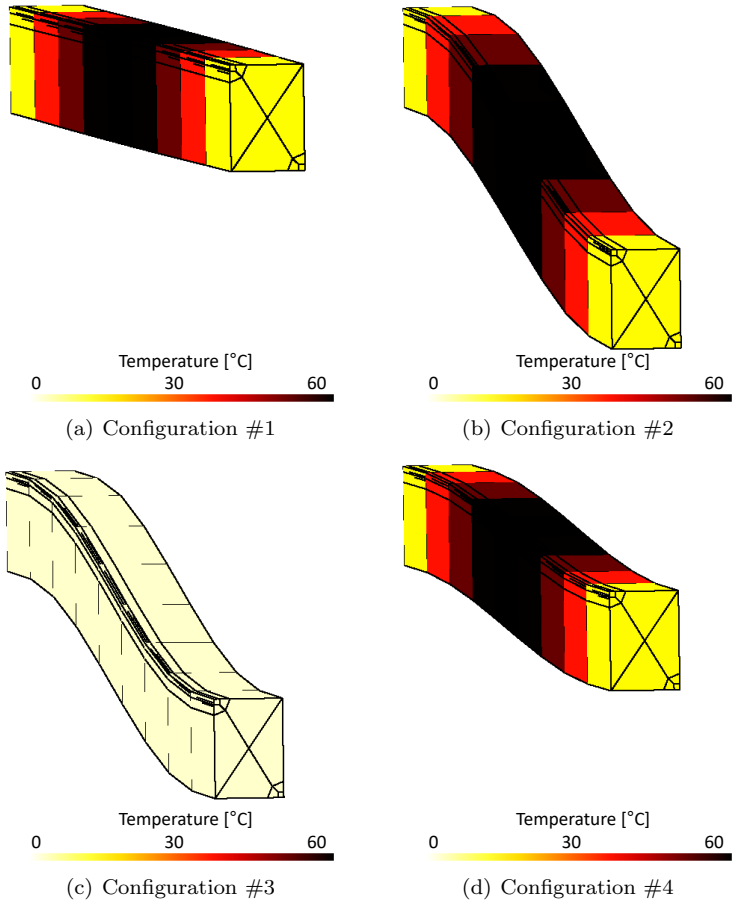

(a) Configuration #1 (b) Configuration #2

(c) Configuration #3 (d) Configuration #4

Fig. 13 Snapshots of the extruded unit cell under bending during the Electro-Thermo-Mechanical cycle. #1: after applying an electric potential of 0.35 [V] to heat the unit cell above the glass transition temperature. #2: after applying the load to bend the beam. #3: after removing the load at 0 [V] of electric potential. #4: after reapplying an electric potential of 0.35 [V] to recover the initial configuration.

pairs of fluxes and fields gradients, the SIPG method has been derived as a consistent weak form to solve the various interacting physics in the coupled simulations.

In particular, the stability of the method and its optimal convergence rate with the mesh-size have been demonstrated in the context of linearized mechanical equations, but with non-linear electro-thermal coupling. A numerical simulation was carried out to verify these properties.

Moreover, advantage has been taken of the DG feature to develop an efficient parallel implementation of the method based on the concept of ghost elements. This implementation only requires as communication –besides the system resolution– the exchange of the nodal values of these ghost elements corresponding to neighboring elements on other processors, ensuring a good scalability of the method.

Finally the DG method has been used to study the behavior of shape memory polymer composite unit-cells. A multi-physic micro-model of unidirectional carbon fibers embedded in a shape memory polymer matrix was formulated by considering the interaction of electrical, thermal, and mechanical fields, and it was shown that when mechanical and electrical loads are applied, the heat induced due to the Joule effect triggers the shape memory behavior.

In the future it is intended to formulate the multi-physic micro-model, in particular the constraints on the boundary conditions, to embed it in a computational multi-scale framework with a view to the simulation of smart structures.

Acknowledgements This project has been funded with support of the European Commission under the grant number 2012-2624/001-001-EM. This publication reflects the view only of the author, and the Commission cannot be held responsible for any use which may be made of the information contained therein.
Computational resources have been provided by the supercomputing facilities of the "Consortium des Équipements de Calcul Intensif en Fédération Wallonie Bruxelles (CÉCI)" funded by the "Fond de la Recherche Scientifique de Belgique (FRS-FNRS)".
Compliance with Ethical Standards: The authors declare that they have no conflict of interest.

References

1. Ainsworth, M., Kay, D.: The approximation theory for the p-version finite element method and application to non-linear elliptic pdes. Numerische Mathematik **82**(3), 351–388 (1999)
2. Ainsworth, M., Kay, D.: Approximation theory for the hp-version finite element method and application to the non-linear laplacian. Applied numerical mathematics **34**(4), 329–344 (2000)
3. Amestoy, P., Duff, I., L'Excellent, J.Y.: Multifrontal parallel distributed symmetric and unsymmetric solvers. Computer Methods in Applied Mechanics and Engineering **184**(2), 501 – 520 (2000). DOI http://dx.doi.org/10.1016/S0045-7825(99)00242-X. URL http://www.sciencedirect.com/science/article/pii/S004578259900242X
4. Anand, L.: On H. Hencky's approximate strain-energy function for moderate deformations. J. Appl. Mech. **46**, 78–82 (1979). DOI 10.1115/1.3424532
5. Arnold, D.N., Brezzi, F., Cockburn, B., Marini, L.D.: Unified analysis of discontinuous galerkin methods for elliptic problems. SIAM journal on numerical analysis **39**(5), 1749–1779 (2002)
6. Arnold, D.N., Brezzi, F., Marini, L.D.: A family of discontinuous galerkin finite elements for the reissner-mindlin plate. Journal of Scientific Computing **22-23**, 25–45 (2005)
7. Babuška, I., Suri, M.: The *hp* version of the finite element method with quasiuniform meshes. RAIRO-Modélisation mathématique et analyse numérique **21**(2), 199–238 (1987)
8. Becker, G., Noels, L.: A full-discontinuous galerkin formulation of nonlinear kirchhofflove shells: elasto-plastic finite deformations, parallel computation, and fracture applications. International Journal for Numerical Methods in Engineering **93**(1), 80–117 (2013). DOI 10.1002/nme.4381. URL http://dx.doi.org/10.1002/nme.4381
9. Behl, M., Lendlein, A.: Shape-memory polymers. Materials today **10**(4), 20–28 (2007)
10. Bonet, J., Burton, A.: A simple orthotropic, transversely isotropic hyperelastic constitutive equation for large strain computations. Computer methods in applied mechanics and engineering **162**(1), 151–164 (1998)
11. Chung, D.D.: {CHAPTER} 4 - properties of carbon fibers. In: D.D. Chung (ed.) Carbon Fiber Composites, pp. 65 – 78. Butterworth-Heinemann, Boston (1994). DOI http://dx.doi.org/10.1016/B978-0-08-050073-7.50008-7. URL //www.sciencedirect.com/science/article/pii/B9780080500737500087
12. Ciarlet, P.: Conforming Finite Element Methods for Second-Order Problems, chap. 3, pp. 110–173. SIAM (2002). DOI 10.1137/1.9780898719208.ch3. URL http://epubs.siam.org/doi/abs/10.1137/1.9780898719208.ch3
13. Cockburn, B., Karniadakis, G.E., Shu, C.W.: The development of discontinuous Galerkin methods. Springer (2000)

14. Culebras, M., Gómez, C.M., Cantarero, A.: Review on polymers for thermoelectric applications. Materials **7**(9), 6701–6732 (2014)
15. Douglas, J., Dupont, T.: Interior Penalty Procedures for Elliptic and Parabolic Galerkin Methods, pp. 207–216. Springer Berlin Heidelberg, Berlin, Heidelberg (1976). DOI 10.1007/BFb0120591. URL http://dx.doi.org/10.1007/BFb0120591
16. Engel, G., Garikipati, K., Hughes, T.J.R., Larson, M.G., Mazzei, L., Taylor, R.L.: Continuous/discontinuous finite element approximations of fourth-order elliptic problems in structural and continuum mechanics with applications to thin beams and plates, and strain gradient elasticity. Computer Methods in Applied Mechanics and Engineering **191**(34), 3669–3750 (2002)
17. Fabré, M., Binst, J., Bocsan, I., De Smet, C., Ivens, J.: Heating shape memory polymers with alternative ways: microwave and direct electrical heating. In: 15th European Conference on Composite Materials, pp. 1–8. University of Padova (2012)
18. Ferreira, A.D.B.L., Nóvoa, P.R.O., Torres Marques, A.: Multifunctional material systems: A state-of-the-art review. Composite Structures **151**, 3 – 35 (2016). DOI http://dx.doi.org/10.1016/j.compstruct.2016.01.028. Smart composites and composite structures In honour of the 70th anniversary of Professor Carlos Alberto Mota Soares
19. Georgoulis, E.H.: Discontinuous Galerkin methods on shape-regular and anisotropic meshes. University of Oxford D. Phil. Thesis (2003)
20. Geuzaine, C., Remacle, J.F.: Gmsh: A 3-d finite element mesh generator with built-in pre- and post-processing facilities. International Journal for Numerical Methods in Engineering **79**(11), 1309–1331 (2009). DOI 10.1002/nme.2579. URL http://dx.doi.org/10.1002/nme.2579
21. Gilbarg, D., Trudinger, N.S.: Elliptic partial differential equations of second order. springer (2015)
22. Gudi, T.: Discontinuous galerkin methods for nonlinear elliptic problems. Ph.D. thesis, Indian Institute of Technology, Bombay (2006)
23. Gudi, T., Nataraj, N., Pani, A.K.: hp-discontinuous galerkin methods for strongly nonlinear elliptic boundary value problems. Numerische Mathematik **109**(2), 233–268 (2008)
24. Hansbo, P., Larson, M.G.: A discontinuous galerkin method for the plate equation. Calcolo **39**(1), 41–59 (2002)
25. Hansbo, P., Larson, M.G.: Discontinuous galerkin methods for incompressible and nearly incompressible elasticity by nitsche's method. Computer Methods in Applied Mechanics and Engineering **191**(17-18), 1895–1908 (2002)
26. Homsi, L.: Development of non-linear electro-thermo-mechanical discontinuous galerkin formulations. Ph.D. thesis, University of Liège, Belgium (2017)
27. Homsi, L., Geuzaine, C., Noels, L.: A coupled electro-thermal discontinuous galerkin method. Journal of Computational Physics **348**, 231–258 (2017)
28. Houston, P., Robson, J., Süli, E.: Discontinuous galerkin finite element approximation of quasilinear elliptic boundary value problems i: The scalar case. IMA journal of numerical analysis **25**(4), 726–749 (2005)
29. Huang, W., Yang, B., An, L., Li, C., Chan, Y.: Water-driven programmable polyurethane shape memory polymer: demonstration and mechanism. Applied Physics Letters **86**(11), 114,105 (2005)
30. Issi, J.P.: Electronic and Thermal Properties of Carbon Fibers, pp. 207–216. World of Carbon. CRC Press (2003). DOI 10.1201/9780203166789.ch3. URL http://dx.doi.org/10.1201/9780203166789.ch3. 0
31. Karypis, G., Kumar, V.: A fast and high quality multilevel scheme for partitioning irregular graphs. SIAM Journal on Scientific Computing **20**(1), 359–392 (1998)
32. Kaufmann, P., Martin, S., Botsch, M., Gross, M.: Flexible simulation of deformable models using discontinuous galerkin fem. Graphical Models **71**(4), 153 – 167 (2009). DOI http://dx.doi.org/10.1016/j.gmod.2009.02.002. URL http://www.sciencedirect.com/science/article/pii/S1524070309000125. Special Issue of ACM SIGGRAPH / Eurographics Symposium on Computer Animation 2008
33. Keith, J.M., Janda, N.B., King, J.A., Perger, W.F., Oxby, T.J.: Shielding effectiveness density theory for carbon fiber/nylon 6, 6 composites. Polymer composites **26**(5), 671–678 (2005)
34. Langer, R., Tirrell, D.A.: Designing materials for biology and medicine. Nature **428**(6982), 487–492 (2004)
35. Lendlein, A., Jiang, H., Jünger, O., Langer, R.: Light-induced shape-memory polymers. Nature **434**(7035), 879–882 (2005)

36. Leng, J., Lan, X., Liu, Y., Du, S.: Shape-memory polymers and their composites: stimulus methods and applications. Progress in Materials Science **56**(7), 1077–1135 (2011)
37. Liang, C., Rogers, C., Malafeew, E.: Investigation of shape memory polymers and their hybrid composites. Journal of Intelligent Material Systems and Structures **8**(4), 380–386 (1997)
38. Liu, L.: A continuum theory of thermoelectric bodies and effective properties of thermoelectric composites. International Journal of Engineering Science **55**, 35–53 (2012)
39. Liu, R., Wheeler, M., Dawson, C.: A three-dimensional nodal-based implementation of a family of discontinuous galerkin methods for elasticity problems. Computers & Structures **87**(3-4), 141 – 150 (2009). DOI http://dx.doi.org/10.1016/j.compstruc.2008.11.009
40. Liu, R., Wheeler, M., Dawson, C., Dean, R.: Modeling of convection-dominated thermoporomechanics problems using incomplete interior penalty galerkin method. Computer Methods in Applied Mechanics and Engineering **198**(9-12), 912 – 919 (2009). DOI http://dx.doi.org/10.1016/j.cma.2008.11.012
41. Lu, H., Liu, Y., Leng, J., Du, S.: Qualitative separation of the physical swelling effect on the recovery behavior of shape memory polymer. European Polymer Journal **46**(9), 1908–1914 (2010)
42. Mahan, G.D.: Density variations in thermoelectrics. Journal of Applied Physics **87**(10), 7326–7332 (2000)
43. McBride, A., Reddy, B.: A discontinuous galerkin formulation of a model of gradient plasticity at finite strains. Computer Methods in Applied Mechanics and Engineering **198**(21-26), 1805 – 1820 (2009). DOI http://dx.doi.org/10.1016/j.cma.2008.12.034. Advances in Simulation-Based Engineering Sciences Honoring J. Tinsley Oden
44. Meng, H., Li, G.: A review of stimuli-responsive shape memory polymer composites. Polymer **54**(9), 2199–2221 (2013)
45. Meng, Q., Hu, J.: A review of shape memory polymer composites and blends. Composites Part A: Applied Science and Manufacturing **40**(11), 1661–1672 (2009)
46. Miehe, C.: Aspects of the formulation and finite element implementation of large strain isotropic elasticity. International Journal for Numerical Methods in Engineering **37**(12), 1981–2004 (1994)
47. Muliana, A., Li, K.A.: Time-dependent response of active composites with thermal, electrical, and mechanical coupling effect. International Journal of Engineering Science **48**(11), 1481–1497 (2010)
48. Noels, L.: A discontinuous galerkin formulation of non-linear kirchhoff-love shells. International Journal for Numerical Methods in Engineering **78**(3), 296–323 (2009)
49. Noels, L., Radovitzky, R.: A general discontinuous galerkin method for finite hyperelasticity. formulation and numerical applications. International Journal for Numerical Methods in Engineering **68**(1), 64–97 (2006)
50. Noels, L., Radovitzky, R.: An explicit discontinuous galerkin method for non-linear solid dynamics: Formulation, parallel implementation and scalability properties. International Journal for Numerical Methods in Engineering **74**(9), 1393–1420 (2008)
51. Pilate, F., Toncheva, A., Dubois, P., Raquez, J.M.: Shape-memory polymers for multiple applications in the materials world. European Polymer Journal **80**, 268–294 (2016)
52. Prudhomme, S., Pascal, F., Oden, J., Romkes, A.: Review of a priori error estimation for discontinuous galerkin methods. Tech. rep., TICAM, UTexas (2000)
53. Reed, W., Hill, T.: Triangular mesh methods for the neutron transport equation. Tech. Rep. LA-UR-73-479, Los Alamos Scientific Laboratory (1973). URL http://www.osti.gov/scitech/servlets/purl/4491151
54. Romkes, A., Prudhomme, S., Oden, J.: A priori error analyses of a stabilized discontinuous galerkin method. Computers & Mathematics with Applications **46**(8), 1289–1311 (2003)
55. Rothe, S., Schmidt, J.H., Hartmann, S.: Analytical and numerical treatment of electro-thermo-mechanical coupling. Archive of Applied Mechanics **85**(9-10), 1245–1264 (2015)
56. Schmidt, A.M.: Electromagnetic activation of shape memory polymer networks containing magnetic nanoparticles. Macromolecular Rapid Communications **27**(14), 1168–1172 (2006)
57. Spencer, A.: The formulation of constitutive equations for anisotropic solids, pp. 3–26. Nijhoff, Amsterdam (1982)
58. Spencer, A.J.M.: Modelling of finite deformations of anisotropic materials. In: J. Gittus, J. Zarka, S. Nemat-Nasser (eds.) Large Deformations of Solids: Physical Basis and Mathematical Modelling. Springer Netherlands, Dordrecht (1986). DOI 10.1007/978-94-009-3407-8_3. URL https://doi.org/10.1007/978-94-009-3407-8_3

59. Srivastava, V., Chester, S.A., Anand, L.: Thermally actuated shape-memory polymers: Experiments, theory, and numerical simulations. Journal of the Mechanics and Physics of Solids **58**(8), 1100–1124 (2010)
60. Sun, S., Wheeler, M.F.: Discontinuous galerkin methods for coupled flow and reactive transport problems. Applied Numerical Mathematics **52**(2), 273–298 (2005)
61. Ten Eyck, A., Celiker, F., Lew, A.: Adaptive stabilization of discontinuous galerkin methods for nonlinear elasticity: Motivation, formulation, and numerical examples. Computer Methods in Applied Mechanics and Engineering **197**(45-48), 3605–3622 (2008). DOI 10.1016/j.cma.2008.02.020
62. Ten Eyck, A., Lew, A.: Discontinuous galerkin methods for non-linear elasticity. International Journal for Numerical Methods in Engineering **67**(9), 1204–1243 (2006). DOI 10.1002/nme.1667
63. Truster, T.J., Chen, P., Masud, A.: Finite strain primal interface formulation with consistently evolving stabilization. International Journal for Numerical Methods in Engineering **102**(3-4), 278–315 (2015). DOI 10.1002/nme.4763. URL http://dx.doi.org/10.1002/nme.4763
64. Truster, T.J., Chen, P., Masud, A.: On the algorithmic and implementational aspects of a discontinuous galerkin method at finite strains. Computers & Mathematics with Applications **70**(6), 1266 – 1289 (2015). DOI http://dx.doi.org/10.1016/j.camwa.2015.06.035. URL http://www.sciencedirect.com/science/article/pii/S0898122115003211
65. Vilčáková, J., Sáha, P., Quadrat, O.: Electrical conductivity of carbon fibres/polyester resin composites in the percolation threshold region. European Polymer Journal **38**(12), 2343–2347 (2002)
66. Wells, G.N., Dung, N.T.: A c0 discontinuous galerkin formulation for kirchhoff plates. Computer Methods in Applied Mechanics and Engineering **196**(35-36), 3370–3380 (2007)
67. Wells, G.N., Garikipati, K., Molari, L.: A discontinuous galerkin formulation for a strain gradient-dependent damage model. Computer Methods in Applied Mechanics and Engineering **193**(33-35), 3633 – 3645 (2004)
68. Wen, S., Chung, D.: Seebeck effect in carbon fiber-reinforced cement. Cement and Concrete Research **29**(12), 1989–1993 (1999)
69. Wheeler, M.F.: An elliptic collocation-finite element method with interior penalties. SIAM Journal on Numerical Analysis **15**(1), 152–161 (1978)
70. Wu, L., Tjahjanto, D., Becker, G., Makradi, A., Jérusalem, A., Noels, L.: A micro–meso-model of intra-laminar fracture in fiber-reinforced composites based on a discontinuous galerkin/cohesive zone method. Engineering Fracture Mechanics **104**, 162–183 (2013)
71. Yadav, S., Pani, A., Park, E.J.: Superconvergent discontinuous galerkin methods for nonlinear elliptic equations. Mathematics of Computation **82**(283), 1297–1335 (2013)
72. Yang, Y., Xie, S., Ma, F., Li, J.: On the effective thermoelectric properties of layered heterogeneous medium. Journal of Applied Physics **111**(1), 013,510 (2012)
73. Zheng, X.P., Liu, D.H., Liu, Y.: Thermoelastic coupling problems caused by thermal contact resistance: A discontinuous galerkin finite element approach. Science China Physics, Mechanics and Astronomy **54**(4), 666–674 (2011)
74. Zhupanska, O.I., Sierakowski, R.L.: Electro-thermo-mechanical coupling in carbon fiber polymer matrix composites. Acta mechanica **218**(3-4), 319–332 (2011)

A Constitutive behaviors

The objective of this section is to summarize large deformation constitutive theories in order to model the response of Shape Memory Polymers composites (SMPC) subjected to a variety of Electro-Thermo-Mechanical histories. The composite material system is obtained by defining two separate models, one for carbon fiber and another one for shape memory polymers. For carbon fibers, a transversely isotropic hyperelastic model is considered while an elasto-viscoplastic model is considered for the shape memory polymers.

A.1 Material model of carbon fiber

Carbon fiber is a transversely isotropic material and subsequently the number of mechanical constants is reduced to 5 because of the in-plane isotropy:

$$\begin{aligned} &E^{\mathrm{T}} = E_1 = E_2 \neq E_3 = E^{\mathrm{L}}, \quad \nu^{\mathrm{TT}} = \nu_{12} = \nu_{21} \neq \nu_{13} = \nu_{23} = \nu^{\mathrm{TL}} \\ &G^{\mathrm{LT}} = G_{13} = G_{23} = G_3 = G^{\mathrm{L}}\,. \end{aligned} \tag{113}$$

The missing in-plane shear modulus G^{TT} is obtained from ν^{TT} and E^{T}, with

$$G^{\mathrm{TT}} = G_{12} = \frac{E^{\mathrm{T}}}{2(1+\nu^{\mathrm{TT}})}. \tag{114}$$

In the previous relations, the subscript 3 or the superscript L refers to the fiber direction and 1, 2, or T is a direction transverse to the fiber direction. Along the longitudinal direction the Poisson ratios are not symmetric but instead satisfy $\frac{\nu_{ij}}{E_i} = \frac{\nu_{ji}}{E_j}$.

In order to model the carbon fiber, we have considered the equation proposed by Bonet *et al.* [10], with some modifications proposed by Wu *et al.* [70], since the original formulation considered that $\nu^{\mathrm{TL}} = \nu^{\mathrm{TT}}$, to describe the isotropic hyperelastic solids in the large strain regime. In addition, we have added the thermal contribution, characterized by the thermal expansion term α_{th}. In this formulation, the strain energy density ψ consists of an isotropic component ψ^{is} and of an orthotropic transversely isotropic component ψ^{tr} such that $\psi = \psi^{\mathrm{is}} + \psi^{\mathrm{tr}}$. The Neo-Hookean equation is used to model the isotropic part, such that

$$\psi^{\mathrm{is}} = \frac{1}{2}G^{\mathrm{TT}}(\mathrm{tr}\boldsymbol{C} - 3) - G^{\mathrm{TT}}\ln J + \frac{1}{2}\lambda(\ln J - 3\alpha'_{\mathrm{th}}(T - T_0))^2, \tag{115}$$

where this energy density function has been defined by C. Miehe in [46], and where $\alpha'_{\mathrm{th}} = \alpha_{\mathrm{th}}\frac{\lambda+2/3G^{\mathrm{TT}}}{\lambda}$ in order to recover the usual dilation coefficient definition of isotropic materials. The orthotropic transversely isotropic component is obtained from a generalization of the model proposed by Bonet *et al.* [10] and enhanced by Wu *et al.* [70]:

$$\psi^{\mathrm{tr}} = \left[\alpha^{\mathrm{tr}} + 2\beta^{\mathrm{tr}}(\ln J - 3\alpha'_{\mathrm{th}}(T - T_0)) + \gamma^{\mathrm{tr}}(\mathrm{I}_4 - 1)\right](\mathrm{I}_4 - 1) - \frac{1}{2}\alpha^{\mathrm{tr}}(\mathrm{I}_5 - 1), \tag{116}$$

where I_4 and I_5 denote the two new pseudo invariants of $\mathbf{C}$ expressed as [57,58],

$$\mathrm{I}_4 = \boldsymbol{A}\cdot\boldsymbol{C}\cdot\boldsymbol{A} \quad \text{and} \quad \mathrm{I}_5 = \boldsymbol{A}\cdot\boldsymbol{C}^2\cdot\boldsymbol{A}\,, \tag{117}$$

with the unit vector $\boldsymbol{A}$ defining the main direction of orthotropy (fiber direction) in the undeformed configuration.

The parameters of the model Eq. (116), λ, G^{TT}, α^{tr}, β^{tr} and γ^{tr} are obtained from the measured properties Eqs. (113, 114) as

$$\begin{aligned} &\lambda = \frac{E^{\mathrm{T}}(\nu^{\mathrm{TT}} + n{\nu^{\mathrm{TL}}}^2)}{m(1+\nu^{\mathrm{TT}})}, \quad G^{\mathrm{TT}} = \frac{E^{\mathrm{T}}}{2(1+\nu^{\mathrm{TT}})},\ \alpha^{\mathrm{tr}} = G^{\mathrm{TT}} - G^{\mathrm{LT}}\,, \\ &\beta^{\mathrm{tr}} = \frac{E^{\mathrm{T}}\left[n\nu^{\mathrm{TL}}(1+\nu^{\mathrm{TT}} - \nu^{\mathrm{TL}}) - \nu^{\mathrm{TT}}\right]}{4m(1+\nu^{\mathrm{TT}})},\ \gamma^{\mathrm{tr}} = \frac{E^{\mathrm{T}}(1-\nu^{\mathrm{TT}})}{8m} - \frac{\lambda + 2G^{\mathrm{TT}}}{8} + \frac{\alpha^{\mathrm{tr}}}{2} - \beta^{\mathrm{tr}}, \\ &m = 1 - \nu^{\mathrm{TT}} - 2n{\nu^{\mathrm{TL}}}^2\,, \quad n = \frac{E^{\mathrm{L}}}{E^{\mathrm{T}}}. \end{aligned} \tag{118}$$

The second Piola-Kirchhoff stress tensor can be obtained by differentiating the free energy in terms of the right Cauchy-Green strain tensor $\boldsymbol{S} = 2\frac{\partial\psi}{\partial\boldsymbol{C}}$ leading to

$$\boldsymbol{S} = \boldsymbol{S}^{\mathrm{is}} + \boldsymbol{S}^{\mathrm{tr}}, \text{ with} \tag{119}$$

$$\boldsymbol{S}^{\mathrm{is}} = \lambda\ln J\boldsymbol{C}^{-1} + G^{\mathrm{TT}}(\boldsymbol{I} - \mathbf{C}^{-1}) - 3\lambda\alpha'_{\mathrm{th}}(T - T_0)\boldsymbol{C}^{-1}, \tag{120}$$

where $\boldsymbol{I}$ is the identity tensor, and with

$$\begin{aligned}\boldsymbol{S}^{\mathrm{tr}} = 2\beta^{\mathrm{tr}}(\mathrm{I}_4 - 1)\boldsymbol{C}^{-1} + 2\left[\alpha^{\mathrm{tr}} + 2\beta^{\mathrm{tr}}(\ln J - 3\alpha'_{\mathrm{th}}(T - T_0)) + 2\gamma^{\mathrm{tr}}(\mathrm{I}_4 - 1)\right]\boldsymbol{A}\otimes\boldsymbol{A} \\ - \alpha^{\mathrm{tr}}(\boldsymbol{C}\cdot\boldsymbol{A}\otimes\boldsymbol{A} + \boldsymbol{A}\otimes\boldsymbol{C}\cdot\boldsymbol{A}).\end{aligned} \tag{121}$$

Then the first Piola-Kirchhoff stress tensor is evaluated from the second Piola-Kirchhoff stress tensor as

$$\boldsymbol{P} = \boldsymbol{F}\cdot\boldsymbol{S}. \tag{122}$$

The stiffness is computed following [10, 70].

A.2 Elasto-visco-plastic formulation for SMP

In this section, we summarize the work of Srivastava *et al.* [59] to model the shape memory polymer behavior above and below glass transition.

A.2.1 Kinematics

To model the inelastic response of the amorphous polymeric materials, it is assumed that the deformation gradient $\boldsymbol{F}$ may be multiplicatively decomposed into elastic and plastic parts

$$\boldsymbol{F} = \boldsymbol{F}^{\mathrm{e}(\alpha)}\cdot\boldsymbol{F}^{\mathrm{p}(\alpha)} \text{ with } \det\boldsymbol{F}^{\mathrm{e}(\alpha)} = J^{\mathrm{e}(\alpha)} = J > 0 \text{ and } \det\boldsymbol{F}^{\mathrm{p}(\alpha)} = 1\,, \tag{123}$$

where $\boldsymbol{F}^{\mathrm{e}(\alpha)}$ is the elastic distortion and $\boldsymbol{F}^{\mathrm{p}(\alpha)}$ is the inelastic distortion with $\boldsymbol{F}^{\mathrm{p}(\alpha)}(\boldsymbol{X}, 0) = \boldsymbol{I}$. In these equations we have considered the possibility to account for several mechanisms $\alpha = 1, 2, 3$. Moreover, the elastic decomposition of the deformation gradient can be written as

$$\boldsymbol{F}^{\mathrm{e}(\alpha)} = \boldsymbol{R}^{\mathrm{e}(\alpha)}\cdot\boldsymbol{U}^{\mathrm{e}(\alpha)}\,, \tag{124}$$

with the elastic right and left Cauchy-Green strain tensors respectively equal to

$$\boldsymbol{C}^{\mathrm{e}(\alpha)} = \boldsymbol{U}^{\mathrm{e}(\alpha)^2} = \boldsymbol{F}^{\mathrm{e}(\alpha)\mathrm{T}}\cdot\boldsymbol{F}^{\mathrm{e}(\alpha)} \text{ and } \boldsymbol{B}^{\mathrm{e}(\alpha)} = \boldsymbol{F}^{\mathrm{e}(\alpha)}\cdot\boldsymbol{F}^{\mathrm{e}(\alpha)\mathrm{T}}\,. \tag{125}$$

A.2.2 Elasto-visco-plasticity

The material may be idealized to be isotropic. Accordingly, all constitutive functions are presumed to be isotropic in character. Let us assume that the free energy has the separable form

$$\psi_R = \sum_{\alpha}\ \psi^{(\alpha)}(\Phi_{\boldsymbol{C}^{\mathrm{e}(\alpha)}}, T), \tag{126}$$

where $\Phi_{\boldsymbol{c}^{\mathrm{e}(\alpha)}}$ represents a list of the principle invariants of $\boldsymbol{C}^{\mathrm{e}(\alpha)}$ and T is the temperature. The Cauchy stress is decomposed in terms of the mechanisms $\boldsymbol{\sigma} = \sum_{(\alpha)}\boldsymbol{\sigma}^{(\alpha)}$ with

$$\boldsymbol{\sigma}^{(\alpha)} = \frac{1}{J}\,\boldsymbol{F}\,\boldsymbol{S}^{(\alpha)}\,\boldsymbol{F}^{\mathrm{T}} = \frac{1}{J}\,\boldsymbol{F}^{\mathrm{e}(\alpha)}\,\boldsymbol{S}^{e(\alpha)}\,\boldsymbol{F}^{\mathrm{e}(\alpha)\mathrm{T}}, \tag{127}$$

where $\boldsymbol{S}^{e(\alpha)}$ is the symmetric elastic second Piola-Kirchhoff stress

$$\boldsymbol{S}^{e(\alpha)} = 2\frac{\partial\psi^{(\alpha)}(\Phi_{\boldsymbol{c}^{\mathrm{e}(\alpha)}}, T)}{\partial\boldsymbol{C}^{\mathrm{e}(\alpha)}}. \tag{128}$$

Moreover, the first Piola-Kirchhoff stress tensor can be computed following

$$\boldsymbol{P}^{(\alpha)} = J\,\boldsymbol{\sigma}^{(\alpha)}\boldsymbol{F}^{-\mathrm{T}} = \boldsymbol{F}^{\mathrm{e}(\alpha)}\,\boldsymbol{S}^{\mathrm{e}(\alpha)}\,\boldsymbol{F}^{\mathrm{p}(\alpha)-\mathrm{T}} = \boldsymbol{F}\,\boldsymbol{F}^{\mathrm{p}(\alpha)-1}\,\boldsymbol{S}^{\mathrm{e}(\alpha)}\,\boldsymbol{F}^{\mathrm{p}(\alpha)-\mathrm{T}}\,. \tag{129}$$

The driving stress of the plastic flow is the symmetric Mandel stress, which is defined as

$$\boldsymbol{M}^{\mathrm{e}(\alpha)} = J\,\boldsymbol{R}^{\mathrm{e}(\alpha)\mathrm{T}}\boldsymbol{\sigma}^{(\alpha)}\boldsymbol{R}^{\mathrm{e}(\alpha)} = \boldsymbol{U}^{\mathrm{e}(\alpha)}\boldsymbol{S}^{\mathrm{e}(\alpha)}\boldsymbol{U}^{\mathrm{e}(\alpha)} = \boldsymbol{C}^{\mathrm{e}(\alpha)}\boldsymbol{S}^{\mathrm{e}(\alpha)}, \tag{130}$$

where $\boldsymbol{M}^{\mathrm{e}(\alpha)}$ is the elastic Mandel stress, $\boldsymbol{R}^{\mathrm{e}(\alpha)}$ is the rotation matrix, and where it has been assumed that $\boldsymbol{C}^{\mathrm{e}(\alpha)}$ and $\boldsymbol{S}^{\mathrm{e}(\alpha)}$ permute. The corresponding equivalent shear stress is given by

$$\bar{\tau}^{(\alpha)} = \frac{1}{\sqrt{2}}|\boldsymbol{M}_0^{\mathrm{e}(\alpha)}|, \tag{131}$$

where $\boldsymbol{M}_0^{\mathrm{e}(\alpha)}$ is the deviatoric part of the Mandel stress

$$\boldsymbol{M}_0^{\mathrm{e}(\alpha)} = \boldsymbol{M}^{\mathrm{e}(\alpha)} + \bar{p}\boldsymbol{I}\,,\ \text{with}\ \bar{p} = -\frac{1}{3}\mathrm{tr}\boldsymbol{M}^{\mathrm{e}(\alpha)}\,, \tag{132}$$

and $|\boldsymbol{M}_0^{\mathrm{e}(\alpha)}| = \sqrt{\boldsymbol{M}_0^{\mathrm{e}(\alpha)} : \boldsymbol{M}_0^{\mathrm{e}(\alpha)}}$ is the norm of the deviatoric part of the Mandel stress.

In order to account for the major strain-hardening and softening characteristics of polymeric materials observed during visco-plastic deformation, Srivastava *et al.* [59] have introduced macroscopic internal variables $\boldsymbol{\xi}^{(\alpha)}$ to represent important aspects of the microstructural resistance to plastic flow. The plastic flow follows

$$\dot{\boldsymbol{F}}^{\mathrm{p}(\alpha)} = \boldsymbol{D}^{\mathrm{p}(\alpha)}\boldsymbol{F}^{\mathrm{p}(\alpha)}, \tag{133}$$

where each $\boldsymbol{F}^{\mathrm{p}(\alpha)}$ is to be regarded as an internal variable part of $\boldsymbol{\xi}^{(\alpha)}$, and which is defined as a solution of the differential equation

$$\boldsymbol{D}^{\mathrm{p}(\alpha)} = \dot{\epsilon}^{\mathrm{p}(\alpha)}\left(\frac{\boldsymbol{M}_0^{\mathrm{e}(\alpha)}}{2\bar{\tau}^{\alpha}}\right), \tag{134}$$

where $\boldsymbol{D}^{\mathrm{p}}$ is the plastic stretching tensor, and $\dot{\epsilon}^{\mathrm{p}(\alpha)} = \sqrt{2}|\boldsymbol{D}^{\mathrm{p}(\alpha)}|$ is the equivalent plastic shear strain rate.

Therefore for given $\bar{\tau}^{(\alpha)}$ and $\boldsymbol{\Lambda}^{(\alpha)} = (\boldsymbol{C}^{\mathrm{e}(\alpha)}, \boldsymbol{B}^{\mathrm{p}(\alpha)}, \boldsymbol{\xi}^{(\alpha)}, T)$ a list of constitutive variables, the equivalent plastic shear strain rate $\dot{\epsilon}^{\mathrm{p}(\alpha)}$ is obtained by solving a scalar strength relation such as

$$\bar{\tau}^{(\alpha)} = \Upsilon^{(\alpha)}(\boldsymbol{\Lambda}^{(\alpha)}, \dot{\epsilon}^{\mathrm{p}(\alpha)}), \tag{135}$$

where the strength function $\Upsilon^{(\alpha)}(\boldsymbol{\Lambda}^{(\alpha)}, \dot{\epsilon}^{\mathrm{p}(\alpha)})$ is an isotropic function of its arguments.

A.2.3 Partial differential governing equations

In order to complete Eq. (7), y, the internal energy per unit mass, is defined as $y = c_{\mathrm{v}}T$, where the volumetric heat capacity per unit mass is a function of the glass transition temperature, and is defined as follows

$$c_{\mathrm{v}} = \begin{cases} c_0 - c_1(T - T_{\mathrm{g}}) & \text{if}\, T \le T_{\mathrm{g}} \\ c_0 & \text{if}\, T > T_{\mathrm{g}}. \end{cases} \tag{136}$$

Moreover, $\bar{F}$, the body source of heat, is expressed as

$$\bar{F} = Q_{\mathrm{r}} + \sum_{\alpha} \bar{\tau}^{(\alpha)}\dot{\epsilon}^{\mathrm{p}(\alpha)} + T\frac{\partial^2\psi^{\mathrm{e}(\alpha)}}{\partial\boldsymbol{C}^{\mathrm{e}(\alpha)}\partial\mathrm{T}} : \dot{\boldsymbol{C}}^{\mathrm{e}(\alpha)}, \tag{137}$$

where Q_{r} is the scalar heat supply measured per unit reference volume and the last term of the right hand side is the thermo-elastic damping term which is neglected. Instead it is assumed that only a fraction v of the rate of the plastic dissipation contributes to the temperature change

$$\bar{F} = Q_{\mathrm{r}} + v\sum_{\alpha} \bar{\tau}^{(\alpha)}\dot{\epsilon}^{\mathrm{p}(\alpha)}, \tag{138}$$

where $0 \le v \le 1$.

The glass transition in amorphous polymers depends on the equivalent shear strain rate $\dot{\epsilon} = \sqrt{2}|\boldsymbol{D}_0|$ to which the material is subjected, where $\boldsymbol{D}_0 = \boldsymbol{D} - \frac{1}{3}\mathrm{tr}\boldsymbol{D}\ \boldsymbol{I}$ denotes the total deviatoric stretching tensor, with

$$\boldsymbol{D} = \frac{1}{2}(\dot{\boldsymbol{F}}\ \boldsymbol{F}^{-1} + \boldsymbol{F}^{-\mathrm{T}}\dot{\boldsymbol{F}}^{\mathrm{T}})\,. \tag{139}$$

Eventually, the glass transition T_{g} is calculated from the following expression

$$T_{\mathrm{g}} = \begin{cases} T_{\mathrm{r}} & \text{if } \dot{\epsilon} \leq \epsilon_{\mathrm{r}}, \\ T_{\mathrm{r}} + n\log(\dfrac{\dot{\epsilon}}{\epsilon_{\mathrm{r}}}) & \text{if } \dot{\epsilon} > \epsilon_{\mathrm{r}}, \end{cases} \tag{140}$$

where T_{r} is the reference glass transition temperature at low strain rate, $\dot{\epsilon}$ is the shear strain rate, and ϵ_{r} is the reference strain rate.

A.2.4 The first micromechanism ($\alpha = 1$)

The first micromechanism ($\alpha = 1$) represents an elastic resistance due to intermolecular energetic bond-stretching and a dissipation due to the thermally-activated plastic flow following chain segment rotation and relative slippage of the polymer chains between neighboring cross-linkage points.

The following simple generalization of the classical strain energy function of infinitesimal isotropic elasticity is considered, and uses a logarithmic measure

$$\boldsymbol{E}^{\mathrm{e}(1)} = \frac{1}{2}\ln \boldsymbol{C}^{\mathrm{e}(1)}\,, \tag{141}$$

of the finite elastic strain [4]. The form of the elastic free energy is thus defined as

$$\psi^{\mathrm{e}(1)} = G|\boldsymbol{E}_0^{\mathrm{e}(1)}|^2 + \frac{1}{2}K\left(\mathrm{tr}\boldsymbol{E}^{\mathrm{e}(1)}\right)^2 - 3K\left(\mathrm{tr}\boldsymbol{E}^{\mathrm{e}(1)}\right)\alpha_{\mathrm{th}}(T - T_0) + \tilde{f}(T)\,, \tag{142}$$

where the deviatoric part of the logarithmic strain is denoted by $\boldsymbol{E}_0^{\mathrm{e}}$, $\tilde{f}(T)$ is an entropy contribution to the free energy related to the temperature dependent specific heat of the material, and where the temperature dependent parameters $G(T)$, $K(T)$, $\alpha_{\mathrm{th}}(T)$ are respectively the shear modulus, bulk modulus, and the coefficient of thermal expansion.

The Mandel stress is thus obtained from

$$\boldsymbol{M}^{\mathrm{e}(1)} = 2\boldsymbol{C}^{\mathrm{e}(1)}\frac{\partial\psi^{\mathrm{e}(1)}(\boldsymbol{E}^{\mathrm{e}(1)},\mathrm{T})}{\partial\boldsymbol{C}^{\mathrm{e}(1)}} = \frac{\partial\psi^{\mathrm{e}(1)}(\boldsymbol{E}^{\mathrm{e}(1)},T)}{\partial\boldsymbol{E}^{\mathrm{e}(1)}}\,, \tag{143}$$

if $\boldsymbol{C}^{\mathrm{e}(1)}$ and $\boldsymbol{M}^{\mathrm{e}(1)}$ permute. It should be noted that in this work $\boldsymbol{E}^{\mathrm{e}(1)}$ is computed by using a Taylor series approximation of Eq. (141), and not through the eigenvalue decomposition. Substituting Eq. (142) in Eq. (143), as $|\boldsymbol{E}_0^{\mathrm{e}(1)}| = \boldsymbol{E}_0^{\mathrm{e}(1)} : \boldsymbol{E}_0^{\mathrm{e}(1)}$ one can get directly $\boldsymbol{M}^{\mathrm{e}(1)}$ as

$$\boldsymbol{M}^{\mathrm{e}(1)} = 2G\boldsymbol{E}_0^{\mathrm{e}(1)} + K\left(\mathrm{tr}\boldsymbol{E}^{\mathrm{e}(1)}\right)\boldsymbol{I}\ - 3K\alpha_{\mathrm{th}}(T - T_0)\boldsymbol{I}\,. \tag{144}$$

The thermal expansion is taken to have a bilinear temperature dependence, with the slope $\alpha_{\mathrm{th}} = \alpha_{\mathrm{r}}$ above the glass transition temperature and the slope $\alpha_{\mathrm{th}} = \alpha_{\mathrm{gl}}$ below it.

Moreover, the evaluation equation for $\boldsymbol{F}^{\mathrm{p}(1)}$ follows Eqs. (133-134) with the thermally-activated relation for the equivalent plastic strain rate following

$$\dot{\epsilon}^{\mathrm{p}(1)} = \begin{cases} 0 & \text{if} \quad \tau^{\mathrm{e}(1)} \leq 0, \\ \dot{\epsilon_0^{(1)}}\exp(-\dfrac{1}{\xi})\exp(-\dfrac{Q(T)}{K_{\mathrm{B}}T})[\sinh(\dfrac{\tau^{\mathrm{e}(1)}\,V'}{2\,K_{\mathrm{B}}T})]^{1/m^{(1)}} & \text{if} \quad \tau^{\mathrm{e}(1)} > 0, \end{cases} \tag{145}$$

where $\dot{\epsilon}^{\mathrm{p}(1)}$ is the plastic strain rate, the parameter $\dot{\epsilon_0^{(1)}}$ is a pre-exponential factor with units of 1/time, K_{B} is Boltzmann's constant, V' is an activation volume, $m^{(1)}$ is the sensitive

parameter for the strain rate, $Q(T)$ is the temperature dependent activation energy, and $\tau^{e(1)}$ denotes a net shear stress for the thermally activated flow

$$\tau^{\mathrm{e}(1)} = \bar{\tau}^{(1)} - (S_\mathrm{a} + S_\mathrm{b} + \alpha_\mathrm{p}\bar{p}), \tag{146}$$

with $\alpha_\mathrm{p} \geqslant 0$ a parameter introduced to account for the pressure sensitivity. The term $\exp(-\frac{1}{\xi})$ in Eq. (145) represents a concentration of flow defects, with

$$\xi = \begin{cases} \xi_\mathrm{gl} & \text{if} \quad T \leq T_\mathrm{g}\,, \\ \xi_\mathrm{gl} + d(T - T_\mathrm{g}) & \text{if} \quad T > T_\mathrm{g}\,. \end{cases} \tag{147}$$

For the first micromechanism, besides the plastic strain gradient, the list $\boldsymbol{\xi}^1 = (\varphi, S_\mathrm{a}, S_\mathrm{b})$ of internal variables consists of three positive scalars, where the variable $\varphi \geq 0$ and $S_\mathrm{a} \geq 0$ are introduced to model the yield peak which is observed in the stress-strain response of glassy polymers and $S_\mathrm{b} \geq 0$ is introduced to model the isotropic hardening at high strain. The evolution equations of $\dot{S}_\mathrm{a}$ and $\dot{\varphi}$ are governed by

$$\dot{S}_\mathrm{a} = h_\mathrm{a}\left[b(\varphi^* - \varphi) - S_\mathrm{a}\right]\dot{\epsilon}^{\mathrm{p}(1)} \quad \text{with initial value } S_\mathrm{a} = S_{\mathrm{a}0}\,, \tag{148}$$

$$\dot{\varphi} = g(\varphi^* - \varphi)\dot{\epsilon}^{\mathrm{p}(1)} \quad \text{with initial value } \varphi = \varphi_0\,, \tag{149}$$

with φ^* as

$$\varphi^*(\dot{\epsilon}^{\mathrm{p}(1)},\, T) = \begin{cases} z\left((1 - \dfrac{T}{T_\mathrm{g}})^r + h_\mathrm{g}\right)\,(\dfrac{\dot{\epsilon}^{\mathrm{p}(1)}}{\epsilon_\mathrm{r}})^s & \text{if } T \leq T_\mathrm{g} \text{ and } \dot{\epsilon}^{\mathrm{p}(1)} > 0\,, \\ z\,h_\mathrm{g}\,(\dfrac{\dot{\epsilon}^{\mathrm{p}(1)}}{\epsilon_\mathrm{r}})^s & \text{if } T > T_\mathrm{g} \text{ and } \dot{\epsilon}^{\mathrm{p}(1)} > 0\,, \end{cases} \tag{150}$$

which represents the temperature and strain rate dependency of φ, where z, r, h_g, and s are taken to be constants. In particular we have introduced h_g to get a small value for φ^* when $T > T_\mathrm{g}$, instead of 0 in order to improve the convergence of the numerical model. Then the evolution of S_b is governed by

$$S_\mathrm{b} = S_{\mathrm{b}0} + H_\mathrm{b}(\bar{\lambda} - 1)^a, \;\; \bar{\lambda} = \sqrt{\mathrm{tr}\boldsymbol{C}/3}, \tag{151}$$

where $\bar{\lambda}$ is an effective stretch which increases or decreases as the overall stretch increases or decreases, and where $H_\mathrm{b}(T)$ is a temperature dependent hardening parameter.

The temperature evolutions of H_b, $Q(T)$, $G(T)$, and of the Poisson ratio $\nu(T)$ follow a law

$$\cdot(T) = \frac{1}{2}(\cdot_\mathrm{gl} + \cdot_\mathrm{r}) - \frac{1}{2}(\cdot_\mathrm{gl} - \cdot_\mathrm{r})\tanh(\frac{1}{\Delta}(T - T_\mathrm{g})) - L_\cdot(T - T_\mathrm{g})\,, \tag{152}$$

where $\cdot_\mathrm{gl}$ and $\cdot_\mathrm{r}$ are the values in glassy and rubbery regions, and where $L_\cdot$ represents the slope of the temperature variation of $\cdot$, and takes the value of $L_\cdot = L_{\cdot_\mathrm{gl}}$ if $T \leq T_\mathrm{g}$ and $L_\cdot = L_{\cdot_\mathrm{r}}$ if $T > T_\mathrm{g}$. The temperature dependence of the bulk modulus $K(T)$ is then obtained by using the standard relation for isotropic materials $K(T) = G(T)\frac{2(1+\nu(T))}{3(1-2\,\nu(T))}$.

A.2.5 The second micromechanism ($\alpha = 2$)

The second micromechanism ($\alpha = 2$) represents the molecular chains between mechanical crosslinks. At temperatures below T_g the polymer exhibits a significant amount of mechanical crosslinking which disintegrates when the temperature is increased above T_g.

Only deviatoric contributions are considered in the free energy function

$$\psi^{(2)} = \bar{\psi}^{(2)}(\bar{\boldsymbol{C}}^{e(2)},\, T) = -\frac{1}{2}\,\mu^{(2)} I_\mathrm{m}^{(2)} \ln(1 - \frac{\mathrm{tr}\bar{\boldsymbol{C}}^{\mathrm{e}(2)} - 3}{I_\mathrm{m}^{(2)}})\,, \tag{153}$$

where $\bar{\boldsymbol{C}}^{\mathrm{e}(2)} = \bar{\boldsymbol{F}}^{\mathrm{e}(2)\mathrm{T}}\bar{\mathbf{F}}^{\mathrm{e}(2)} = \mathrm{J}^{-\frac{2}{3}}\boldsymbol{C}^{\mathrm{e}(2)}$ denotes the distrotional (or volume preserving) right Cauchy strain tensor, the parameter $I_{\mathrm{m}}^{(2)}$ is taken to be temperature constant, and where $\mu^{(2)}$ is the rubbery shear modulus, which follows

$$\mu^{(2)} = \mu_{\mathrm{g}}\exp(-N(T - T_{\mathrm{g}}))\,, \tag{154}$$

with μ_{g} the value of $\mu^{(2)}$ at the glass transition temperature, and N a parameter that represents the slope of temperature variation on a logarithmic scale.

The corresponding Mandel stress is evaluated from Eq. (130) and Eq. (153) as

$$\boldsymbol{M}^{\mathrm{e}(2)} = \boldsymbol{C}^{\mathrm{e}(2)}\; 2\,\frac{\partial\bar{\psi}^{(2)}}{\partial\boldsymbol{C}^{\mathrm{e}(2)}} = \mu^{(2)}(1 - \frac{\mathrm{tr}\bar{\mathbf{C}}^{\mathrm{e}(2)} - 3}{I_{\mathrm{m}}^{(2)}})^{-1}\bar{\boldsymbol{C}}_0^{\mathrm{e}(2)}, \tag{155}$$

where $\bar{\boldsymbol{C}}_0^{\mathrm{e}(2)} = \bar{\boldsymbol{C}}^{\mathrm{e}(2)} - \frac{1}{3}\mathrm{tr}\bar{\boldsymbol{C}}^{\mathrm{e}(2)}\boldsymbol{I}$ is the deviatoric part of $\boldsymbol{C}^{\mathrm{e}(2)}$ the right Cauchy Green tensor. Clearly, as $\bar{\boldsymbol{C}}^{\mathrm{e}(2)}$ and $\boldsymbol{C}^{\mathrm{e}(2)}$ permute, $\boldsymbol{M}^{\mathrm{e}(2)}$ and $\bar{\boldsymbol{C}}^{\mathrm{e}(2)}$ permute as well.

For the second mechanism, the equivalent plastic strain rate follows

$$\dot{\epsilon}^{\mathrm{p}(2)} = \dot{\epsilon}_0^{(2)}(\frac{\bar{\tau}^{(2)}}{S^{(2)}})^{\frac{1}{m^{(2)}}}\,, \tag{156}$$

where $\dot{\epsilon}_0^{(2)}$ is a reference plastic shear strain rate, $m^{(2)}$ is the positive valued strain rate sensitivity parameter, and $S^{(2)}$ is a temperature dependent parameter which follows (152).

A.2.6 The third micromechanism ($\alpha = 3$)

The third micromechanism ($\alpha = 3$) introduces the molecular chains between chemical crosslinks and represents the resistance due to changes in the free energy upon stretching of the molecular chains between the crosslinks.

The free energy is a function of the deviatoric tensor $\bar{\boldsymbol{C}} = \bar{\boldsymbol{F}}^{\mathrm{T}}\bar{\boldsymbol{F}} = J^{-\frac{2}{3}}\boldsymbol{C}$, and is given by a deviatoric form

$$\psi^{(3)} = \bar{\psi}^{(3)}(\bar{\boldsymbol{C}}) = -\frac{1}{2}\,\mu^{(3)}I_{\mathrm{m}}^{(3)}\,\ln(1 - \frac{\mathrm{tr}\bar{\boldsymbol{C}} - 3}{I_{\mathrm{m}}^{(3)}}), \tag{157}$$

where the material constants $\mu^{(3)} > 0$ and $I_{\mathrm{m}}^{(3)} > 0$ are assumed to be temperature-independent.

The free energy (157) yields the corresponding second Piola stress $\boldsymbol{S}^{(3)}$ as

$$\boldsymbol{S}^{(3)} = 2\frac{\partial\bar{\psi}^{(3)}}{\partial\bar{\boldsymbol{C}}} : \frac{\partial\bar{\boldsymbol{C}}}{\partial\boldsymbol{C}} = J^{-\frac{2}{3}}\mu^{(3)}(1 - \frac{\mathrm{tr}\bar{\mathbf{C}} - 3}{\boldsymbol{I}_{\mathrm{m}}^{(3)}})^{-1}[\boldsymbol{I} - \frac{1}{3}(\mathrm{tr}\bar{\boldsymbol{C}})\bar{\mathbf{C}}^{-1}]\,. \tag{158}$$

A.2.7 Finite increment form of the Shape Memory Polymer constitutive law

The constitutive laws are formulated in a finite strain setting and solved following the predictor-corrector scheme during the time interval $[t_n;\ t_{n+1}]$, where we use the subscript n for the previous time t_n and $n+1$ for the current time t_{n+1}. The formulation can be summarized as follows:

- Prediction step: The plastic deformation gradient is initialized to the value at the previous step $\boldsymbol{F}_{(\mathrm{pr})}^{\mathrm{p}(\alpha)} = \boldsymbol{F}_n^{\mathrm{p}(\alpha)}$, and the elastic deformation follows

$$\boldsymbol{F}_{n+1}^{\mathrm{e}(\alpha)} = \boldsymbol{F}_{n+1}\boldsymbol{F}_n^{\mathrm{p}(\alpha)^{-1}}\,. \tag{159}$$

- Correction step: In this step we solve the system of equations that has been presented for each mechanism. To extract the plastic increment using the evaluation equation of the plastic deformation gradient during the time step between the configurations n and $n+1$, we consider

$$\boldsymbol{F}_{n+1}^{\mathrm{p}(\alpha)} = \exp(\Delta\mathbf{D}^{\mathrm{p}(\alpha)})\boldsymbol{F}_n^{\mathrm{p}(\alpha)}\,, \tag{160}$$

with

$$\Delta\boldsymbol{D}^{\mathrm{p}(\alpha)} = (\epsilon_{n+1}^{\mathrm{p}(\alpha)} - \epsilon_n^{\mathrm{p}(\alpha)})\frac{\boldsymbol{M}^{\mathrm{e}(\alpha)}}{2\bar{\tau}^{(\alpha)}} = \Delta\epsilon^{\mathrm{p}(\alpha)}\left(\frac{\boldsymbol{M}^{\mathrm{e}(\alpha)}}{2\bar{\tau}^{(\alpha)}}\right)\,. \tag{161}$$

More details about the predictor-corrector algorithm and the stiffness computation can be found in [26].

B The finite element formulation

Using the interpolations (33-34), the gradients are readily obtained by:

$$\nabla_0 \boldsymbol{u}_\mathrm{h} = \mathbf{u}^a \otimes \nabla_0 N^a_\mathbf{u} \,, \quad \nabla_0 \mathbf{M}_\mathrm{h} = \nabla_0 \mathbf{N}^a_\mathbf{M}\, \mathbf{M}^a \,, \tag{162}$$

$$\nabla_0 \delta\boldsymbol{u}_\mathrm{h} = \delta\mathbf{u}^a \otimes \nabla_0 N^a_\mathbf{u} \,, \quad \nabla_0 \delta\mathbf{M}_\mathrm{h} = \nabla_0 \mathbf{N}^a_\mathbf{M}\, \delta\mathbf{M}^a \,, \tag{163}$$

where $\nabla_0 N^a_\mathbf{u}$ and $\nabla_0 \mathbf{N}^a_\mathbf{M} = \begin{pmatrix} \nabla_0 N^a_{\mathrm{f_V}} & \mathbf{0} \\ \mathbf{0} & \nabla_0 N^a_{\mathrm{f_T}} \end{pmatrix}$ are the gradients of the shape functions at node a.

B.1 Nodal forces

The expressions of the nodal forces (36) are obtained by substituting the interpolations (33-34) and (162-163) in the weak formulation (31).

First the mechanical contribution reads

$$\begin{aligned}
\mathbf{F}^a_{\mathbf{u}\mathrm{ext}} &= \sum_\mathrm{s} \int_{(\partial_\mathrm{N}\Omega_0)^\mathrm{s}} N^a_\mathbf{u} \bar{\boldsymbol{T}} \mathrm{d}S_0 - \sum_\mathrm{s} \int_{(\partial_\mathrm{D}\Omega_0)^\mathrm{s}} (\bar{\boldsymbol{u}} \otimes \boldsymbol{N} : \boldsymbol{\mathcal{H}}) \cdot \nabla_0 N^a_\mathbf{u} \mathrm{d}S_0 \\
&\quad + \sum_\mathrm{s} \int_{(\partial_\mathrm{D}\Omega_0)^\mathrm{s}} \left(\bar{\boldsymbol{u}} \otimes \boldsymbol{N} : \frac{\boldsymbol{\mathcal{H}}\mathcal{B}}{h_\mathrm{s}} \right) \cdot \boldsymbol{N} N^a_\mathbf{u} \mathrm{d}S_0 \\
&\quad - \int_{\partial_\mathrm{D}\Omega_{0\mathrm{h}}} \left(\boldsymbol{\mathcal{Y}}(\bar{\mathbf{M}})\bar{\mathbf{M}} - \boldsymbol{\mathcal{Y}}(\bar{\mathbf{M}}_0)\bar{\mathbf{M}}_0 \right) \cdot \boldsymbol{N} N^a_\mathbf{u} \mathrm{d}S_0 \,,
\end{aligned} \tag{164}$$

$$\mathbf{F}^a_{\mathbf{u}\mathrm{int}} = \sum_\mathrm{e} \int_{\Omega^\mathrm{e}_0} \boldsymbol{P}(\boldsymbol{F}_\mathrm{h}, \mathbf{M}_\mathrm{h}) \cdot \nabla_0 N^a_\mathbf{u} \mathrm{d}\Omega_0, \text{ and} \tag{165}$$

$$\mathbf{F}^{a\pm}_{\mathbf{u}\mathrm{I}} = \mathbf{F}^{a\pm}_{\mathbf{u}\mathrm{I}1} + \mathbf{F}^{a\pm}_{\mathbf{u}\mathrm{I}2} + \mathbf{F}^{a\pm}_{\mathbf{u}\mathrm{I}3} \,, \tag{166}$$

with the three mechanical contributions to the interface forces related to the degrees of freedom of the nodes $a\pm$ on each side of the interface elements reading[1]

$$\mathbf{F}^{a\pm}_{\mathbf{u}\mathrm{I}1} = \sum_\mathrm{s} \int_{(\partial_\mathrm{I}\Omega_0)^\mathrm{s}} (\pm N^{a\pm}_\mathbf{u}) \langle \boldsymbol{P}(\boldsymbol{F}_\mathrm{h}, \mathbf{M}_\mathrm{h}) \rangle \cdot \boldsymbol{N}^- \mathrm{d}S_0, \tag{167}$$

$$\mathbf{F}^{a\pm}_{\mathbf{u}\mathrm{I}2} = \frac{1}{2} \sum_\mathrm{s} \int_{(\partial_\mathrm{I}\Omega_0)^\mathrm{s}} [\![\boldsymbol{u}_\mathrm{h}]\!] \otimes \boldsymbol{N}^- : \boldsymbol{\mathcal{H}}^\pm \cdot \nabla_0 N^{a\pm}_\mathbf{u} \mathrm{d}S_0, \tag{168}$$

$$\mathbf{F}^{a\pm}_{\mathbf{u}\mathrm{I}3} = \sum_\mathrm{s} \int_{(\partial_\mathrm{I}\Omega_0)^\mathrm{s}} ([\![\boldsymbol{u}_\mathrm{h}]\!] \otimes \boldsymbol{N}^-) : \left\langle \frac{\boldsymbol{\mathcal{H}}\mathcal{B}}{h_\mathrm{s}} \right\rangle \cdot \boldsymbol{N}^- (\pm N^{a\pm}_\mathbf{u}) \mathrm{d}S_0. \tag{169}$$

Secondly, the electro-thermal contributions read

$$\begin{aligned}
\mathbf{F}^a_{\mathbf{M}_\mathrm{ext}} &= \sum_\mathrm{s} \int_{(\partial_\mathrm{N}\Omega_0)^\mathrm{s}} \mathbf{N}^a_\mathbf{M} \bar{\mathbf{J}} \mathrm{d}S_0 - \sum_\mathrm{s} \int_{(\partial_\mathrm{D}\Omega_0)^\mathrm{s}} \nabla_0 \mathbf{N}^{a\,\mathrm{T}}_\mathbf{M} \boldsymbol{Z}_0(\boldsymbol{F}_\mathrm{h}, \bar{\mathbf{M}}) \bar{\mathbf{M}}_\mathbf{N} \mathrm{d}S_0 \\
&\quad + \sum_\mathrm{s} \int_{(\partial_\mathrm{D}\Omega_0)^\mathrm{s}} \mathbf{N}^a_\mathbf{M} \bar{\mathbf{N}}^\mathrm{T}_\mathbf{M} \boldsymbol{Z}_0(\boldsymbol{F}_\mathrm{h}, \bar{\mathbf{M}}) \frac{\mathcal{B}}{h_\mathrm{s}} \bar{\mathbf{M}}_\mathbf{N} \mathrm{d}S_0 \,,
\end{aligned} \tag{170}$$

$$\mathbf{F}^a_{\mathbf{M}_\mathrm{int}} = \sum_\mathrm{e} \int_{\Omega^\mathrm{e}_0} \nabla_0 \mathbf{N}^{a\,\mathrm{T}}_\mathbf{M} \mathbf{J}(\boldsymbol{F}_\mathrm{h}, \mathbf{M}_\mathrm{h}, \nabla \mathbf{M}_\mathrm{h}) \mathrm{d}\Omega_0 + \sum_\mathrm{e} \int_{\Omega^\mathrm{e}_0} \mathbf{N}^{a\,\mathrm{T}}_\mathbf{M} \mathbf{I}_\mathrm{i} \mathrm{d}\Omega_0, \text{ and} \tag{171}$$

$$\mathbf{F}^{a\pm}_{\mathbf{M}_\mathrm{I}} = \mathbf{F}^{a\pm}_{\mathbf{M}_\mathrm{I}1} + \mathbf{F}^{a\pm}_{\mathbf{M}_\mathrm{I}2} + \mathbf{F}^{a\pm}_{\mathbf{M}_\mathrm{I}3}, \tag{172}$$

[1] The contributions on $\partial_\mathrm{D}\Omega_{0\mathrm{h}}$ can be directly deduced by removing the factor (1/2) accordingly to the definition of the average flux on the Dirichlet boundary and by using $\boldsymbol{Z}_0(\boldsymbol{F}_\mathrm{h}, \bar{\mathbf{M}})$ instead of $\boldsymbol{Z}_0(\boldsymbol{F}_\mathrm{h}, \mathbf{M}_\mathrm{h})$. However, there is one more additional term in $\mathbf{F}^{a\pm}_{\mathbf{u}\mathrm{I}1}$ in the Dirichlet boundary, which is $\sum_\mathrm{s} \int_{(\partial_\mathrm{D}\Omega_0)^\mathrm{s}} (-N^a_\mathbf{u}) \left(\boldsymbol{\mathcal{Y}}(\mathbf{M})\mathbf{M} - \boldsymbol{\mathcal{Y}}(\mathbf{M}_0)\mathbf{M}_0 \right) \cdot \boldsymbol{N}^- \mathrm{d}S_0$.

with the three electric contributions to the interface forces[1]

$$\mathbf{F}^{a\pm}_{\mathbf{M}_{\mathrm{I}1}} = \sum_{\mathrm{s}} \int_{(\partial_{\mathrm{I}}\Omega_0)^{\mathrm{s}}} (\pm \mathbf{N}^{a\pm}_{\mathbf{M}}) \left(\bar{\mathbf{N}}^{-}_{\mathbf{M}}\right)^{\mathrm{T}} \langle \mathbf{J}(\boldsymbol{F}_{\mathrm{h}},\, \mathbf{M}_{\mathrm{h}},\, \nabla \mathbf{M}_{\mathrm{h}}) \rangle \, \mathrm{dS}_0, \tag{173}$$

$$\mathbf{F}^{a\pm}_{\mathbf{M}_{\mathrm{I}2}} = \frac{1}{2} \sum_{\mathrm{s}} \int_{(\partial_{\mathrm{I}}\Omega_0)^{\mathrm{s}}} \left(\nabla_0 \mathbf{N}^{a\pm\mathrm{T}}_{\mathbf{M}} \boldsymbol{Z}^{\pm}_0(\boldsymbol{F}_{\mathrm{h}},\, \mathbf{M}_{\mathrm{h}}) \right) [\![\mathbf{M}_{\mathrm{h}_{\mathbf{N}}}]\!] \, \mathrm{dS}_0, \tag{174}$$

$$\mathbf{F}^{a\pm}_{\mathbf{M}_{\mathrm{I}3}} = \sum_{\mathrm{s}} \int_{(\partial_{\mathrm{I}}\Omega_0)^{\mathrm{s}}} (\pm \mathbf{N}^{a\pm}_{\mathbf{M}}) \left(\bar{\mathbf{N}}^{-}_{\mathbf{M}}\right)^{\mathrm{T}} \left\langle \boldsymbol{Z}_0(\boldsymbol{F}_{\mathrm{h}},\, \mathbf{M}_{\mathrm{h}}) \frac{\mathcal{B}}{h_{\mathrm{s}}} \right\rangle [\![\mathbf{M}_{\mathrm{h}_{\mathbf{N}}}]\!] \, \mathrm{dS}_0 \,. \tag{175}$$

B.2 Tangent operators

In order to derive the tangent matrix $\mathbb{K}^{ab}_{\mathbf{G}} = \frac{\partial \mathbf{F}^a_{\mathrm{ext}}}{\partial \mathbf{G}^b} - \frac{\partial \mathbf{F}^a_{\mathrm{int}}}{\partial \mathbf{G}^b} - \frac{\partial \mathbf{F}^a_{\mathrm{I}}}{\partial \mathbf{G}^b}$, the system (38) is rewritten

$$\begin{pmatrix} \mathbb{K}_{\mathbf{uu}} & \mathbb{K}_{\mathbf{uM}} \\ \mathbb{K}_{\mathbf{Mu}} & \mathbb{K}_{\mathbf{MM}} \end{pmatrix} \begin{pmatrix} \Delta\mathbf{u} \\ \Delta\mathbf{M} \end{pmatrix} = - \begin{pmatrix} \mathbf{R}_{\mathbf{u}}(\mathbf{u},\mathbf{M}) \\ \mathbf{R}_{\mathbf{M}}(\mathbf{u},\mathbf{M}) \end{pmatrix}. \tag{176}$$

The stiffness matrix has been decomposed into four sub-matrices as shown in Eq. (176) with respect to the discretization of the five independent field variables (d for displacement $\mathbf{u}$, and 2 for $\mathbf{M}$ (for $\mathrm{f_V}$, and $\mathrm{f_T}$)), and can be obtained in a straighforward way from the internal forces, see details in [26].

C Derivation of the numerical properties

C.1 Taylor's remainders

The remainder terms of Eqs. (60-61) are obtained by defining $\mathbf{V}^{\mathrm{t}} = \mathbf{G} + t(\mathbf{V} - \mathbf{G})$, $\nabla\mathbf{Q}^{\mathrm{t}} = \nabla\mathbf{G} + t(\nabla\mathbf{Q} - \nabla\mathbf{G})$. They can thus be evaluated by

$$\bar{\mathbf{w}}_{\mathbf{G}}(\mathbf{G}, \nabla\mathbf{G}) = \int_0^1 \mathbf{w}_{\mathbf{G}}(\mathbf{V}^{\mathrm{t}}, \nabla\mathbf{Q}^{\mathrm{t}}) \mathrm{d}t, \quad \bar{\mathbf{w}}_{\nabla\mathbf{G}}(\mathbf{G}) = \int_0^1 \mathbf{w}_{\nabla\mathbf{G}}(\mathbf{V}^{\mathrm{t}}) \mathrm{d}t \,, \tag{177}$$

and by

$$\bar{\mathbf{w}}_{\mathbf{GG}}(\mathbf{V}, \nabla\mathbf{Q}) = \int_0^1 (1-t) \mathbf{w}_{\mathbf{GG}}(\mathbf{V}^{\mathrm{t}}, \nabla\mathbf{Q}^{\mathrm{t}}) \mathrm{d}t \,, \; \bar{\mathbf{w}}_{\mathbf{G}\nabla\mathbf{G}}(\mathbf{V}) = \int_0^1 (1-t) \mathbf{w}_{\mathbf{G}\nabla\mathbf{G}}(\mathbf{V}^{\mathrm{t}}) \mathrm{d}t \,, \tag{178}$$

with the partial derivatives $\mathbf{w}_{\mathbf{GG}}(\mathbf{G}, \nabla\mathbf{G}) = \mathbf{v}_{\mathbf{GG}}(\mathbf{G}) \nabla\mathbf{G}$, and $\mathbf{w}_{\mathbf{G}\nabla\mathbf{G}}(\mathbf{G}) = \mathbf{v}_{\mathbf{G}}(\mathbf{G})$ of $\mathbf{w}(\mathbf{G}, \nabla\mathbf{G})$, since $\mathbf{w}_{\nabla\mathbf{G}\nabla\mathbf{G}}(\mathbf{G}) = 0$.

The remainder terms of Eqs. (62-63) read

$$\bar{\mathbf{d}}_{\mathbf{G}}(\mathbf{G}, \nabla\mathbf{G}) = \int_0^1 \mathbf{d}_{\mathbf{G}}(\mathbf{V}^{\mathrm{t}}, \nabla\mathbf{Q}^{\mathrm{t}}) \mathrm{d}t, \quad \bar{\mathbf{d}}_{\nabla\mathbf{G}}(\mathbf{G}) = \int_0^1 \mathbf{d}_{\nabla\mathbf{G}}(\mathbf{V}^{\mathrm{t}}) \mathrm{d}t \,, \tag{179}$$

and

$$\bar{\mathbf{d}}_{\mathbf{GG}}(\mathbf{V}, \nabla\mathbf{Q}) = \int_0^1 (1-t) \mathbf{d}_{\mathbf{GG}}(\mathbf{V}^{\mathrm{t}}, \nabla\mathbf{Q}^{\mathrm{t}}) \mathrm{d}t \,, \; \bar{\mathbf{d}}_{\mathbf{G}\nabla\mathbf{G}}(\mathbf{V}) = \int_0^1 (1-t) \mathbf{d}_{\mathbf{G}\nabla\mathbf{G}}(\mathbf{V}^{\mathrm{t}}) \mathrm{d}t \,. \tag{180}$$

Finally, the remainder terms of Eqs. (64-65) read

$$\bar{\mathbf{p}}_{\mathbf{G}}(\mathbf{G}) = \int_0^1 \mathbf{p}_{\mathbf{G}}(\mathbf{V}^{\mathrm{t}}) \mathrm{d}t, \quad \bar{\mathbf{p}}_{\mathbf{GG}}(\mathbf{V}) = \int_0^1 (1-\mathrm{t}) \mathbf{p}_{\mathbf{GG}}(\mathbf{V}^{\mathrm{t}}) \mathrm{d}t \,. \tag{181}$$

C.2 Application of the Taylor's expansion

The first term of Eq. (70) is rewritten, using the Taylor's expansion defined in Eq. (60), as

$$\int_{\Omega_\mathrm{h}} (\nabla\delta\mathbf{G}_\mathrm{h})^\mathrm{T}(\mathbf{w}(\mathbf{G}^\mathrm{e},\nabla\mathbf{G}^\mathrm{e}) - \mathbf{w}(\mathbf{G}_\mathrm{h},\nabla\mathbf{G}_\mathrm{h}))\mathrm{d}\Omega = \int_{\Omega_\mathrm{h}} (\nabla\delta\mathbf{G}_\mathrm{h})^\mathrm{T}(\mathbf{w}_\mathbf{G}(\mathbf{G}^\mathrm{e},\nabla\mathbf{G}^\mathrm{e})(\mathbf{G}^\mathrm{e}-\mathbf{G}_\mathrm{h}))\mathrm{d}\Omega$$
$$+\int_{\Omega_\mathrm{h}} (\nabla\delta\mathbf{G}_\mathrm{h})^\mathrm{T}(\mathbf{w}_{\nabla\mathbf{G}}(\mathbf{G}^\mathrm{e})(\nabla\mathbf{G}^\mathrm{e}-\nabla\mathbf{G}_\mathrm{h}))\mathrm{d}\Omega - \int_{\Omega_\mathrm{h}} (\nabla\delta\mathbf{G}_\mathrm{h})^\mathrm{T}(\bar{\mathbf{R}}_\mathbf{w}(\mathbf{G}^\mathrm{e}-\mathbf{G}_\mathrm{h},\nabla\mathbf{G}^\mathrm{e}-\nabla\mathbf{G}_\mathrm{h}))\mathrm{d}\Omega\,. \tag{182}$$

Similarly, the second term of Eq. (70) is rewritten, using the Taylor's expansion defined in Eq. (62), as

$$\begin{aligned}
&\int_{\Omega_\mathrm{h}} \delta\mathbf{G}_\mathrm{h}^\mathrm{T}\left(\tilde{\mathbf{o}}(\mathbf{G}^\mathrm{e})\nabla\mathbf{G}^\mathrm{e} - \tilde{\mathbf{o}}(\mathbf{G}_\mathrm{h})\nabla\mathbf{G}_\mathrm{h}\right)\mathrm{d}\Omega = \int_{\Omega_\mathrm{h}} \delta\mathbf{G}_\mathrm{h}^\mathrm{T}\left(\mathbf{d}(\mathbf{G}^\mathrm{e},\nabla\mathbf{G}^\mathrm{e}) - \mathbf{d}(\mathbf{G}_\mathrm{h},\nabla\mathbf{G}_\mathrm{h})\right)\mathrm{d}\Omega\\
&= \int_{\Omega_\mathrm{h}} \delta\mathbf{G}_\mathrm{h}^\mathrm{T}\mathbf{d}_\mathbf{G}(\mathbf{G}^\mathrm{e},\nabla\mathbf{G}^\mathrm{e})(\mathbf{G}^\mathrm{e}-\mathbf{G}_\mathrm{h}))\mathrm{d}\Omega + \int_{\Omega_\mathrm{h}} \delta\mathbf{G}_\mathrm{h}^\mathrm{T}\mathbf{d}_{\nabla\mathbf{G}}(\mathbf{G}^\mathrm{e})(\nabla\mathbf{G}^\mathrm{e}-\nabla\mathbf{G}_\mathrm{h}))\mathrm{d}\Omega\\
&- \int_{\Omega_\mathrm{h}} \delta\mathbf{G}_\mathrm{h}^\mathrm{T}\bar{\mathbf{R}}_\mathbf{d}(\mathbf{G}^\mathrm{e}-\mathbf{G}_\mathrm{h},\nabla\mathbf{G}^\mathrm{e}-\nabla\mathbf{G}_\mathrm{h})\mathrm{d}\Omega\,.
\end{aligned} \tag{183}$$

Likewise, the third term is rewritten, using the Taylor's expansion defined in Eq. (60), as

$$\begin{aligned}
&\int_{\partial_\mathrm{I}\Omega_\mathrm{h}\cup\partial_\mathrm{D}\Omega_\mathrm{h}} \left[\!\left[\delta\mathbf{G}_{\mathrm{h}_\mathbf{n}}^\mathrm{T}\right]\!\right] \langle\mathbf{w}(\mathbf{G}^\mathrm{e},\nabla\mathbf{G}^\mathrm{e}) - \mathbf{w}(\mathbf{G}_\mathrm{h},\nabla\mathbf{G}_\mathrm{h})\rangle\,\mathrm{dS} =\\
&\int_{\partial_\mathrm{I}\Omega_\mathrm{h}\cup\partial_\mathrm{D}\Omega_\mathrm{h}} \left[\!\left[\delta\mathbf{G}_{\mathrm{h}_\mathbf{n}}^\mathrm{T}\right]\!\right] \langle\mathbf{w}_\mathbf{G}(\mathbf{G}^\mathrm{e},\nabla\mathbf{G}^\mathrm{e})(\mathbf{G}^\mathrm{e}-\mathbf{G}_\mathrm{h})\rangle\,\mathrm{dS} +\\
&\int_{\partial_\mathrm{I}\Omega_\mathrm{h}\cup\partial_\mathrm{D}\Omega_\mathrm{h}} \left[\!\left[\delta\mathbf{G}_{\mathrm{h}_\mathbf{n}}^\mathrm{T}\right]\!\right] \langle\mathbf{w}_{\nabla\mathbf{G}}(\mathbf{G}^\mathrm{e})(\nabla\mathbf{G}^\mathrm{e}-\nabla\mathbf{G}_\mathrm{h})\rangle\,\mathrm{dS} -\\
&\int_{\partial_\mathrm{I}\Omega_\mathrm{h}\cup\partial_\mathrm{D}\Omega_\mathrm{h}} \left[\!\left[\delta\mathbf{G}_{\mathrm{h}_\mathbf{n}}^\mathrm{T}\right]\!\right] \langle\bar{\mathbf{R}}_\mathbf{w}(\mathbf{G}^\mathrm{e}-\mathbf{G}_\mathrm{h},\nabla\mathbf{G}^\mathrm{e}-\nabla\mathbf{G}_\mathrm{h})\rangle\,\mathrm{dS}.
\end{aligned} \tag{184}$$

The fifth term of Eq. (70) is developed by using the definition of $\mathbf{p}^\mathrm{T}(\mathbf{G}) = \mathbf{G}^\mathrm{T}\mathbf{o}^\mathrm{T}(\mathbf{G})$ and using the Taylor's expansion defined in Eq. (64), leading to

$$\begin{aligned}
&-\int_{\partial_\mathrm{I}\Omega_\mathrm{h}\cup\partial_\mathrm{D}\Omega_\mathrm{h}} \left[\!\left[\mathbf{G}^{\mathrm{e}^\mathrm{T}}\mathbf{o}^\mathrm{T}(\mathbf{G}^\mathrm{e}) - \mathbf{G}_\mathrm{h}^\mathrm{T}\mathbf{o}^\mathrm{T}(\mathbf{G}_\mathrm{h})\right]\!\right] \langle\delta\mathbf{G}_{\mathrm{h}_\mathbf{n}}\rangle\,\mathrm{dS} =\\
&-\int_{\partial_\mathrm{I}\Omega_\mathrm{h}\cup\partial_\mathrm{D}\Omega_\mathrm{h}} \left[\!\left[(\mathbf{G}^{\mathrm{e}^\mathrm{T}} - \mathbf{G}_\mathrm{h}^\mathrm{T})\mathbf{p}_\mathbf{G}^\mathrm{T}(\mathbf{G}^\mathrm{e})\right]\!\right] \langle\delta\mathbf{G}_{\mathrm{h}_\mathbf{n}}\rangle\,\mathrm{dS} + \int_{\partial_\mathrm{I}\Omega_\mathrm{h}\cup\partial_\mathrm{D}\Omega_\mathrm{h}} \left[\!\left[\bar{\mathbf{R}}_\mathbf{p}^\mathrm{T}(\mathbf{G}^\mathrm{e}-\mathbf{G}_\mathrm{h})\right]\!\right] \langle\delta\mathbf{G}_{\mathrm{h}_\mathbf{n}}\rangle\,\mathrm{dS}.
\end{aligned} \tag{185}$$

However, as $\mathbf{p}_\mathbf{G}^\mathrm{T} = -\mathbf{o}^\mathrm{T}(\mathbf{G})$, using Eq. (66), this last term is also rewritten as

$$\begin{aligned}
&-\int_{\partial_\mathrm{I}\Omega_\mathrm{h}\cup\partial_\mathrm{D}\Omega_\mathrm{h}} \left[\!\left[\mathbf{G}^{\mathrm{e}^\mathrm{T}}\mathbf{o}^\mathrm{T}(\mathbf{G}^\mathrm{e}) - \mathbf{G}_\mathrm{h}^\mathrm{T}\mathbf{o}^\mathrm{T}(\mathbf{G}_\mathrm{h})\right]\!\right] \langle\delta\mathbf{G}_{\mathrm{h}_\mathbf{n}}\rangle\,\mathrm{dS} =\\
&\int_{\partial_\mathrm{I}\Omega_\mathrm{h}\cup\partial_\mathrm{D}\Omega_\mathrm{h}} \left[\!\left[(\mathbf{G}^{\mathrm{e}^\mathrm{T}} - \mathbf{G}_\mathrm{h}^\mathrm{T})\mathbf{o}^\mathrm{T}(\mathbf{G}^\mathrm{e})\right]\!\right] \langle\delta\mathbf{G}_{\mathrm{h}_\mathbf{n}}\rangle\,\mathrm{dS}\\
&-\int_{\partial_\mathrm{I}\Omega_\mathrm{h}\cup\partial_\mathrm{D}\Omega_\mathrm{h}} \left[\!\left[(\mathbf{G}^\mathrm{e}-\mathbf{G}_\mathrm{h})^\mathrm{T}\bar{\mathbf{o}}_\mathbf{G}^\mathrm{T}(\mathbf{G}_\mathrm{h})(\mathbf{G}^\mathrm{e}-\mathbf{G}_\mathrm{h})\right]\!\right] \langle\delta\mathbf{G}_{\mathrm{h}_\mathbf{n}}\rangle\,\mathrm{dS}.
\end{aligned} \tag{186}$$

Finally, using the definition of the $\tilde{\cdot}$ operator $\mathbf{G}^{\mathrm{T}}\mathbf{o}^{\mathrm{T}}(\mathbf{G}')\delta\mathbf{G}_{\mathbf{n}} = \mathbf{G}_{\mathbf{n}}^{\mathrm{T}}\tilde{\mathbf{o}}^{\mathrm{T}}(\mathbf{G}')\delta\mathbf{G}^2$, and Eq. (186) is rewritten as

$$\begin{aligned}
&-\int_{\partial_{\mathrm{I}}\Omega_{\mathrm{h}}\cup\partial_{\mathrm{D}}\Omega_{\mathrm{h}}} \left[\!\!\left[\mathbf{G}^{\mathrm{e}^{\mathrm{T}}}\mathbf{o}^{\mathrm{T}}(\mathbf{G}^{\mathrm{e}}) - \mathbf{G}_{\mathrm{h}}^{\mathrm{T}}\mathbf{o}^{\mathrm{T}}(\mathbf{G}_{\mathrm{h}})\right]\!\!\right] \langle\delta\mathbf{G}_{\mathrm{h}_{\mathbf{n}}}\rangle \,\mathrm{dS} = \\
&\int_{\partial_{\mathrm{I}}\Omega_{\mathrm{h}}\cup\partial_{\mathrm{D}}\Omega_{\mathrm{h}}} \left[\!\!\left[(\mathbf{G}_{\mathbf{n}}^{\mathrm{e}^{\mathrm{T}}} - \mathbf{G}_{\mathrm{h}_{\mathbf{n}}}^{\mathrm{T}})\tilde{\mathbf{o}}^{\mathrm{T}}(\mathbf{G}^{\mathrm{e}})\right]\!\!\right] \langle\delta\mathbf{G}_{\mathrm{h}}\rangle \,\mathrm{dS} \\
&-\int_{\partial_{\mathrm{I}}\Omega_{\mathrm{h}}\cup\partial_{\mathrm{D}}\Omega_{\mathrm{h}}} \left[\!\!\left[(\mathbf{G}^{\mathrm{e}} - \mathbf{G}_{\mathrm{h}})^{\mathrm{T}}\bar{\mathbf{o}}_{\mathbf{G}}^{\mathrm{T}}(\mathbf{G}_{\mathrm{h}})(\mathbf{G}^{\mathrm{e}} - \mathbf{G}_{\mathrm{h}})\right]\!\!\right] \langle\delta\mathbf{G}_{\mathrm{h}_{\mathbf{n}}}\rangle \,\mathrm{dS}.
\end{aligned} \tag{187}$$

C.3 General properties of the finite element method and Hilbert spaces

The following properties will be used in the numerical properties derivation.

Lemma 5 (Interpolation inequality) *For all $\boldsymbol{G} \in (H^s(\Omega^e))^n$ there exists a sequence $\boldsymbol{G}^h \in \left(\mathbb{P}^k(\Omega^e)\right)^n$ and a positive constant $C_{\mathcal{D}}^k$ depending on s and k but independent of $\boldsymbol{G}$ and h_s, such that*

1. *for any $0 \leq n \leq s$*

$$\| \boldsymbol{G} - \boldsymbol{G}^h \|_{H^n(\Omega^e)} \leq C_{\mathcal{D}}^k h_s^{\mu-n} \| \boldsymbol{G} \|_{H^s(\Omega^e)}, \tag{188}$$

2. *for any $0 \leq n \leq s - 1 + \frac{2}{r}$*

$$\| \boldsymbol{G} - \boldsymbol{G}^h \|_{W_r^n(\Omega^e)} \leq C_{\mathcal{D}}^k h_s^{\mu-n-1+\frac{2}{r}} \| \boldsymbol{G} \|_{H^s(\Omega^e)}, \text{ if } d = 2, \tag{189}$$

3. *for any $s > n + \frac{1}{2}$*

$$\| \boldsymbol{G} - \boldsymbol{G}^h \|_{H^n(\partial\Omega^e)} \leq C_{\mathcal{D}}^k h_s^{\mu-n-\frac{1}{2}} \| \boldsymbol{G} \|_{H^s(\Omega^e)}, \tag{190}$$

where $\mu = min\{s, k+1\}$.
The proof of the first and third properties can be found in [7], and the proof of the second property in the particular case of $d = 2$ can be found in [1, 2], see also the discussion by [23].
Remarks
i) The approximation property in (2) is still valid for $r = \infty$, see [1].
ii) For $\boldsymbol{G} \in X_s$, let us define the interpolant $I_h\boldsymbol{G} \in X^k$ by $I_h\boldsymbol{G}|_{\Omega^e} = \boldsymbol{G}^h(\boldsymbol{G}|_{\Omega^e})$, which means $I_h\boldsymbol{G}$ satisfies the interpolant inequality property provided in Lemma 5 on Ω_h, see [28].

Lemma 6 (Trace inequality) *For all $\boldsymbol{G} \in \left(H^{s+1}(\Omega^e)\right)^n$, there exists a positive constant $C_{\mathcal{T}}$, such that*

$$\| \boldsymbol{G} \|_{W_r^s(\partial\Omega^e)}^r \leq C_{\mathcal{T}} \left(\frac{1}{h_s} \| \boldsymbol{G} \|_{W_r^s(\Omega^e)}^r + \| \boldsymbol{G} \|_{W_{2r-2}^s(\Omega^e)}^{r-1} \| \nabla^{s+1}\boldsymbol{G} \|_{L^2(\Omega^e)} \right), \tag{191}$$

where $s = 0, 1$ and $r = 2, 4$, or in other words

$$\begin{aligned}
\| \boldsymbol{G} \|_{L^2(\partial\Omega^e)}^2 &\leq C_{\mathcal{T}} \left(\frac{1}{h_s} \| \boldsymbol{G} \|_{L^2(\Omega^e)}^2 + \| \boldsymbol{G} \|_{L^2(\Omega^e)} \| \nabla\boldsymbol{G} \|_{L^2(\Omega^e)} \right), \\
\| \boldsymbol{G} \|_{L^4(\partial\Omega^e)}^4 &\leq C_{\mathcal{T}} \left(\frac{1}{h_s} \| \boldsymbol{G} \|_{L^4(\Omega^e)}^4 + \| \boldsymbol{G} \|_{L^6(\Omega^e)}^3 \| \nabla\boldsymbol{G} \|_{L^2(\Omega^e)} \right).
\end{aligned} \tag{192}$$

The first equation, $s = 0$ and $r = 2$, is proved in [52], and the second one, $r = 4$ and $s = 0$, is proved in [22].

[2] In this case $\mathbf{G}^{\mathrm{T}}\mathbf{o}^{\mathrm{T}}(\mathbf{G}')\delta\mathbf{G}_{\mathbf{n}} = \mathbf{G}_{\mathbf{n}}^{\mathrm{T}}\tilde{\mathbf{o}}^{\mathrm{T}}(\mathbf{G}')\delta\mathbf{G} = -\frac{3K}{f_{\mathrm{T}}^{2'}} f_{\mathrm{T}}\alpha_{\mathrm{th}} n_{\mathrm{x}}^{-}\delta u_{\mathrm{x}} - \frac{3K}{f_{\mathrm{T}}^{2'}} f_{\mathrm{T}}\alpha_{\mathrm{th}} n_{\mathrm{y}}^{-}\delta u_{\mathrm{y}} - \frac{3K}{f_{\mathrm{T}}^{2'}} f_{\mathrm{T}}\alpha_{\mathrm{th}} n_{\mathrm{z}}^{-}\delta u_{\mathrm{z}}$

Lemma 7 (Trace inequality on the finite element space) *For all* $\boldsymbol{G}_h \in \left(\mathbb{P}^k(\Omega^e)\right)^n$ *there exists a constant* $C^k_{\mathcal{K}} > 0$ *depending on* k*, such that*

$$\| \nabla^l \boldsymbol{G}_h \|_{L^2(\partial\Omega^e)} \leq C^k_{\mathcal{K}} h_s^{-\frac{1}{2}} \| \nabla^l \boldsymbol{G}_h \|_{L^2(\Omega^e)} \qquad l = 0,\, 1, \tag{193}$$

where $C^k_{\mathcal{K}} = sup_{\boldsymbol{G}_h \in (P_k(\Omega^e))^n} \frac{h_s \|\nabla \boldsymbol{G}_h\|^2_{L^2(\partial\Omega^e)}}{\|\nabla \boldsymbol{G}_h\|^2_{L^2(\Omega^e)}}$ *is a constant which depends on the degree of the polynomial approximation only with* $h_s = \frac{|\Omega^e|}{|\partial\Omega^e|}$*, see [25] for more details.*

Lemma 8 (Inverse inequality) *For* $\boldsymbol{G}_h \in \left(\mathbb{P}^k(\Omega^e)\right)^n$ *and* $r \geq 2$*, there exists* $C^k_{\mathcal{I}} > 0$*, such that*

$$\| \boldsymbol{G}_h \|_{L^r(\Omega^e)} \leq C^k_{\mathcal{I}} h_s^{\frac{d}{r} - \frac{d}{2}} \| \boldsymbol{G}_h \|_{L^2(\Omega^e)}, \tag{194}$$

$$\| \boldsymbol{G}_h \|_{L^r(\partial\Omega^e)} \leq C^k_{\mathcal{I}} h_s^{\frac{d-1}{r} - \frac{d-1}{2}} \| \boldsymbol{G}_h \|_{L^2(\partial\Omega^e)}, \tag{195}$$

$$\| \nabla \boldsymbol{G}_h \|_{L^2(\Omega^e)} \leq C^k_{\mathcal{I}} h_s^{-1} \| \boldsymbol{G}_h \|_{L^2(\Omega^e)} . \tag{196}$$

The proof of these properties can be found in [12, Theorem 3.2.6]. Note that Eqs. (194-195) involve the space dimension d*.*

Lemma 9 (Relation between energy norms on the finite element space) *From [69], for* $\boldsymbol{G}_h \in X^k$*, there exists a positive constant* C^k*, depending on* k*, such that*

$$|\!|\!| \boldsymbol{G}_h |\!|\!|_1 \leq C^k \, |\!|\!| \boldsymbol{G}_h |\!|\!| . \tag{197}$$

The demonstration directly follows by bounding the extra terms $\sum_e h_s \| \boldsymbol{G} \|^2_{H^1(\partial\Omega^e)}$ *of the norm defined by Eq. (77), in comparison to the norm defined by Eq. (76), using successively the trace inequality, Eq. (192), and the inverse inequality, Eq. (196), for the first term, and the trace inequality on the finite element space, Eq. (193), for the second term.*

Lemma 10 (Energy bound of interpolant error) *Let* $\boldsymbol{G}^e \in X_s, s \geq 2$*, and let* $I_h \boldsymbol{G} \in X^k$*, be its interpolant. Therefore, there is a constant* $C^k > 0$ *independent of* h_s*, such that*

$$|\!|\!| \boldsymbol{G}^e - I_h \boldsymbol{G} |\!|\!|_1 \leq C^k h_s^{\mu - 1} \| \boldsymbol{G}^e \|_{H^s(\Omega_h)}, \tag{198}$$

with $\mu = min\{s,\, k+1\}$*. The proof follows from Lemma 5, Eq. (188), and Eq. (190), applied on the mesh dependent norm (77).*

C.4 The bound of the non-linear term $\mathcal{N}(\mathbf{G}^{\mathrm{e}}, \mathbf{y}; \delta\mathbf{G}_{\mathrm{h}})$

C.4.1 Intermediate bounds

To bound the terms of $\mathcal{N}(\mathbf{G}^{\mathrm{e}}, \mathbf{y}; \delta\mathbf{G}_{\mathrm{h}})$, we have recourse to the following intermediate bounds, which are derived for the particular case of $d = 2$.

Lemma 11 (Intermediate bounds) *Let* $\boldsymbol{\xi} = I_h \boldsymbol{G} - \boldsymbol{y}$*,* $\delta \boldsymbol{G}_h \in X^k$*,* $\boldsymbol{\eta} = \boldsymbol{G}^e - I_h \boldsymbol{G} \in X$ *and* $\boldsymbol{\zeta} = \boldsymbol{\xi} + \boldsymbol{\eta}$*. The terms in* $\boldsymbol{\xi}$ *can be bounded by recourse to the trace inequality, see Lemma 6, and to the inverse inequality, see Lemma 8, while bounding the terms in* $\boldsymbol{\eta}$ *makes use of the trace inequality, see Lemma 6 and of the interpolation inequality, see Lemma 5 for* $d = 2$*. Using the definition of the ball (92-93) thus leads to the different contributions, see [23, 26] for details,*

$$\left(\sum_e \| \boldsymbol{\zeta} \|^2_{L^2(\Omega^e)} \right)^{\frac{1}{2}} \leq C^k \sigma \leq C^k h_s^{\mu - 1 - \varepsilon} \| \boldsymbol{G}^e \|_{H^s(\Omega_h)} , \tag{199}$$

$$\left(\sum_e \| \boldsymbol{\zeta} \|^4_{L^4(\Omega^e)} \right)^{\frac{1}{4}} \leq C^k h_s^{-\frac{1}{2}} \sigma \leq C^k h_s^{\mu - \frac{3}{2} - \varepsilon} \| \boldsymbol{G}^e \|_{H^s(\Omega_h)} , \tag{200}$$

$$\left(\sum_e \| \nabla\boldsymbol{\zeta} \|^2_{L^2(\Omega^e)}\right)^{\frac{1}{2}} \leq C^k\sigma \leq C^k h_s^{\mu-1-\varepsilon} \| \boldsymbol{G}^e \|_{H^s(\Omega_h)}\,, \tag{201}$$

$$\left(\sum_e \| \boldsymbol{\zeta} \|^4_{L^4(\partial\Omega^e)}\right)^{\frac{1}{4}} \leq C^k h_s^{-\frac{3}{4}}\sigma \leq C^k h_s^{\mu-\frac{7}{4}-\varepsilon} \| \boldsymbol{G}^e \|_{H^s(\Omega_h)}\,, \tag{202}$$

$$\left(\sum_e \| [\![\boldsymbol{\zeta}]\!] \|^4_{L^4(\partial\Omega^e)}\right)^{\frac{1}{4}} \leq C^k h_s^{\frac{1}{4}}\sigma \leq C^k h_s^{\mu-\frac{3}{4}-\varepsilon} \| \boldsymbol{G}^e \|_{H^s(\Omega_h)}\,, \tag{203}$$

$$\left(\sum_e \| \nabla\boldsymbol{\zeta} \|^4_{L^4(\partial\Omega^e)}\right)^{\frac{1}{4}} \leq C^k h_s^{-\frac{3}{4}}\sigma \leq C^k h_s^{\mu-\frac{7}{4}-\varepsilon} \| \boldsymbol{G}^e \|_{H^s(\Omega_h)} \tag{204}$$

with $\mu = min\{s,\, k+1\}$. *Moreover, using the inverse inequality, see Lemma 8, one has*

$$\begin{cases} \| \delta\boldsymbol{G}_h \|_{W^1_4(\Omega^e)} & \leq C^k_{\mathcal{I}} h_s^{-\frac{1}{2}} \| \delta\boldsymbol{G}_h \|_{H^1(\Omega^e)}\,, \\ | \delta\boldsymbol{G}_h |_{W^1_4(\Omega^e)} & \leq C^k_{\mathcal{I}} h_s^{-\frac{1}{2}} | \delta\boldsymbol{G}_h |_{H^1(\Omega^e)}\ . \end{cases} \tag{205}$$

C.4.2 Bounds of the different contributions

The bound of $\mathcal{N}(\mathbf{G}^{\mathrm{e}}, \mathbf{y}; \delta\mathbf{G}_{\mathrm{h}})$ follows from the argumentation reported in [23] and is nominated by the term with the largest bound.

The first term of $\mathcal{N}(\mathbf{G}^{\mathrm{e}}, \mathbf{y}; \delta\mathbf{G}_{\mathrm{h}})$, defined in Eq. (74), can be expanded using Eq. (61) as

$$\begin{aligned} \mathcal{I}_1 &= \int_{\Omega_{\mathrm{h}}} (\nabla\delta\mathbf{G})^{\mathrm{T}}_{\mathrm{h}} \bar{\mathbf{R}}_{\mathbf{w}}(\boldsymbol{\zeta}, \nabla\boldsymbol{\zeta}) \mathrm{d}\Omega = \sum_{\mathrm{e}} \int_{\Omega^{\mathrm{e}}} (\nabla\delta\mathbf{G}_{\mathrm{h}})^{\mathrm{T}} (\boldsymbol{\zeta}^{\mathrm{T}} \bar{\mathbf{w}}_{\mathbf{GG}}(\mathbf{y}, \nabla\mathbf{y})\boldsymbol{\zeta}) \mathrm{d}\Omega \\ &+ 2\sum_{\mathrm{e}} \int_{\Omega^{\mathrm{e}}} (\nabla\delta\mathbf{G})^{\mathrm{T}}_{\mathrm{h}} \left(\boldsymbol{\zeta}^{\mathrm{T}} \bar{\mathbf{w}}_{\mathbf{G}\nabla\mathbf{G}}(\mathbf{y}) \nabla\boldsymbol{\zeta}\right) \mathrm{d}\Omega = \mathcal{I}_{11} + 2\mathcal{I}_{12}. \end{aligned} \tag{206}$$

The two term of the right hand side of Eq. (206) are bounded by using the generalized Hölder's inequality, the generalized Cauchy-Schwartz' inequality, the definition of C_{y} in Eq. (67), and the bounds (199, 200, 201, and 205) as

$$\begin{aligned} | \mathcal{I}_{11} | &\leq C_{\mathrm{y}} \sum_{\mathrm{e}} \| \boldsymbol{\zeta} \|_{\mathrm{L}^4(\Omega^{\mathrm{e}})} \| \boldsymbol{\zeta} \|_{\mathrm{L}^2(\Omega^{\mathrm{e}})} \| \nabla\delta\mathbf{G}_{\mathrm{h}} \|_{\mathrm{L}^4(\Omega^{\mathrm{e}})} \\ &\leq C_{\mathrm{y}} \left(\sum_{\mathrm{e}} \| \boldsymbol{\zeta} \|^4_{\mathrm{L}^4(\Omega^{\mathrm{e}})}\right)^{\frac{1}{4}} \left(\sum_{\mathrm{e}} \| \boldsymbol{\zeta} \|^2_{\mathrm{L}^2(\Omega^{\mathrm{e}})}\right)^{\frac{1}{2}} \left(\sum_{\mathrm{e}} \| \nabla\delta\mathbf{G}_{\mathrm{h}} \|^4_{\mathrm{L}^4(\Omega^{\mathrm{e}})}\right)^{\frac{1}{4}} \\ &\leq C^k C_{\mathrm{y}} h_{\mathrm{s}}^{\mu-2-\varepsilon}\sigma \, | \delta\mathbf{G}_{\mathrm{h}} |_{\mathrm{H}^1(\Omega_{\mathrm{h}})} \| \mathbf{G}^{\mathrm{e}} \|_{\mathrm{H}^s(\Omega_{\mathrm{h}})}\,, \end{aligned} \tag{207}$$

$$\begin{aligned} | \mathcal{I}_{12} | &\leq C_{\mathrm{y}} \sum_{\mathrm{e}} \| \boldsymbol{\zeta} \|_{\mathrm{L}^4(\Omega^{\mathrm{e}})} \| \nabla\boldsymbol{\zeta} \|_{\mathrm{L}^2(\Omega^{\mathrm{e}})} \| \nabla\delta\mathbf{G}_{\mathrm{h}} \|_{\mathrm{L}^4(\Omega^{\mathrm{e}})} \\ &\leq C_{\mathrm{y}} \left(\sum_{\mathrm{e}} \| \boldsymbol{\zeta} \|^4_{\mathrm{L}^4(\Omega^{\mathrm{e}})}\right)^{\frac{1}{4}} \left(\sum_{\mathrm{e}} \| \nabla\boldsymbol{\zeta} \|^2_{\mathrm{L}^2(\Omega^{\mathrm{e}})}\right)^{\frac{1}{2}} \left(\sum_{\mathrm{e}} \| \nabla\delta\mathbf{G}_{\mathrm{h}} \|^4_{\mathrm{L}^4(\Omega^{\mathrm{e}})}\right)^{\frac{1}{4}} \\ &\leq C^k C_{\mathrm{y}} h_{\mathrm{s}}^{\mu-2-\varepsilon}\sigma \, | \delta\mathbf{G}_{\mathrm{h}} |_{\mathrm{H}^1(\Omega_{\mathrm{h}})} \| \mathbf{G}^{\mathrm{e}} \|_{\mathrm{H}^s(\Omega_{\mathrm{h}})}\ . \end{aligned} \tag{208}$$

Combining the above results leads to

$$| \mathcal{I}_1 | \leq C^k C_{\mathrm{y}} h_{\mathrm{s}}^{\mu-2-\varepsilon}\sigma \, | \delta\mathbf{G}_{\mathrm{h}} |_{\mathrm{H}^1(\Omega_{\mathrm{h}})} \| \mathbf{G}^{\mathrm{e}} \|_{\mathrm{H}^s(\Omega_{\mathrm{h}})}\ . \tag{209}$$

The second term of $\mathcal{N}(\mathbf{G}^{\mathrm{e}}, \mathbf{y}; \delta\mathbf{G}_{\mathrm{h}})$, defined in Eq. (74), becomes by using Eq. (61),

$$\begin{aligned} \mathcal{I}_2 &= \int_{\partial_{\mathrm{I}}\Omega_{\mathrm{h}} \cup \partial_{\mathrm{D}}\Omega_{\mathrm{h}}} \left[\!\!\left[\delta\mathbf{G}^{\mathrm{T}}_{\mathrm{h}_{\mathbf{n}}}\right]\!\!\right] \left\langle \boldsymbol{\zeta}^{\mathrm{T}} \bar{\mathbf{w}}_{\mathbf{GG}}(\mathbf{y}, \nabla\mathbf{y})\boldsymbol{\zeta} \right\rangle \mathrm{dS} \\ &+ 2\int_{\partial_{\mathrm{I}}\Omega_{\mathrm{h}} \cup \partial_{\mathrm{D}}\Omega_{\mathrm{h}}} \left[\!\!\left[\delta\mathbf{G}^{\mathrm{T}}_{\mathrm{h}_{\mathbf{n}}}\right]\!\!\right] \left\langle \boldsymbol{\zeta}^{\mathrm{T}} \bar{\mathbf{w}}_{\mathbf{G}\nabla\mathbf{G}}(\mathbf{y}) \nabla\boldsymbol{\zeta} \right\rangle \mathrm{dS} = \mathcal{I}_{21} + 2\mathcal{I}_{22}\,. \end{aligned} \tag{210}$$

The two terms of the right hand side of Eq. (210) are bounded by using the generalized Hölder's inequality, the generalized Cauchy-Schwartz' inequality, the definition of C_y in Eq. (67), and the bounds (202, 204), yielding

$$\begin{aligned} |\,\mathcal{I}_{21}\,| &\leq C_\mathrm{y} h_\mathrm{s}^{\frac{1}{2}} \left(\sum_\mathrm{e} \| \boldsymbol{\zeta} \|^4_{\mathrm{L}^4(\partial\Omega^\mathrm{e})} \right)^{\frac{1}{2}} \left(\sum_\mathrm{e} h_\mathrm{s}^{-1} \| \left[\!\left[\delta\mathbf{G}^\mathrm{T}_{\mathrm{h}_\mathbf{n}} \right]\!\right] \|^2_{\mathrm{L}^2(\partial\Omega^\mathrm{e})} \right)^{\frac{1}{2}} \\ &\leq C^k C_\mathrm{y} \| \mathbf{G}^\mathrm{e} \|_{\mathrm{H}^s(\Omega_\mathrm{h})} h_\mathrm{s}^{\mu-2-\varepsilon\sigma} \left(\sum_\mathrm{e} h_\mathrm{s}^{-1} \| [\![\delta\mathbf{G}_{\mathrm{h}_\mathbf{n}}]\!] \|^2_{\mathrm{L}^2(\partial\Omega^\mathrm{e})} \right)^{\frac{1}{2}}, \end{aligned} \tag{211}$$

$$\begin{aligned} |\,\mathcal{I}_{22}\,| &\leq C_\mathrm{y} h_\mathrm{s}^{\frac{1}{2}} \left(\sum_\mathrm{e} \| \boldsymbol{\zeta} \|^4_{\mathrm{L}^4(\partial\Omega^\mathrm{e})} \right)^{\frac{1}{4}} \left(\sum_\mathrm{e} \| \nabla\boldsymbol{\zeta} \|^4_{\mathrm{L}^4(\partial\Omega^\mathrm{e})} \right)^{\frac{1}{4}} \left(\sum_\mathrm{e} h_\mathrm{s}^{-1} \| \left[\!\left[\delta\mathbf{G}^\mathrm{T}_{\mathrm{h}_\mathbf{n}} \right]\!\right] \|^2_{\mathrm{L}^2(\partial\Omega^\mathrm{e})} \right)^{\frac{1}{2}} \\ &\leq C^k C_\mathrm{y} \| \mathbf{G}^\mathrm{e} \|_{\mathrm{H}^s(\Omega_\mathrm{h})} h_\mathrm{s}^{\mu-2-\varepsilon\sigma} \left(\sum_\mathrm{e} h_\mathrm{s}^{-1} \| [\![\delta\mathbf{G}_{\mathrm{h}_\mathbf{n}}]\!] \|^2_{\mathrm{L}^2(\partial\Omega^\mathrm{e})} \right)^{\frac{1}{2}}. \end{aligned} \tag{212}$$

We now substitute Eqs. (211, 212) in Eq. (210) to obtain the final bound of the second term of $\mathcal{N}(\mathbf{G}^\mathrm{e}, \mathbf{y}; \delta\mathbf{G}_\mathrm{h})$ as

$$|\,\mathcal{I}_2\,| \leq C^k C_\mathrm{y} \| \mathbf{G}^\mathrm{e} \|_{\mathrm{H}^s(\Omega_\mathrm{h})} h_\mathrm{s}^{\mu-2-\varepsilon\sigma} \left(\sum_\mathrm{e} h_\mathrm{s}^{-1} \| [\![\delta\mathbf{G}_{\mathrm{h}_\mathbf{n}}]\!] \|^2_{\mathrm{L}^2(\partial\Omega^\mathrm{e})} \right)^{\frac{1}{2}}. \tag{213}$$

Furthermore, for the third term of $\mathcal{N}(\mathbf{G}^\mathrm{e}, \mathbf{y}; \delta\mathbf{G}_\mathrm{h})$ as decomposed in Eq. (74), using Taylor's expansion as in Eqs. (60-61), the generalized Hölder's inequality, the generalized Cauchy-Schwartz' inequality, the definition of C_y in Eq. (67), and the bounds (202, 203), leads to

$$\begin{aligned} |\,\mathcal{I}_3\,| &\leq \sum_\mathrm{e} \left| \int_{\partial_\mathrm{I}\Omega^\mathrm{e}} \left[\!\left[\boldsymbol{\zeta}^\mathrm{T}_\mathbf{n} \right]\!\right] \left(\boldsymbol{\zeta}^\mathrm{T} \bar{\mathbf{w}}_{\nabla\mathbf{G}\mathbf{G}}(\mathbf{y}) \nabla\delta\mathbf{G}_\mathrm{h} \right) \mathrm{dS} \right| \\ &\leq C_\mathrm{y} h_\mathrm{s}^{-\frac{1}{2}} \left(\sum_\mathrm{e} \| [\![\boldsymbol{\zeta}]\!] \|^4_{\mathrm{L}^4(\partial\Omega^\mathrm{e})} \right)^{\frac{1}{4}} \left(\sum_\mathrm{e} \| \boldsymbol{\zeta} \|^4_{\mathrm{L}^4(\partial\Omega^\mathrm{e})} \right)^{\frac{1}{4}} \left(\sum_\mathrm{e} h_\mathrm{s} \| \nabla\delta\mathbf{G}_\mathrm{h} \|^2_{\mathrm{L}^2(\partial\Omega^\mathrm{e})} \right)^{\frac{1}{2}} \\ &\leq C_\mathrm{y} C^k \| \mathbf{G}^\mathrm{e} \|_{\mathrm{H}^s(\Omega_\mathrm{h})} h_\mathrm{s}^{\mu-2-\varepsilon\sigma} \left(\sum_\mathrm{e} h_\mathrm{s} \,|\, \delta\mathbf{G}_\mathrm{h} \,|^2_{\mathrm{H}^1(\partial\Omega^\mathrm{e})} \right)^{\frac{1}{2}}. \end{aligned} \tag{214}$$

Likewise, the fourth term of $\mathcal{N}(\mathbf{G}^\mathrm{e}, \mathbf{y}; \delta\mathbf{G}_\mathrm{h})$ defined in Eq. (74) is bounded using a Taylor's expansion as in Eqs. (60-61), the generalized Hölder's inequality, the generalized Cauchy-Schwartz' inequality, the definition of C_y in Eq. (67), and the bounds (202, 203) leading to

$$\begin{aligned} |\,\mathcal{I}_4\,| &\leq \sum_\mathrm{e} \left| \int_{\partial_\mathrm{I}\Omega^\mathrm{e}} \left[\!\left[\boldsymbol{\zeta}^\mathrm{T}_\mathbf{n} \right]\!\right] \left(\frac{\mathcal{B}}{h_\mathrm{s}} \boldsymbol{\zeta}^\mathrm{T} \bar{\mathbf{w}}_{\nabla\mathbf{G}\mathbf{G}}(\mathbf{y}) \right) [\![\delta\mathbf{G}_{\mathrm{h}_\mathbf{n}}]\!] \,\mathrm{dS} \right| \\ &\leq C_\mathrm{y} h_\mathrm{s}^{-\frac{1}{2}} \left(\sum_\mathrm{e} \| [\![\boldsymbol{\zeta}]\!] \|^4_{\mathrm{L}^4(\partial\Omega^\mathrm{e})} \right)^{\frac{1}{4}} \left(\sum_\mathrm{e} \| \boldsymbol{\zeta} \|^4_{\mathrm{L}^4(\partial\Omega^\mathrm{e})} \right)^{\frac{1}{4}} \left(\sum_\mathrm{e} h_\mathrm{s}^{-1} \| [\![\delta\mathbf{G}_{\mathrm{h}_\mathbf{n}}]\!] \|^2_{\mathrm{L}^2(\partial\Omega^\mathrm{e})} \right)^{\frac{1}{2}} \\ &\leq C^k C_\mathrm{y} \| \mathbf{G}^\mathrm{e} \|_{\mathrm{H}^s(\Omega_\mathrm{h})} h_\mathrm{s}^{\mu-2-\varepsilon\sigma} \left(\sum_\mathrm{e} h_\mathrm{s}^{-1} \| [\![\delta\mathbf{G}_{\mathrm{h}_\mathbf{n}}]\!] \|^2_{\mathrm{L}^2(\partial\Omega^\mathrm{e})} \right)^{\frac{1}{2}}. \end{aligned} \tag{215}$$

Then the bound of the fifth term of $\mathcal{N}(\mathbf{G}^\mathrm{e}, \mathbf{y}; \delta\mathbf{G}_\mathrm{h})$ defined in Eq. (74) is derived using Eq. (231) developed in C.4.3, following

$$\begin{aligned} |\,\mathcal{I}_5\,| &\leq 2C_\mathrm{y} \sum_\mathrm{e} \left| \int_{\partial_\mathrm{I}\Omega^\mathrm{e} \cup \partial_\mathrm{D}\Omega^\mathrm{e}} \left[\!\left[(\mathbf{G}^\mathrm{e} - \mathbf{G}_\mathrm{h})^\mathrm{T} \right]\!\right] \mathbf{I} (\mathbf{G}^\mathrm{e} - \mathbf{G}_\mathrm{h}) \delta\mathbf{G}_{\mathrm{h}_\mathbf{n}} \,\mathrm{dS} \right| \\ &\quad + \frac{1}{8} C_\mathrm{y} \sum_\mathrm{e} \left| \int_{\partial_\mathrm{I}\Omega^\mathrm{e}} \left[\!\left[(\mathbf{G}^\mathrm{e} - \mathbf{G}_\mathrm{h})^\mathrm{T} \right]\!\right] \mathbf{I} [\![\mathbf{G}^\mathrm{e} - \mathbf{G}_\mathrm{h}]\!] [\![\delta\mathbf{G}_{\mathrm{h}_\mathbf{n}}]\!] \,\mathrm{dS} \right| = |\,\mathcal{I}_{51}\,| + |\,\mathcal{I}_{52}\,|, \end{aligned} \tag{216}$$

where $\mathbf{I}$ is a matrix of unit norm and has the same size of $\bar{\mathbf{o}}_{\mathbf{G}}^{\mathrm{T}}$. Using the generalized Hölder's inequality, the generalized Cauchy-Schwartz' inequality, and the bounds (202, 203) one has

$$\begin{aligned}
\mid \mathcal{I}_{51} \mid &\leq 2C_{\mathrm{y}} \sum_{\mathrm{e}} \mid \int_{\partial\Omega^{\mathrm{e}}} \left[\!\left[\boldsymbol{\zeta}^{\mathrm{T}}\right]\!\right] \mathbf{I} \left(\boldsymbol{\zeta} \delta \mathbf{G}_{\mathrm{h}_{\mathbf{n}}}\right) \mathrm{dS} \mid \\
&\leq 2C_{\mathrm{y}} h_{\mathrm{s}}^{-\frac{1}{2}} \left(\sum_{\mathrm{e}} \parallel [\![\boldsymbol{\zeta}]\!] \parallel^4_{\mathrm{L}^4(\partial\Omega^{\mathrm{e}})} \right)^{\frac{1}{4}} \left(\sum_{\mathrm{e}} \parallel \boldsymbol{\zeta} \parallel^4_{\mathrm{L}^4(\partial\Omega^{\mathrm{e}})} \right)^{\frac{1}{4}} \left(\sum_{\mathrm{e}} \mathrm{h_s} \parallel \delta \mathbf{G}_{\mathrm{h}} \parallel^2_{\mathrm{L}^2(\partial\Omega^{\mathrm{e}})} \right)^{\frac{1}{2}} \\
&\leq 2C_{\mathrm{y}} C^k \parallel \mathbf{G}^{\mathrm{e}} \parallel_{\mathrm{H}^s(\Omega_{\mathrm{h}})} h_{\mathrm{s}}^{\mu-2-\varepsilon} \sigma \left(\sum_{\mathrm{e}} \mathrm{h_s} \parallel \delta \mathbf{G}_{\mathrm{h}} \parallel^2_{\mathrm{L}^2(\partial\Omega^{\mathrm{e}})} \right)^{\frac{1}{2}},
\end{aligned} \tag{217}$$

$$\begin{aligned}
\mid \mathcal{I}_{52} \mid &\leq \frac{1}{8} C_{\mathrm{y}} \sum_{\mathrm{e}} \mid \int_{\partial\Omega^{\mathrm{e}}} \left[\!\left[\boldsymbol{\zeta}^{\mathrm{T}}\right]\!\right] \mathbf{I} [\![\boldsymbol{\zeta}]\!] [\![\delta \mathbf{G}_{\mathrm{h}_{\mathbf{n}}}]\!] \mathrm{dS} \mid \\
&\leq \frac{1}{8} C_{\mathrm{y}} h_{\mathrm{s}}^{\frac{1}{2}} \left(\sum_{\mathrm{e}} \parallel [\![\boldsymbol{\zeta}]\!] \parallel^4_{\mathrm{L}^4(\partial\Omega^{\mathrm{e}})} \right)^{\frac{1}{4}} \left(\sum_{\mathrm{e}} \parallel [\![\boldsymbol{\zeta}]\!] \parallel^4_{\mathrm{L}^4(\partial\Omega^{\mathrm{e}})} \right)^{\frac{1}{4}} \left(\sum_{\mathrm{e}} h_{\mathrm{s}}^{-1} \parallel [\![\delta \mathbf{G}_{\mathrm{h}}]\!] \parallel^2_{\mathrm{L}^2(\partial\Omega^{\mathrm{e}})} \right)^{\frac{1}{2}} \\
&\leq \frac{1}{8} C_{\mathrm{y}} C^k \parallel \mathbf{G}^{\mathrm{e}} \parallel_{\mathrm{H}^s(\Omega_{\mathrm{h}})} h_{\mathrm{s}}^{\mu-\varepsilon} \sigma \left(\sum_{\mathrm{e}} h_{\mathrm{s}}^{-1} \parallel [\![\delta \mathbf{G}_{\mathrm{h}}]\!] \parallel^2_{\mathrm{L}^2(\partial\Omega^{\mathrm{e}})} \right)^{\frac{1}{2}}.
\end{aligned} \tag{218}$$

Combining Eqs. (217 and 218) leads to the final bound

$$\begin{aligned}
\mid \mathcal{I}_{5} \mid &\leq 2C_{\mathrm{y}} C^k \parallel \mathbf{G}^{\mathrm{e}} \parallel_{\mathrm{H}^s(\Omega_{\mathrm{h}})} h_{\mathrm{s}}^{\mu-2-\varepsilon} \sigma \left(\sum_{\mathrm{e}} \mathrm{h_s} \parallel \delta \mathbf{G}_{\mathrm{h}} \parallel^2_{\mathrm{L}^2(\partial\Omega^{\mathrm{e}})} \right)^{\frac{1}{2}} \\
&\quad + \frac{1}{8} C_{\mathrm{y}} C^k \parallel \mathbf{G}^{\mathrm{e}} \parallel_{\mathrm{H}^s(\Omega_{\mathrm{h}})} h_{\mathrm{s}}^{\mu-\varepsilon} \sigma \left(\sum_{\mathrm{e}} h_{\mathrm{s}}^{-1} \parallel [\![\delta \mathbf{G}_{\mathrm{h}}]\!] \parallel^2_{\mathrm{L}^2(\partial\Omega^{\mathrm{e}})} \right)^{\frac{1}{2}}.
\end{aligned} \tag{219}$$

Finally to bound the last term of $\mathcal{N}(\mathbf{G}^{\mathrm{e}}, \mathbf{y}; \delta \mathbf{G}_{\mathrm{h}})$ defined in Eq. (74), we rewrite it using Eq. (63) as

$$\begin{aligned}
\mathcal{I}_6 &= \int_{\Omega_{\mathrm{h}}} \delta \mathbf{G}_{\mathrm{h}}^{\mathrm{T}} \bar{\mathbf{R}}_{\mathbf{d}}(\boldsymbol{\zeta}, \nabla\boldsymbol{\zeta}) \mathrm{d}\Omega = \sum_{\mathrm{e}} \int_{\Omega^{\mathrm{e}}} \delta \mathbf{G}_{\mathrm{h}}^{\mathrm{T}} (\boldsymbol{\zeta}^{\mathrm{T}} \bar{\mathbf{d}}_{\mathbf{GG}}(\mathbf{y}, \nabla\mathbf{y}) \boldsymbol{\zeta}) \mathrm{d}\Omega \\
&\quad + 2 \sum_{\mathrm{e}} \int_{\Omega^{\mathrm{e}}} \delta \mathbf{G}_{\mathrm{h}}^{\mathrm{T}} (\boldsymbol{\zeta}^{\mathrm{T}} \bar{\mathbf{d}}_{\mathbf{G}\nabla\mathbf{G}}(\mathbf{y}) \nabla\boldsymbol{\zeta}) \mathrm{d}\Omega = \mathcal{I}_{61} + 2\mathcal{I}_{62}.
\end{aligned} \tag{220}$$

The two contributions are bounded using the generalized Hölder's inequality, the generalized Cauchy-Schwartz' inequality, the definition of C_{y} in Eq. (67), the bounds (200, 201), and the inverse inequality of Lemma 8, following

$$\begin{aligned}
\mid \mathcal{I}_{61} \mid &\leq C_{\mathrm{y}} \left(\sum_{\mathrm{e}} \parallel \boldsymbol{\zeta} \parallel^4_{\mathrm{L}^4(\Omega^{\mathrm{e}})} \right)^{\frac{1}{4}} \left(\sum_{\mathrm{e}} \parallel \boldsymbol{\zeta} \parallel^4_{\mathrm{L}^4(\Omega^{\mathrm{e}})} \right)^{\frac{1}{4}} \left(\sum_{\mathrm{e}} \parallel \delta \mathbf{G}_{\mathrm{h}} \parallel^2_{\mathrm{L}^2(\Omega^{\mathrm{e}})} \right)^{\frac{1}{2}} \\
&\leq C^k C_{\mathrm{y}} h_{\mathrm{s}}^{\mu-2-\varepsilon} \sigma \parallel \delta \mathbf{G}_{\mathrm{h}} \parallel_{\mathrm{L}^2(\Omega_{\mathrm{h}})} \parallel \mathbf{G}^{\mathrm{e}} \parallel_{\mathrm{H}^s(\Omega_{\mathrm{h}})}.
\end{aligned} \tag{221}$$

$$\begin{aligned}
\mid \mathcal{I}_{62} \mid &\leq C_{\mathrm{y}} \left(\sum_{\mathrm{e}} \parallel \boldsymbol{\zeta} \parallel^4_{\mathrm{L}^4(\Omega^{\mathrm{e}})} \right)^{\frac{1}{4}} \left(\sum_{\mathrm{e}} \parallel \nabla\boldsymbol{\zeta} \parallel^2_{\mathrm{L}^2(\Omega^{\mathrm{e}})} \right)^{\frac{1}{2}} \left(\sum_{\mathrm{e}} \parallel \delta \mathbf{G}_{\mathrm{h}} \parallel^4_{\mathrm{L}^4(\Omega^{\mathrm{e}})} \right)^{\frac{1}{4}} \\
&\leq C^k C_{\mathrm{y}} h_{\mathrm{s}}^{\mu-2-\varepsilon} \sigma \parallel \delta \mathbf{G}_{\mathrm{h}} \parallel_{\mathrm{L}^2(\Omega_{\mathrm{h}})} \parallel \mathbf{G}^{\mathrm{e}} \parallel_{\mathrm{H}^s(\Omega_{\mathrm{h}})}.
\end{aligned} \tag{222}$$

Substituting Eqs. (221, 222) in Eq. (220) leads to

$$\mid \mathcal{I}_{6} \mid \leq C^k C_{\mathrm{y}} h_{\mathrm{s}}^{\mu-2-\varepsilon} \sigma \parallel \delta \mathbf{G}_{\mathrm{h}} \parallel_{\mathrm{L}^2(\Omega_{\mathrm{h}})} \parallel \mathbf{G}^{\mathrm{e}} \parallel_{\mathrm{H}^s(\Omega_{\mathrm{h}})}. \tag{223}$$

Combining Eqs. (209, 213, 214, 215, 216, and 223), yields

$$| \mathcal{N}(\mathbf{G}^{\mathrm{e}}, \mathbf{y}; \delta\mathbf{G}_{\mathrm{h}}) | \leq \mathrm{C}^k \mathrm{C}_{\mathrm{y}} \parallel \mathbf{G}^{\mathrm{e}} \parallel_{\mathrm{H}^s(\Omega_{\mathrm{h}})} h_{\mathrm{s}}^{\mu-2-\varepsilon} \sigma \left[\parallel \delta\mathbf{G}_{\mathrm{h}} \parallel_{\mathrm{H}^1(\Omega_{\mathrm{h}})} + \left(\sum_{\mathrm{e}} h_{\mathrm{s}} \parallel \delta\mathbf{G}_{\mathrm{h}} \parallel^2_{\mathrm{H}^1(\partial\Omega^{\mathrm{e}})} \right)^{\frac{1}{2}} + \left(\sum_{\mathrm{e}} h_{\mathrm{s}}^{-1} \parallel [\![\delta\mathbf{G}_{\mathrm{h}_{\mathbf{n}}}]\!] \parallel^2_{\mathrm{L}^2(\partial\Omega^{\mathrm{e}})} \right)^{\frac{1}{2}} \right] . \tag{224}$$

Finally, using the definition of the energy norm (77), this results yields the bound (95) of $\mathcal{N}(\mathbf{G}^{\mathrm{e}}, \mathbf{y}; \delta\mathbf{G}_{\mathrm{h}})$.

C.4.3 Declaration related to the fifth term of $\mathcal{N}(\boldsymbol{G}^e, \boldsymbol{y}; \delta\boldsymbol{G}_h)$

Using the identities $[\![\mathrm{ab}]\!] = [\![\mathrm{a}]\!] \langle \mathrm{b} \rangle + \langle \mathrm{a} \rangle [\![\mathrm{b}]\!]$ and $\langle \mathrm{a} \rangle \langle \mathrm{b} \rangle = \langle \mathrm{ab} \rangle - \frac{1}{4} [\![\mathrm{a}]\!] [\![\mathrm{b}]\!]$ on $\partial_{\mathrm{I}}\Omega_{\mathrm{h}}$, the term $[\![(\mathbf{G}^{\mathrm{e}} - \mathbf{G}_{\mathrm{h}})^{\mathrm{T}} \bar{\mathbf{o}}^{\mathrm{T}}_{\mathbf{G}}(\mathbf{G}_{\mathrm{h}})(\mathbf{G}^{\mathrm{e}} - \mathbf{G}_{\mathrm{h}})]\!] \langle \delta\mathbf{G}_{\mathrm{h}_{\mathbf{n}}} \rangle$ can be rewritten with an abuse of notations on the product operator as

$$\begin{aligned} &[\![(\mathbf{G}^{\mathrm{e}} - \mathbf{G}_{\mathrm{h}})^{\mathrm{T}} \bar{\mathbf{o}}^{\mathrm{T}}_{\mathbf{G}}(\mathbf{G}_{\mathrm{h}})(\mathbf{G}^{\mathrm{e}} - \mathbf{G}_{\mathrm{h}})]\!] \langle \delta\mathbf{G}_{\mathrm{h}_{\mathbf{n}}} \rangle = \left\langle (\mathbf{G}^{\mathrm{e}} - \mathbf{G}_{\mathrm{h}})^{\mathrm{T}} \bar{\mathbf{o}}^{\mathrm{T}}_{\mathbf{G}}(\mathbf{G}_{\mathrm{h}}) \delta\mathbf{G}_{\mathrm{h}_{\mathbf{n}}} \right\rangle [\![\mathbf{G}^{\mathrm{e}} - \mathbf{G}_{\mathrm{h}}]\!] \\ &- \frac{1}{4} [\![(\mathbf{G}^{\mathrm{e}} - \mathbf{G}_{\mathrm{h}})^{\mathrm{T}} \bar{\mathbf{o}}^{\mathrm{T}}_{\mathbf{G}}(\mathbf{G}_{\mathrm{h}})]\!] [\![\mathbf{G}^{\mathrm{e}} - \mathbf{G}_{\mathrm{h}}]\!] [\![\delta\mathbf{G}_{\mathrm{h}_{\mathbf{n}}}]\!] + [\![(\mathbf{G}^{\mathrm{e}} - \mathbf{G}_{\mathrm{h}})^{\mathrm{T}} \bar{\mathbf{o}}^{\mathrm{T}}_{\mathbf{G}}(\mathbf{G}_{\mathrm{h}})]\!] \langle \mathbf{G}^{\mathrm{e}} - \mathbf{G}_{\mathrm{h}} \rangle \langle \delta\mathbf{G}_{\mathrm{h}_{\mathbf{n}}} \rangle . \end{aligned} \tag{225}$$

Now, we need to solve explicitly the term $[\![(\mathbf{G}^{\mathrm{e}} - \mathbf{G}_{\mathrm{h}})^{\mathrm{T}} \bar{\mathbf{o}}^{\mathrm{T}}_{\mathbf{G}}(\mathbf{G}_{\mathrm{h}})]\!]$, where $\bar{\mathbf{o}}_{\mathbf{G}}(\mathbf{G}_{\mathrm{h}})$ corresponds to $-\bar{\mathbf{p}}_{\mathbf{GG}}(\mathbf{G}_{\mathrm{h}})$ defined in Eq. (181) with $\mathbf{p}_{\mathbf{GG}}(\mathbf{V}^{\mathrm{t}}) = -\mathbf{o}_{\mathbf{G}}(\mathbf{V}^{\mathrm{t}})$, yielding

$$\bar{\mathbf{o}}_{\mathbf{G}}(\mathbf{G}_{\mathrm{h}}) = \int_0^1 (1 - \mathrm{t}) \mathbf{o}_{\mathbf{G}}(\mathbf{V}^{\mathrm{t}}) \mathrm{dt}, \tag{226}$$

with $\mathbf{V}^{\mathrm{t}} = \mathbf{G}^{\mathrm{e}} + \mathrm{t}(\mathbf{G}_{\mathrm{h}} - \mathbf{G}^{\mathrm{e}})$. As $\mathbf{o}_{\mathbf{G}}$ only involves terms in $\frac{2}{\mathrm{f}_{\mathrm{T}}^3}$, we compute $\bar{\alpha}$ the nonzero component.

$$\bar{\alpha} = 3\mathrm{K}\alpha_{\mathrm{th}} \int_0^1 (1 - \mathrm{t}) \left(\frac{2}{[\mathrm{f}^{\mathrm{e}}_{\mathrm{T}} + \mathrm{t}(\mathrm{f}_{\mathrm{T}} - \mathrm{f}^{\mathrm{e}}_{\mathrm{T}})]^3} \right) \mathrm{dt}. \tag{227}$$

For simplicity, let us define λ as

$$\lambda = \int_0^1 (1 - \mathrm{t}) \frac{2}{[\mathrm{f}^{\mathrm{e}}_{\mathrm{T}} + \mathrm{t}(\mathrm{f}_{\mathrm{T}} - \mathrm{f}^{\mathrm{e}}_{\mathrm{T}})]^3} \mathrm{dt} = \frac{1}{\mathrm{f}_{\mathrm{T}} \mathrm{f}^{\mathrm{e}^2}_{\mathrm{T}}} . \tag{228}$$

It can be noticed that to evaluate $[\![(\mathbf{G}^{\mathrm{e}} - \mathbf{G}_{\mathrm{h}})^{\mathrm{T}} \bar{\mathbf{o}}^{\mathrm{T}}_{\mathbf{G}}(\mathbf{G}_{\mathrm{h}})]\!]$, we need $\lambda(\mathrm{f}^{\mathrm{e}}_{\mathrm{T}} - \mathrm{f}_{\mathrm{T}})$ which reads

$$\lambda(\mathrm{f}^{\mathrm{e}}_{\mathrm{T}} - \mathrm{f}_{\mathrm{T}}) = \frac{1}{\mathrm{f}_{\mathrm{T}} \mathrm{f}^{\mathrm{e}^2}_{\mathrm{T}}} (\mathrm{f}^{\mathrm{e}}_{\mathrm{T}} - \mathrm{f}_{\mathrm{T}}) = \frac{1}{\mathrm{f}^{\mathrm{e}}_{\mathrm{T}}} \left(\frac{1}{\mathrm{f}_{\mathrm{T}}} - \frac{1}{\mathrm{f}^{\mathrm{e}}_{\mathrm{T}}} \right), \tag{229}$$

and the jump of the last result is

$$[\![\lambda(\mathrm{f}^{\mathrm{e}}_{\mathrm{T}} - \mathrm{f}_{\mathrm{T}})]\!] = \begin{cases} \frac{1}{\mathrm{f}^{\mathrm{e}}_{\mathrm{T}}} \left(\frac{1}{\mathrm{f}^{+}_{\mathrm{T}}} - \frac{1}{\mathrm{f}^{\mathrm{e}}_{\mathrm{T}}} - \frac{1}{\mathrm{f}^{-}_{\mathrm{T}}} + \frac{1}{\mathrm{f}^{\mathrm{e}}_{\mathrm{T}}} \right) = -\frac{1}{\mathrm{f}^{\mathrm{e}}_{\mathrm{T}} \mathrm{f}^{+}_{\mathrm{T}} \mathrm{f}^{-}_{\mathrm{T}}} [\![\mathrm{f}_{\mathrm{T}} - \mathrm{f}^{\mathrm{e}}_{\mathrm{T}}]\!] \text{ on } \partial_{\mathrm{I}}\Omega_{\mathrm{h}} \\ \frac{1}{\mathrm{f}_{\mathrm{T}} \mathrm{f}^{\mathrm{e}^2}_{\mathrm{T}}} (\mathrm{f}_{\mathrm{T}} - \mathrm{f}^{\mathrm{e}}_{\mathrm{T}}) = -\frac{1}{\mathrm{f}_{\mathrm{T}} \mathrm{f}^{\mathrm{e}^2}_{\mathrm{T}}} [\![\mathrm{f}_{\mathrm{T}} - \mathrm{f}^{\mathrm{e}}_{\mathrm{T}}]\!] \text{ on } \partial_{\mathrm{D}}\Omega_{\mathrm{h}}. \end{cases} \tag{230}$$

Hence considering this equation in the matrix form, then substituting it in Eq. (225), and using the definition of C_{y} in Eq. (67), lead to

$$
\begin{aligned}
&| \sum_{\mathrm{e}} \int_{\partial_{\mathrm{I}}\Omega^{\mathrm{e}}\cup\partial_{\mathrm{D}}\Omega^{\mathrm{e}}} \Big[\!\Big[(\mathbf{G}^{\mathrm{e}}-\mathbf{G}_{\mathrm{h}})^{\mathrm{T}} \bar{\mathbf{o}}_{\mathbf{G}}^{\mathrm{T}} (\mathbf{G}_{\mathrm{h}})(\mathbf{G}^{\mathrm{e}}-\mathbf{G}_{\mathrm{h}}) \Big]\!\Big] \langle \delta\mathbf{G}_{\mathrm{h}_{\mathbf{n}}} \rangle \,\mathrm{dS} \,| \\
&\leq C_{\mathrm{y}} \sum_{\mathrm{e}} | \int_{\partial_{\mathrm{I}}\Omega^{\mathrm{e}}} (\mathbf{G}^{\mathrm{e}}-\mathbf{G}_{\mathrm{h}})^{\mathrm{T}} \mathbf{I} \, [\![\mathbf{G}^{\mathrm{e}}-\mathbf{G}_{\mathrm{h}}]\!] \, \delta\mathbf{G}_{\mathrm{h}_{\mathbf{n}}} \mathrm{dS} \,| \\
&+ \frac{1}{8} C_{\mathrm{y}} \sum_{\mathrm{e}} | \int_{\partial_{\mathrm{I}}\Omega^{\mathrm{e}}} \Big[\!\Big[(\mathbf{G}^{\mathrm{e}}-\mathbf{G}_{\mathrm{h}})^{\mathrm{T}} \Big]\!\Big] \mathbf{I} \, [\![\mathbf{G}^{\mathrm{e}}-\mathbf{G}_{\mathrm{h}}]\!] \, [\![\delta\mathbf{G}_{\mathrm{h}_{\mathbf{n}}}]\!] \,\mathrm{dS} \,| \\
&+ C_{\mathrm{y}} \sum_{\mathrm{e}} | \int_{\partial_{\mathrm{I}}\Omega^{\mathrm{e}}} \Big[\!\Big[(\mathbf{G}^{\mathrm{e}}-\mathbf{G}_{\mathrm{h}})^{\mathrm{T}} \Big]\!\Big] \mathbf{I} (\mathbf{G}^{\mathrm{e}}-\mathbf{G}_{\mathrm{h}}) \delta\mathbf{G}_{\mathrm{h}_{\mathbf{n}}} \mathrm{dS} \,| \\
&+ C_{\mathrm{y}} \sum_{\mathrm{e}} | \int_{\partial_{\mathrm{D}}\Omega^{\mathrm{e}}} \Big[\!\Big[(\mathbf{G}^{\mathrm{e}}-\mathbf{G}_{\mathrm{h}})^{\mathrm{T}} \Big]\!\Big] \mathbf{I} (\mathbf{G}^{\mathrm{e}}-\mathbf{G}_{\mathrm{h}}) \delta\mathbf{G}_{\mathrm{h}_{\mathbf{n}}} \mathrm{dS} \,| \,,
\end{aligned}
\tag{231}
$$

where $\mathbf{I}$ is a matrix of unit norm and has the same size of $\bar{\mathbf{o}}_{\mathbf{G}}^{\mathrm{T}}$.